

A Decade of Lessons Learned from the 2011 Tohoku-oki Earthquake

Naoki Uchida¹ and Roland Burgmann²

¹Tohoku University

²University of California, Berkeley

November 22, 2022

Abstract

The 2011 Mw 9.0 Tohoku-oki earthquake is one of the world's best-recorded ruptures. In the aftermath of this devastating event, it is important to learn from the complete record. We describe the state of knowledge of the megathrust earthquake generation process before the earthquake, and what has been learned in the decade since the historic event. Prior to 2011, there were a number of studies suggesting the potential of a great megathrust earthquake in NE Japan from geodesy, geology, seismology, geomorphology, and paleoseismology, but results from each field were not enough to enable a consensus assessment of the hazard. A transient unfastening of interplate coupling and foreshock activity were recognized before the earthquake, but did not lead to alerts. Since the mainshock, follow-up studies have (1) documented that the rupture occurred in an area with a large interplate slip deficit, (2) established large near-trench coseismic slip, (3) examined structural anomalies and fault-zone materials correlated with the coseismic slip, (4) clarified the historical and paleoseismic recurrence of M[~]9 earthquakes, and (5) identified various kinds of possible precursors. The studies have also illuminated the heterogeneous distribution of coseismic rupture, aftershocks, slow earthquakes and aseismic afterslip, and the enduring viscoelastic response, which together make up the complex megathrust earthquake cycle. Given these scientific advances, the enhanced seismic hazard of an impending great earthquake can now be more accurately established, although we do not believe such an event could be predicted with confidence.

1
2
3
4
5
6
7
8
9
10
11
12
13
14
15
16
17
18
19
20
21
22
23
24
25
26
27
28
29

A Decade of Lessons Learned from the 2011 Tohoku-oki Earthquake

N. Uchida¹, and R. Bürgmann²

¹Graduate School of Science and International Research Institute of Disaster Science, Tohoku University

²Department of Earth and Planetary Science, University of California, Berkeley

Corresponding author: Naoki Uchida (naoki.uchida.b6@tohoku.ac.jp)

Key Points:

- The lessons learned in the last decade highlight more realistic estimation of seismic hazard and importance of interdisciplinary study.
- Pre-2011 studies based on a variety of evidence did not result in a consensus assessment of the great-earthquake hazard.
- Despite the precursory foreshocks and slow slip and improved monitoring capabilities, prediction of such events still appears impossible.

30 **Abstract**

31 The 2011 Mw 9.0 Tohoku-oki earthquake is one of the world's best-recorded ruptures. In the
32 aftermath of this devastating event, it is important to learn from the complete record. We
33 describe the state of knowledge of the megathrust earthquake generation process before the
34 earthquake, and what has been learned in the decade since the historic event. Prior to 2011, there
35 were a number of studies suggesting the potential of a great megathrust earthquake in NE Japan
36 from geodesy, geology, seismology, geomorphology, and paleoseismology, but results from each
37 field were not enough to enable a consensus assessment of the hazard. A transient unfastening of
38 interplate coupling and foreshock activity were recognized before the earthquake, but did not
39 lead to alerts. Since the mainshock, follow-up studies have (1) documented that the rupture
40 occurred in an area with a large interplate slip deficit, (2) established large near-trench coseismic
41 slip, (3) examined structural anomalies and fault-zone materials correlated with the coseismic
42 slip, (4) clarified the historical and paleoseismic recurrence of M~9 earthquakes, and (5)
43 identified various kinds of possible precursors. The studies have also illuminated the
44 heterogeneous distribution of coseismic rupture, aftershocks, slow earthquakes and aseismic
45 afterslip, and the enduring viscoelastic response, which together make up the complex
46 megathrust earthquake cycle. Given these scientific advances, the enhanced seismic hazard of an
47 impending great earthquake can now be more accurately established, although we do not believe
48 such an event could be predicted with confidence.

49 **Plain Language Summary**

50 The Mw 9 Tohoku-oki earthquake was one of the most disastrous earthquakes in recent history.
51 In this review, we first clarify the knowledge of the earthquake and tsunami potential before the
52 earthquake. Pre-Tohoku-oki studies partly recognized the potential of Mw 8 or larger
53 earthquakes. However, the knowledge based on different types of observations was incomplete
54 and the occurrence of such a great event was not considered in the official earthquake
55 probabilities. The improved understanding of earthquake-cycle and rupture processes since the
56 Tohoku-oki earthquake advanced the leading edge of efforts to characterize megathrust
57 earthquake hazards. We can summarize the lessons as follows. 1) The incorporation of
58 interdisciplinary research is essential to advance our understanding of the processes underlying
59 the occurrence of earthquakes. 2) The recognition of earthquake potential informed by geologic
60 evidence extending beyond available instrumental records is essential for assessing the largest
61 possible earthquake in a subduction zone. 3) The development of advanced scientific
62 infrastructure, especially ocean-bottom observations is necessary to evaluate earthquake potential
63 and monitor dynamic megathrust fault-zone processes. 4) Although post-Tohoku-oki studies
64 have better characterized the hazard and a number of possible precursors have been identified,
65 the confident prediction of such events appears impossible in the near future.

66

67 **1 Introduction**

68 The Mw 9.0 Tohoku-oki earthquake occurred off the Pacific coast of the Tohoku region
69 of Japan, on March 11, 2011 (Fig. 1). A M7-8 earthquake with rupture dimensions of about
70 ~100km was expected along this segment of the subduction zone but it was far larger with a
71 rupture area of about 300 x 200 km (Fig. 2). The strong shaking and tsunami from the event
72 caused devastating damage. The loss of life was as large as 19,729 and more than 121,996

73 houses were completely destroyed [*Fire and disaster management agency*, 2020]. Earthquake
74 early warning and tsunami warnings were issued by the Japan Meteorological Agency (JMA) as
75 part of the routine operation of Japan's earthquake monitoring system, but the initial warnings
76 underestimated the impending shaking and tsunami [*Hoshiwa and Iwakiri*, 2011].

77 The earthquake is probably one of the most scientifically important recent subduction
78 zone ruptures. There have been many studies on the earthquake, including several review papers
79 focused on various aspects of the earthquake. Previous reviews illuminate the observations and
80 characteristics of the coseismic rupture [*Lay*, 2018; *Satake and Fujii*, 2014; *Tajima et al.*, 2013],
81 provide insights gained from geodetic deformation measurements [*Nishimura et al.*, 2014],
82 examine the environment, structure and mechanical properties of the shallow megathrust from
83 ocean bottom drilling [*Brodsky et al.*, 2020], describe preseismic processes from seismicity and
84 geodetic observations [*Hasegawa and Yoshida*, 2015], summarize the tsunami source mechanism
85 [*Pararas-Carayannis*, 2014], and assess post-earthquake changes in earthquake hazard
86 [*Somerville*, 2014]. There are also early overviews of broad knowledge about the earthquake
87 gained within a few years following the mainshock [*Hino*, 2015; *Tajima et al.*, 2013]. However,
88 there are no comprehensive reviews that summarize the advancement of knowledge across a
89 broad range of scientific disciplines after a decade of investigations of the earthquake. Our
90 review targets the whole earthquake-cycle process (before, during and after the earthquake),
91 draws on evidence from a wide range of disciplines (seismology, geodesy, geology,
92 geomorphology, and paleoseismology), and covers up-to-date information based on research up
93 to ~10 years after the earthquake.

94 While there had been many studies of this subduction zone before the earthquake, the
95 knowledge did not lead to awareness of the potential of an M~9 earthquake and scenarios
96 considering large near-trench slip in official hazard assessments at Tohoku. One of the missing
97 pieces was an interdisciplinary understanding of the potential of great megathrust earthquakes
98 based on the wide range of available evidence. Here, we integrate the lessons learned from this
99 event and review insights about the earthquake occurrence process derived from various
100 disciplines. We summarize and evaluate retrospective investigations of pre-earthquake processes
101 and highlight new ocean bottom observations established after the earthquake, which are another
102 missing piece of the pre-Tohoku-oki level of understanding. We believe that such an assessment
103 is also important to make good use of the lessons in scientific studies and hazard mitigation
104 efforts in other subduction zones around the world, where there is a great need to better
105 understand the potential of future damaging earthquakes.

106 **2 Knowledge before the earthquake**

107 **2.1 Seismic and geodetic coupling**

108 Since megathrust ruptures occur to release accumulated stress due to the coupling on the
109 plate interface, it is important to know the distribution of coupled areas to identify the potential
110 source areas of interplate earthquakes. There are two primary methods to infer the interplate
111 coupling, which rely on the slip of known historic interplate seismic events and the interseismic
112 surface deformation of the upper plate. We refer to the coupling derived from seismic and
113 geodetic data as seismic and geodetic coupling, respectively. The seismic coupling is the ratio of
114 the rate of slip released by observed earthquakes to the rate of relative plate motion and
115 associated slip-deficit accumulation across the seismogenic depth extent of the megathrust. For
116 offshore Tohoku, the seismic coupling ratio was estimated to be 0.18-0.24 [*Pacheco et al.*, 1993;

117 *Peterson and Seno, 1984*] from just under one hundred years of data. On the other hand, the
 118 geodetic coupling was estimated to be substantially higher off Tohoku (0.5 – 1.0) [*C Hashimoto*
 119 *et al., 2009; Loveless and Meade, 2010; Nishimura et al., 2000; Suwa et al., 2006*] (Fig. 3). This
 120 indicates a factor of two to five discrepancy between the estimates of seismic and geodetic
 121 coupling.

122 The major source of uncertainty for the seismic coupling estimates is the limited
 123 observation period. If the observation period does not include occurrences of the largest
 124 earthquakes, the estimation becomes very uncertain. On the other hand, major uncertainties of
 125 the geodetic estimates based on on-land data are due to the possibility of temporal coupling
 126 changes during the interseismic period, low resolution of the degree of coupling near the trench,
 127 and unknown mechanisms in the release of the slip deficit (i.e., by earthquakes or slow slip
 128 events). Nevertheless, the evaluation of the interplate locking state represents a fundamental
 129 objective to infer the potential of large earthquakes and the discrepancy in seismic and geodetic
 130 coupling estimates was not thoroughly discussed in most studies. One important discussion of
 131 the discrepancy, which was made before the Tohoku-oki earthquake, is that by *Kanamori et al.*
 132 [2006]. Based on their estimate of much smaller seismic coupling (~0.25) than geodetic coupling
 133 (~1) in the central part (offshore Miyagi, Fig. 2a) of the future Tohoku-oki earthquake rupture,
 134 they proposed the possibility that the accumulated slip deficit will eventually be released by large
 135 megathrust events. However, *Kanamori et al.* [2006] also considered other possibilities,
 136 including resolution problems in the estimates from geodetic data, and strain release by slow
 137 tsunami earthquakes or silent earthquakes. The recognition of silent earthquakes and afterslip,
 138 which can release moments comparable to that of large earthquakes [e.g., *K. Heki et al., 1997;*
 139 *Kawasaki et al., 2001*], was behind the consideration of such aseismic process. Offshore
 140 observation of ocean-bottom geodetic observations using GPS-Acoustic ranging had just started
 141 in 2005, 6-years before the Tohoku-oki earthquake [*Sato et al., 2011b*], however the number of
 142 stations was small and the data had not yet been used to formally reassess the degree of coupling
 143 in the wide near-trench area.

144 2.2 Geologic and historic evidence of megathrust earthquakes

145 The geologic and historic evidence of past $M > 8$ earthquakes provides one of the most
 146 direct ways to document the possibility of such great events. Written records of a very large
 147 earthquake and tsunami in the Tohoku area exist for the 869 Jyogan and 1611 Keicho
 148 earthquakes [*H Abe et al., 1990; T Usami, 1996*]. In addition, oral legends pertaining to the 869
 149 Jyogan earthquake and tsunami persisted along the coast of Miyagi prefecture to Ibaraki
 150 prefecture (Fig. 4a, [*H Watanabe, 2001*]), although it is difficult to assign accurate timing and
 151 size of the earthquake from this type of information. Importantly, tsunami deposits of the Jyogan
 152 earthquake were found in the Sendai plain [*H Abe et al., 1990; Minoura and Nakaya, 1991*],
 153 suggesting the occurrence of a large interplate earthquake and tsunami that carried water several
 154 kilometers inland. The distribution of young tsunami deposits that are possibly associated with
 155 the 869 and 1611 Keicho earthquakes was found to extend over a wide area of the Sendai
 156 [*Minoura and Nakaya, 1991; Sawai et al., 2007*] and Ishinomaki [*Shishikura et al., 2007*] plains,
 157 years before the Tohoku-oki earthquake (Fig. 4a). Some of the tsunami deposits initially
 158 attributed to the 1611 Keicho earthquake were later associated with the 1454 Kyotoku
 159 earthquake [*Sawai et al., 2012*]. These studies also found additional tsunami deposits older than
 160 the 869 event and estimated the recurrence interval to be 600 -1400 years [*Sawai et al., 2007*]
 161 and 500 - 1000 years [*Shishikura et al., 2007*]. *Satake et al.* [2008], *Namegaya et al.* [2010] and

162 *Sugawara et al.* [2011] used numerical simulations to infer the source fault of the 869 Jyogan
 163 earthquake from the tsunami deposit data and estimated a rupture of Mw >8.4, 8.4 and 8.3,
 164 respectively.

165 The discrepancy between the long-term deformation at geological time scales and short-
 166 term deformation measured by geodetic methods in the land area of Tohoku provides additional
 167 constraints on the probability of rare very large events. The geodetic observations in the last 100
 168 years have revealed strain accumulation rates as high as 10^{-7} per year. However, geologically
 169 observed strain rates, based on slip rates on active faults and folding are as low as 10^{-8} per year
 170 [*Ikeda*, 1996; *Kaizuka and Imaizumi*, 1984]. This suggests that while the elastic rebound is likely
 171 incomplete, it still accounts for most of the geodetically observed deformation in this area. Thus,
 172 *Ikeda* [1996] suggested that the strain accumulated at high rates in the last 100 years will be
 173 released by big earthquake(s) with magnitude 8 or greater, rather than by distributed deformation
 174 away from the plate interface.

175 In summary, studies of the distribution of tsunami deposits, written records and oral
 176 legends, and the discrepancy in the deformation rate at geodetic and geologic time scales all
 177 suggested the occurrence of megathrust events much larger than the instrumentally observed
 178 earthquakes offshore Tohoku (Fig. 5), although the detailed nature of such earthquakes remained
 179 unclear.

180 2.3 Other indicators of earthquake potential

181 There are other approaches to assess the potential of very large megathrust earthquakes.
 182 *Ruff and Kanamori* [1980] investigated correlations between variations in coupling and other
 183 physical features of subduction zones and suggested that fast plate convergence rates and young
 184 plate ages are correlated with the occurrence of great earthquakes. Since the convergence rate at
 185 Tohoku-oki region is relatively high (~ 9 cm/yr) but the subducting Pacific slab is old (~ 130 Ma),
 186 the relationship suggested by *Ruff and Kanamori* [1980] would suggest a maximum earthquake
 187 of roughly M 8.2. However, the 2004 Sumatra earthquake (Mw 9.1), which occurred in a slow
 188 subduction zone with an old slab, had already clearly violated such a general relationship [e.g.,
 189 *McCaffrey*, 2008]. The earthquake size distribution, such as the Gutenberg–Richter frequency-
 190 magnitude law, can also be used to statistically infer the maximum earthquake size in a region.
 191 For example, *Kagan* [1997] estimated M8.6 as the maximum size for the Japan-Kurile-
 192 Kamchatka region, a relatively high value close to the magnitude of the eventual Tohoku-oki
 193 earthquake. Other attempts for estimating earthquake probabilities prospectively were based on a
 194 variety of methods, and efforts by the Collaboratory for the Study of Earthquake Predictability
 195 (CSEP) to assess such efforts had started before the Tohoku-oki earthquake [*Nanjo et al.*, 2011].
 196 A total of 35 forecast models had been submitted before the Tohoku-oki earthquake, but they did
 197 not intend to estimate the potential of very large earthquakes.

198 2.4 Long-term earthquake forecast

199 Figure 6 shows the segments offshore Tohoku considered in the official assessment of the
 200 long-term subduction earthquake probabilities, which was effective at the time of the 2011
 201 Tohoku-oki earthquake [*Headquarters of Earthquake Research Promotion*, 2002]. The offshore
 202 Tohoku area was divided into source regions based on 11 earthquakes since 1611 (Fig. 5). The
 203 maximum considered magnitude was M8.2 in the near-trench area off northern Sanriku to off-
 204 Boso and southern Sanriku-oki. The earthquake probabilities were estimated for each individual
 205 segment. In the near-trench area from northern Sanriku-oki to Boso-oki, compound hazard from

206 interplate and normal-faulting earthquakes in the Pacific plate were also considered. The
 207 possibility of earthquakes with larger rupture areas was not considered, with one exception; in
 208 the off Miyagi area, simultaneous rupture was allowed for the Miyagi-ken oki and southern
 209 Sanriku-oki regions (pink shaded area), and the size of the compound rupture was estimated to
 210 be M8.2. The considered segment failures were too small compared to the eventual rupture area
 211 of the 2011 Tohoku-oki earthquake, which ruptured a wide area that encompassed at least five
 212 segments considered in the long-term forecast (Fig. 6).

213 There was evidence that earthquake ruptures had occurred repeatedly in some of the
 214 smaller segments. Figure 5a shows the distribution of the slip areas for $M_w \geq 7$ earthquakes in
 215 1930-2002 from *Yamanaka and Kikuchi* [2004] and *Murotani et al.* [2003]. They show that
 216 some of the slip areas appear to be overlapping and may represent repeat failures. The
 217 compilation of aftershock areas and tsunami source areas from instrumental data spanning 85
 218 and 118 years, respectively, (Fig. 5b and c) also shows that some of the sources are located in the
 219 same area. The evidence for repeating ruptures was established for $M \sim 7$ [*Yamanaka and Kikuchi*,
 220 2004] and much smaller repeating earthquakes [*Igarashi et al.*, 2003] in the same subduction
 221 zone, as well as for some other historical plate boundary earthquakes [e.g., *Murray and Langbein*,
 222 2006]. Therefore, it came natural to infer that the same fault area repeatedly produces
 223 characteristic earthquakes of nearly the same size [*Hasegawa et al.*, 2009; *Schwartz and*
 224 *Coppersmith*, 1984]. However, there was also evidence of multisegment ruptures and partial
 225 rupture of previous large megathrust slip zones in the Aleutian subduction zone [*Shennan et al.*,
 226 2009], Kuril subduction zone [*Nanayama et al.*, 2003], Sumatra subduction zone [*Konca et al.*,
 227 2008], and Nankai subduction zone [*M Ando*, 1975]. In addition, there were indications that
 228 smaller sized earthquakes occur within the slip areas of larger ruptures, including frequent partial
 229 ruptures of a middle-sized ($M \sim 5$) off-Kamaishi repeating earthquake sequence [*Uchida et al.*,
 230 2007], suggesting a hierarchical structure of the slip area. Heterogeneous frictional parameters
 231 or multi-scale heterogeneity may explain such observations [*Hori and Miyazaki*, 2010; *Ide and*
 232 *Aochi*, 2005]. This means that if we define likely rupture segments based only on the so far
 233 observed, smaller-sized events, even if they had occurred repeatedly, we neglect the real
 234 possibility of much larger earthquakes. In any case, the official long-term forecast and most
 235 individual studies before 2011 did not consider the occurrence of $M \sim 9$ earthquakes offshore
 236 Tohoku, largely because of insufficient evidence for ruptures of that size.

237 2.5 Reported anomalies before the earthquake

238 The central part of Tohoku-oki, the Miyagi-oki area where $M \sim 7.5$ earthquakes occurred
 239 every ~ 30 years, was considered as one of the most probable locations of pending earthquakes
 240 and the long-term forecast suggested a 90% or larger probability of rupture before 2030
 241 [*Headquarters of Earthquake Research Promotion*, 2000]. Therefore, the area received special
 242 attention, although the expected magnitude of the earthquake was moderate. Notably, a $M 7.3$
 243 earthquake occurred 2 days before the Tohoku-oki earthquake just updip of the expected Miyagi-
 244 oki earthquake (Figs 2 and 5). However, there were no pre-Tohoku-oki reports on the foreshock
 245 and related monitoring results or forecasting attempts.

246 Changes in interplate coupling offshore Tohoku were being investigated based on Global
 247 Positioning System (GPS) time series and repeating earthquake data sets. The 2009 report of a
 248 project “Research and Observation of the Miyagi-Oki Earthquake” under The Headquarters for
 249 Earthquake Research Promotion (HERP), which aimed to quantify coupling and its temporal
 250 changes, indicated that both the GPS and repeating earthquake data show relative uncoupling in

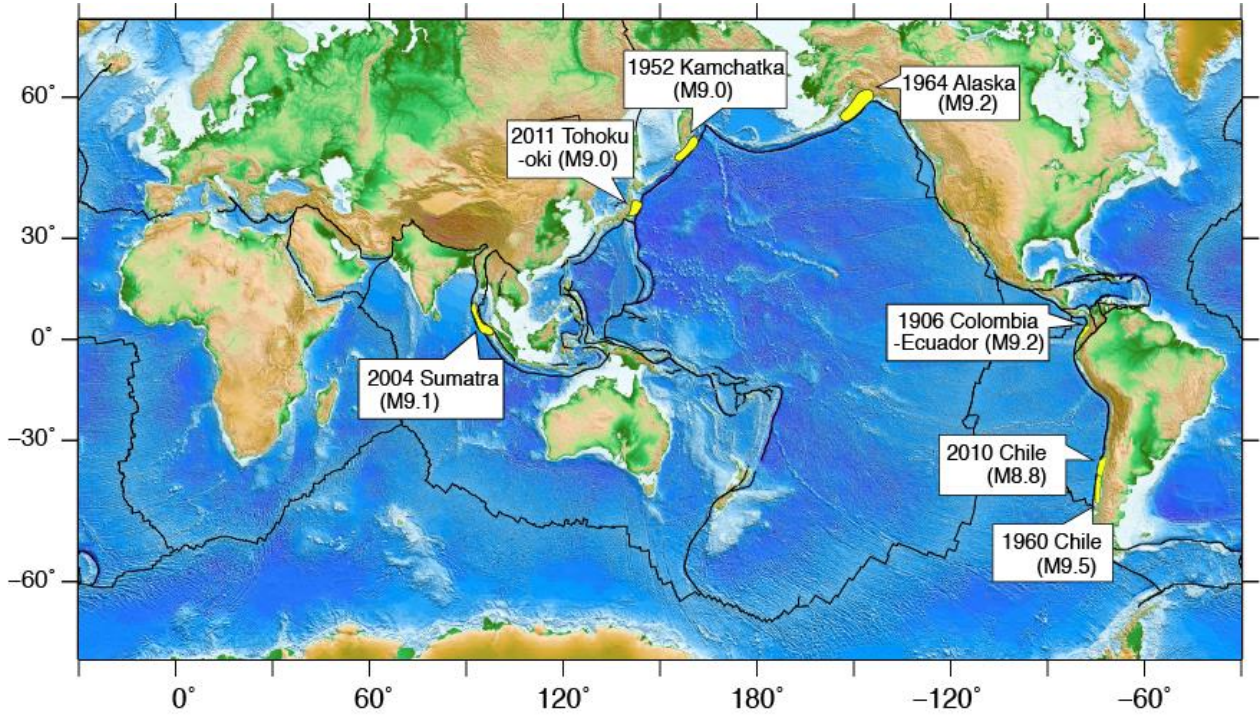
251 the south Tohoku area since 2008 [*Headquarters for Earthquake Research Promotion, Ministry*
252 *of Education, Culture, Sports, Science and Technology, Japan*,, 2009] (Fig. 7). The underlying
253 observations were clear, but the results were not published in peer-reviewed journals until after
254 the earthquake (see section 4.2) and the report did not include discussions of potential future
255 earthquakes.

256 The moderate seismic activity during February of 2011 in the off Miyagi area, which
257 included a M5.5 earthquake, was reported on March 9 (2 days before the Tohoku-oki
258 earthquake) at the monthly meeting of HERP. It was considered to be similar to previous
259 periods of seismic activity including M5-6 earthquakes that occur sometimes in the area
260 [*Headquarters for Earthquake Research Promotion, Ministry of Education, Culture, Sports,*
261 *Science and Technology, Japan, 2011*]. The M7.3 foreshock that occurred later on March 9 (Fig.
262 2a) did not get evaluated by the HERP but several institutes published information on their
263 webpages, mostly on the general information on the earthquake type and previous seismic
264 activity near the source. One detailed posting with interpretation was posted by Tohoku
265 University, which also commented on the apparent uncoupling that had occurred since around
266 2008 [*Research Center for Prediction of Earthquakes and Volcanic Eruptions, 2011*]. However,
267 again there was no discussion of possible future large earthquakes. To the contrary, since the M
268 7.3 slip area was considered to be located in southern Sanriku-oki, where simultaneous rupture
269 with the Miyagi-oki region had been considered (Fig. 6), other researchers considered that the
270 occurrence of the M7.3 earthquake decreased the possibility of large multi-segment earthquakes
271 [e.g., *Kahoku-shinpo, 2011*]. The fact that these geodetic and repeating earthquake anomalies
272 over the last several years and the early 2011 foreshock activity were not investigated in detail
273 and discussed as a potential anomaly related to enhanced megathrust earthquake hazard before
274 the Tohoku-oki earthquake probably reflects the still limited level of knowledge of the
275 subduction zone before the Tohoku-oki earthquake. Other kinds of potential precursory
276 anomalies were, as far as we know, only pointed out retrospectively after the Tohoku-oki
277 earthquake had occurred.

278

279

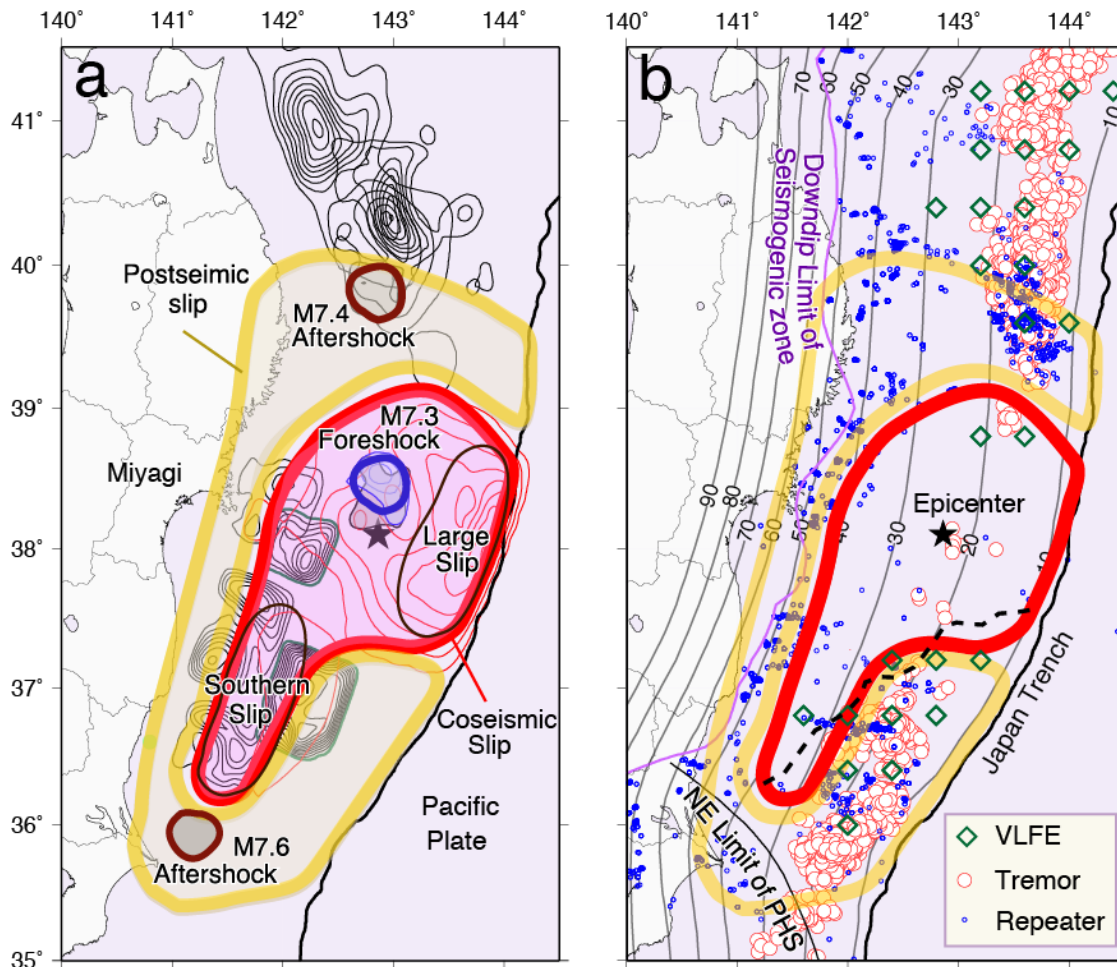
280
281
282



283
284
285
286
287

Figure 1 Global distribution of instrumentally recorded $M > 8.8$ earthquakes. The rupture areas are schematically shown by yellow polygons. The moment magnitudes are based on U. S. Geological Survey except for the Tohoku-oki earthquake which is based on JMA.

288
289
290
291



292
293

Figure 2 A schematic model showing the coseismic (red) and postseismic slip areas (orange) of the 2011 Tohoku-oki earthquake with observed slip areas of previous earthquakes (a) and postseismic distribution of Very Low Frequency Earthquakes (VLFs, green diamonds, Baba et al. 2020), tremors (red circles, Nishikawa et al. [2019]) and repeating earthquakes (small blue circles, Nishikawa et al. [2019]) (b). In (a), the slip distribution of the 2011 Tohoku-oki earthquake is shown with 10 m intervals [Inuma et al., 2012]. The slip distribution of other $M \geq 7$ earthquakes by Yamanaka and Kikuchi [2004] and Murotani et al. [2003] are shown with 0.5 m and 1 m contour intervals, respectively, to the north and south of 37.7°N in black. In (b) the gray contour lines show the depth of the plate boundary and a magenta line indicates the downdip limit of the seismogenic zone [Igarashi et al., 2001; Kita et al., 2010a; Uchida et al., 2009]. The dashed black line show forearc segment boundary from residual topography and gravity anomalies data [Bassett et al., 2016]. The northeastern limit of the Philippine Sea plate (PHS) on the subducting Pacific plate is from [Uchida et al., 2009].

307
308

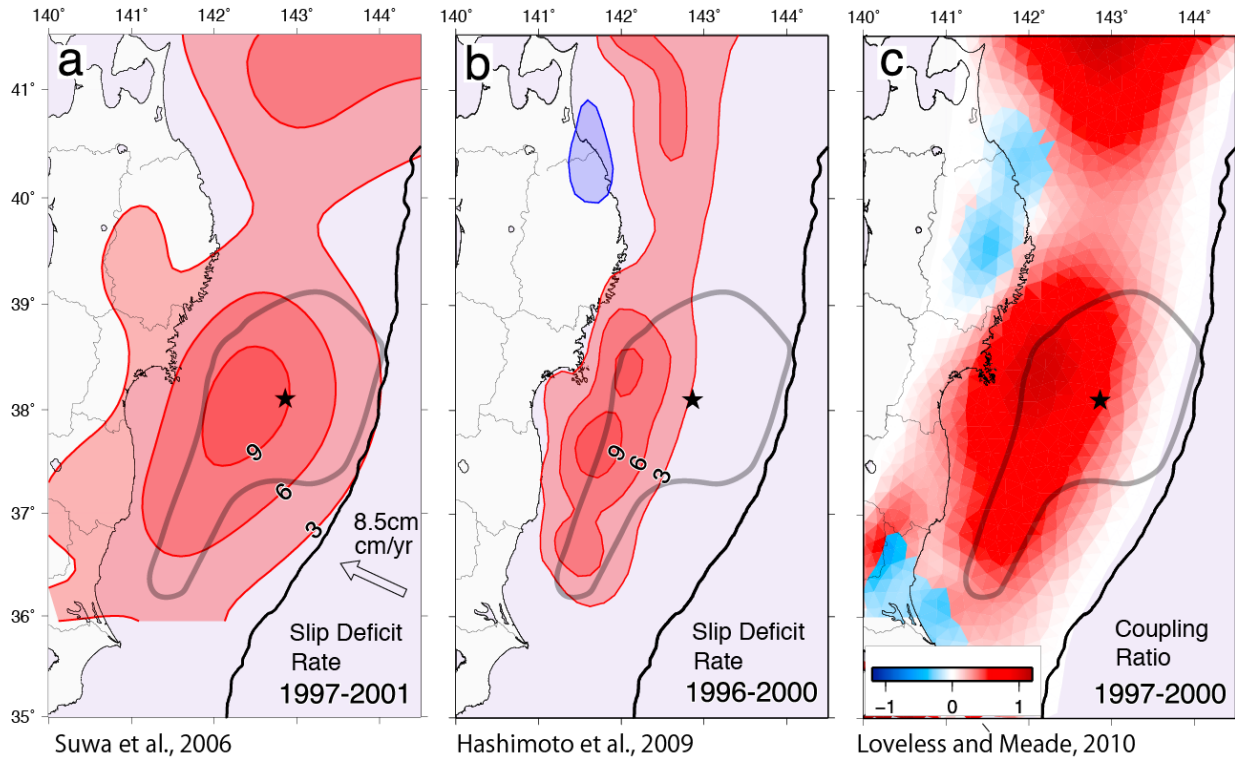
309
310311
312

Figure 3 Distribution of slip deficit rate (a, b) and coupling ratio (c) from model inversions of interseismic on-land GPS velocities. (a) The distribution of slip deficit rate from 1997 to 2001 [Suwa *et al.*, 2006]. (b) The distribution of slip deficit rate from 1996 to 2000 [C Hashimoto *et al.*, 2009]. The contour interval for (a) and (b) is 3 cm/year. (c) The distribution of coupling ratio from January 1997 to May 2000 [Loveless and Meade, 2010]. The stars show the epicenter of the 2011 Tohoku-oki earthquake. Note that there are wide areas of large slip deficit or coupling ratio offshore southern Tohoku in all three models, which correspond to the approximate slip area of the Tohoku-oki earthquake (gray line, the same area as shown in Fig. 2). Note also that the model resolution in the near-trench area is poor and largely depends on the assumed boundary conditions.

323
324
325
326
327

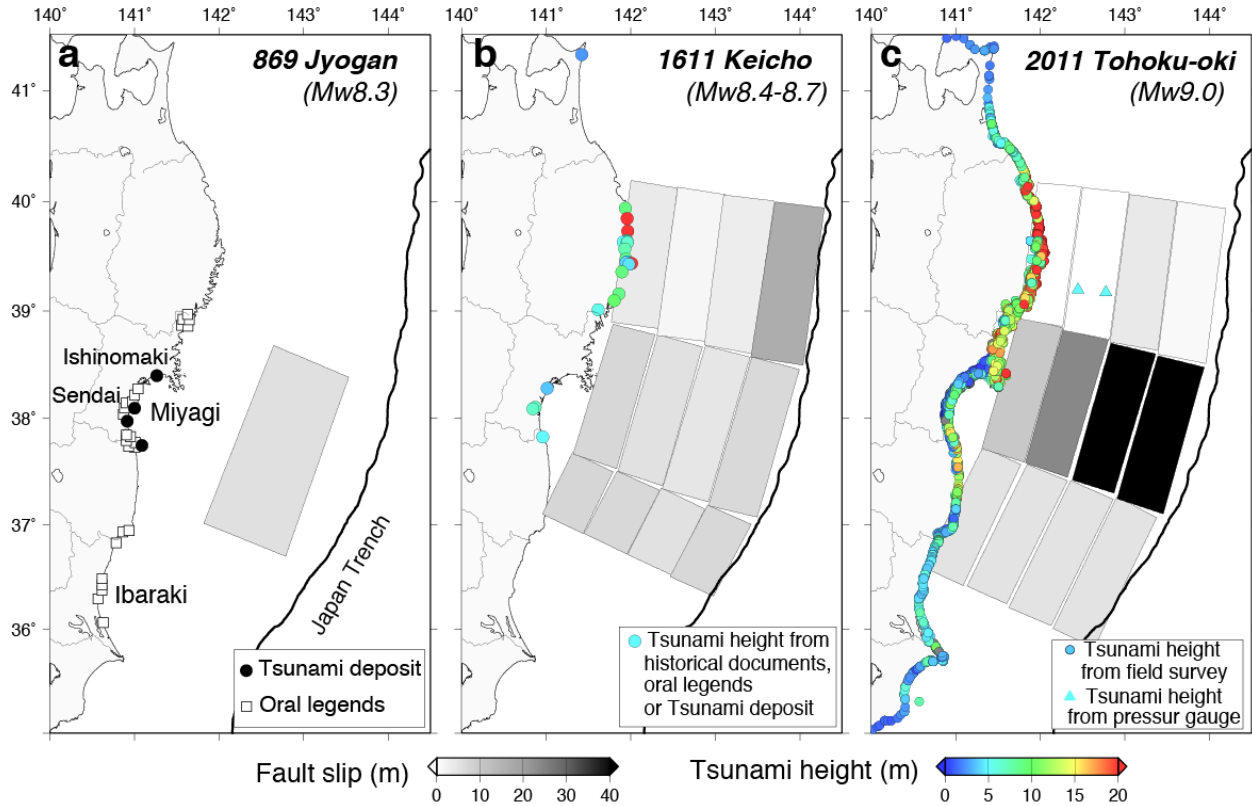
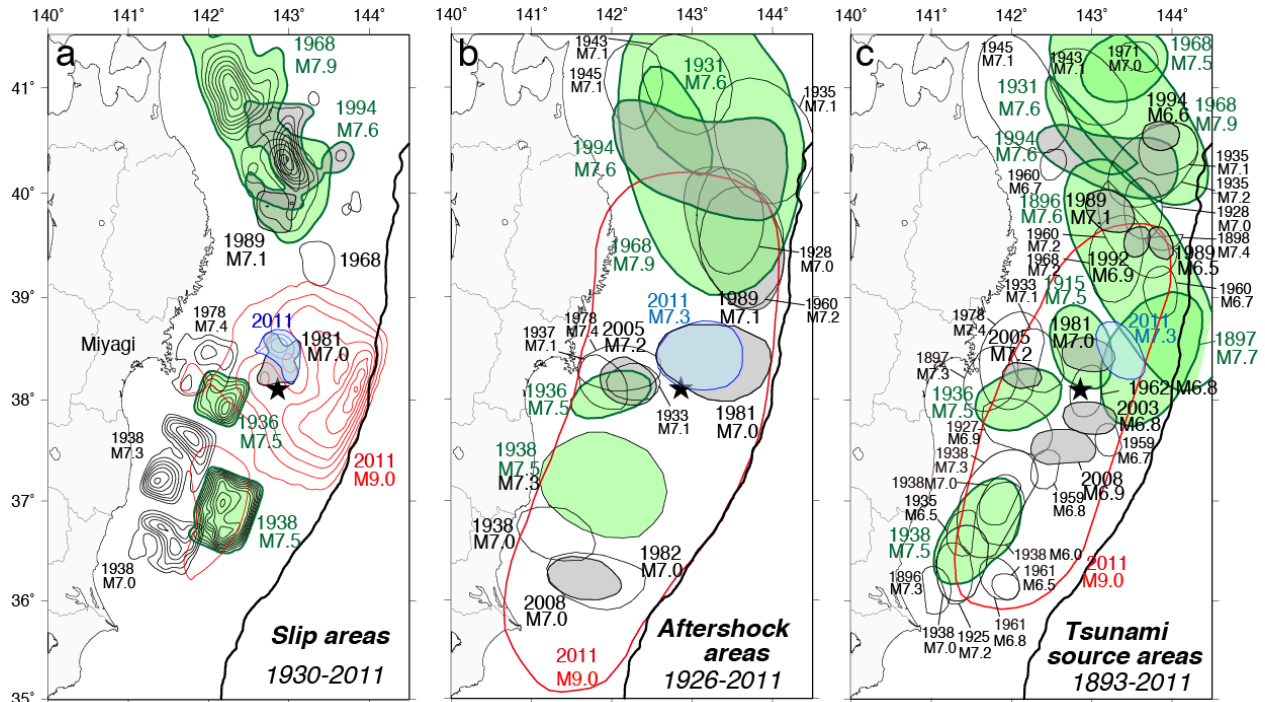
328
329
330331
332

Figure 4. The tsunami observations and source models for the (a) 869 Jyogan, (b) 1611 Keicho and (c) 2011 Tohoku-oki earthquakes. The symbols along the coast and triangles in (c) show the locations of tsunami data. The data in (a) represent oral legends of tsunami at locations shown by squares [H Watanabe, 2001] and excavated tsunami deposits at black circles [H Abe et al., 1990; Minoura et al., 2001; Minoura and Nakaya, 1991; Sawai et al., 2008; Sawai et al., 2007; Shishikura et al., 2007; Sugawara et al., 2010; Sugawara et al., 2001]. These data do not provide tsunami run-up height values. The historical observation data in (b) represent written documents and oral legends except for the northernmost point that is based on the absence of tsunami deposits attributed to the 1611 event. The data are from Ebina and Imai [2014], Hatori [1975], [Yoshinobu Tsuji and Ueda, 1995], Tsuji and Ueda [1995], Yoshinobu Tsuji et al. [2011] and [Yoshinobu Tsuji et al., 2012]. The observation data in (c) show field survey measurements of tsunami height by the Tsunami Joint Survey Group [2011]. Please note both run-up heights and inundation heights are shown. The rectangles show the tsunami source models based on these observations except for (c), which is only based on the waveforms of the two offshore pressure gauges (cyan triangles). The data source are (a) Sugawara et al. [2011] (b) Imai et al. [2015] and (c) Maeda et al. [2011].

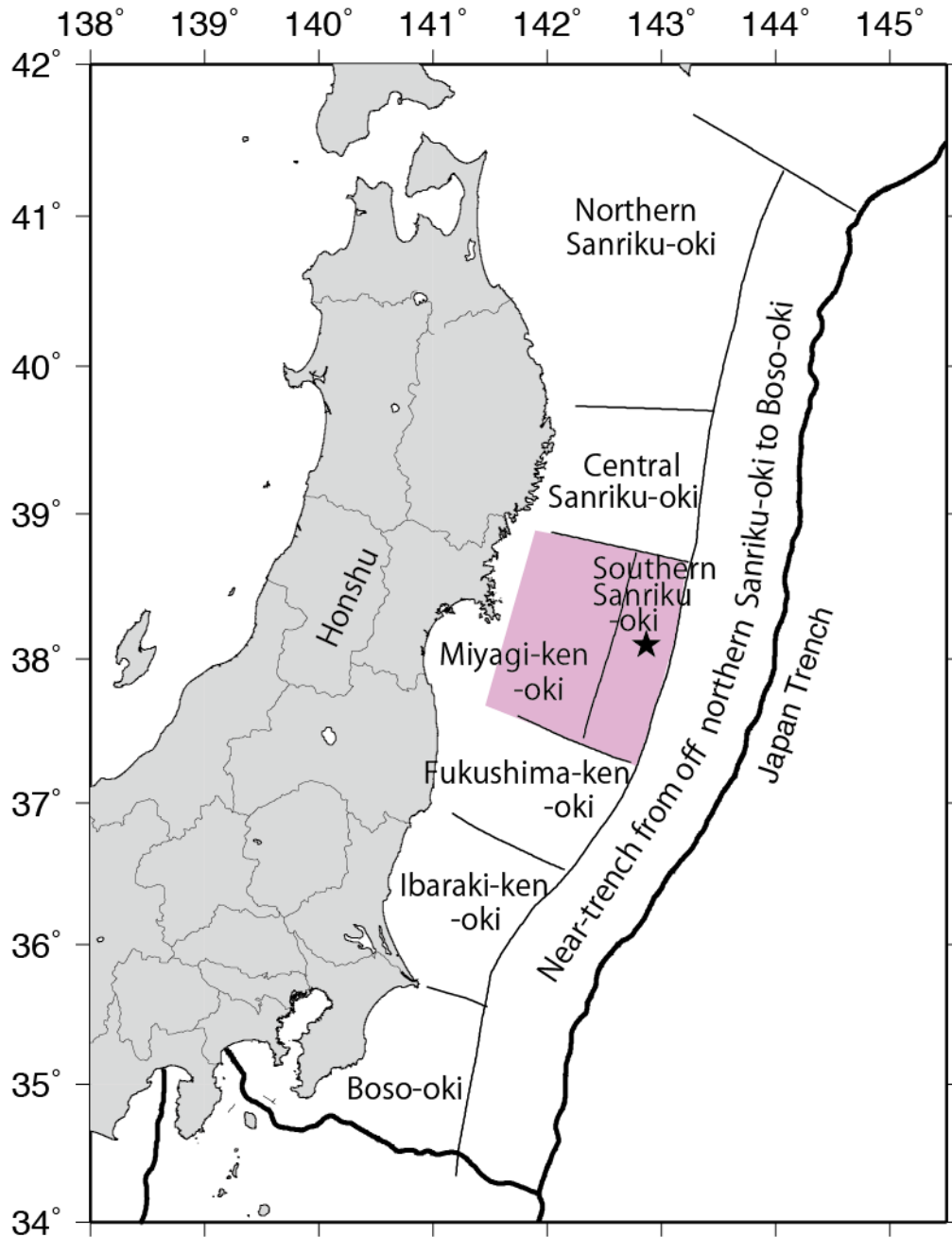
349

350
351
352
353
354



355
356
357
358
359
360
361
362
363
364
365
366
367
368
369
370
371
372
373
374
375

Figure 5 The distribution of interplate earthquake source areas from instrumental records. Green, gray and blue lines show $M \geq 7.5$ or larger earthquake, 1980 or more recent earthquakes, and the March 9, 2011 foreshock, respectively. Red lines and black star show the source area and epicenter of the 2011 Tohoku-oki earthquake. (a) Slip distributions based on seismic waveform inversions. The slip area of the 2011 Tohoku-oki earthquake in 10 m intervals [Inuma *et al.*, 2012] is shown in red and was obtained from terrestrial and seafloor geodetic data. The slip distribution of other $M \geq 7$ earthquakes by Yamanaka and Kikuchi [2004] and Murotani *et al.* [2003] are shown with 0.5 m and 1 m contour intervals, respectively, to the north and south of 37.7°N . The foreshock slip is by Ohta *et al.* [2012a] with 0.5 m contour intervals. (b) Aftershock areas that are thought to delineate the extent of source ruptures for $M \geq 7$ earthquakes. The data are Hasegawa *et al.* [1985] and Uchida *et al.* [2009]. The foreshock and aftershock areas for the 2011 Tohoku-oki earthquake were added in blue and red in this study based on the distribution of aftershocks from the first 24 hours. (c) The tsunami source areas of interplate earthquakes that produced coseismic ocean bottom deformation. The red line shows the 2011 Tohoku-oki earthquake [Hatori, 2012]. The other data are [Hatori, 1972; 1974; 1975; 1976; 1978; 1989; 1996].



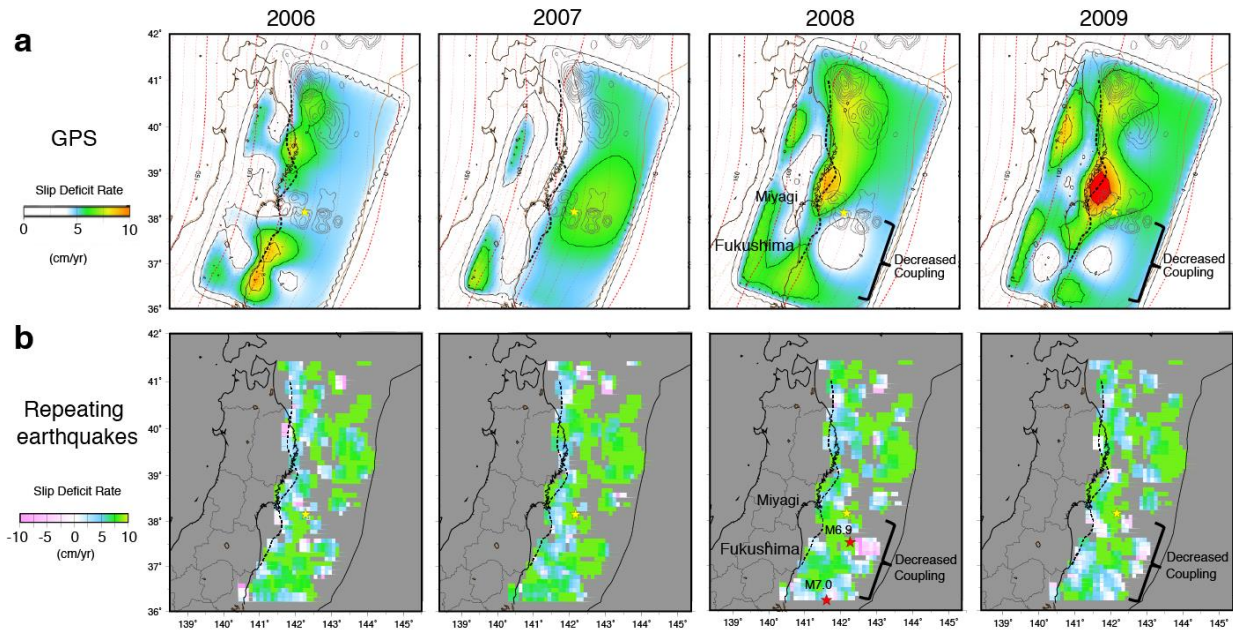
376

377 **Figure 6** Inferred rupture segmentation along the Japan trench for which long-term earthquake
 378 probabilities were estimated by the Earthquake Research Committee of the Headquarters for
 379 Earthquake Research Promotion. The colored patches represent the segments for which multi-
 380 segment rupture was considered. For the near-trench segment, both interplate and intraplate
 381 earthquakes are considered and are not assumed to rupture the whole area simultaneously. The
 382 star shows the epicenter of the Tohoku-oki earthquake. Modified from *Headquarters of*
 383 *Earthquake Research Promotion* [2002].

384

385

386
 387
 388
 389
 390
 391



392
 393
 394
 395
 396
 397
 398
 399
 400
 401

Figure 7 The distribution of slip deficit rate from GPS data and repeating earthquakes from 2006 to 2009. The years are shown at the top of each panel (after Figs 6 and 14 of section 3.1, *Headquarters for Earthquake Research Promotion, Ministry of Education, Culture, Sports, Science and Technology, Japan*, [2009]). As the repeating earthquake analysis estimates slip rate, it was converted to slip deficit rate using the plate convergence rate of 8.5 cm/year. Please also note that the GPS and repeater data suggest zero or negative (slip in excess of long-term rates) slip deficit off Fukushima after 2008.

402 3 The features of the Tohoku-oki earthquake

403 3.1 Co- and postseismic observations of the earthquake

404 The characteristics of the coseismic and postseismic slip processes of the Tohoku-oki
405 earthquake were constrained with better spatio-temporal resolution than previous M~9
406 earthquakes, benefitting from on-land and offshore geophysical observations. The data that were
407 available in real time or near-real time are mostly from land stations and include geodetic
408 observations (high sampling rate GPS, tilt meter, strain meter) and seismic data (broad band
409 seismometer, strong motion, short period seismometer) and far-field geodetic and seismic data.
410 The on-land area (Honshu Island) is one of the most densely instrumented areas in the world but
411 located outside of the slip area. Nonetheless, the real time seismic data were valuable for rapid
412 estimation of seismic intensity and magnitude (for earthquake early warning) and tsunami
413 heights based on the seismic source model, although the station density is of limited advantage
414 for initial source characterization. The tsunami waveforms collected at coastal tide gauges are
415 also available for source parameter studies, but most of the gauges are clipped by the large
416 tsunami (Fig. 8). Two cabled pressure gauges off Sanriku [*Hino et al.*, 2001; *Maeda et al.*,
417 2011]) and GPS buoys [*Satake et al.*, 2013] were also available to obtain data of the sea surface
418 height (tsunami, Fig 9c).

419 The geophysical data acquired by permanently operating networks in the Japanese islands
420 also contributed to more detailed analysis. The seismic network allowed for the detection of local
421 triggered earthquakes [e.g., *Lengliné et al.*, 2012; *Miyazawa*, 2011; *Okada et al.*, 2015], and
422 changes in elastic earth structure [e.g., *Sawazaki et al.*, 2015; *Takagi and Okada*, 2012]. The
423 global broadband seismic network and arrays contributed to understand the source process and
424 offshore seismicity immediately after the earthquake [e.g., *Kiser and Ishii*, 2013; *Lay et al.*,
425 2011b]. Data from the dense GPS network revealed details of the heterogeneous co- and
426 postseismic surface deformation fields in the land area, which contributed to better
427 understanding of the rheological structure beneath the arc [*Meneses-Gutierrez and Sagiya*, 2016;
428 *Muto et al.*, 2016; *Ohzono et al.*, 2013].

429 The offshore geophysical measurement capabilities that were developed in recent
430 decades [e.g., *Bürgmann and Chadwell*, 2014] provided unprecedented data for this earthquake
431 soon after the earthquake. The horizontal movements of the seafloor around the main slip area
432 were measured by seven GPS-Acoustic (combined geodetic technique of GPS and acoustic
433 ranging) stations (Fig. 9a, [*Kido et al.*, 2011; *Sato et al.*, 2011a]). The campaign style repeat
434 observations collected 17-31 days after the Tohoku-oki earthquake revealed as much as 31 m
435 horizontal coseismic sea bottom displacement [*Kido et al.*, 2011; *Sato et al.*, 2011a]). The vertical
436 coseismic movement of the seafloor was also constrained at some of the stations by the GPS-
437 Acoustic system [*Kido et al.*, 2011] as well as by ten campaign-style seafloor pressure gauges
438 near the epicenter that had been deployed before the Tohoku-oki earthquake ([*Iinuma et al.*,
439 2016; *Y Ito et al.*, 2011b]), Fig. 9c). The Deep-ocean Assessment and Reporting of Tsunamis
440 (DART) buoys east of the Japan trench and nearshore GPS-buoys (Fig. 9c) also recorded the
441 tsunami [e.g., *Satake et al.*, 2013].

442 The geophysical and geological surveys conducted (before and) after the earthquake on
443 land and the ocean bottom also provided new constraints on the coseismic rupture process.
444 Multi-beam active source surveys of the bathymetry were performed within 11 days to 5 years
445 after the Tohoku-oki earthquake and compared with data collected before the earthquake.
446 Similarly, a seismic reflection survey was completed 3-20 days after the earthquake to compare

447 with pre-earthquake data [Kodaira *et al.*, 2012]. These data provided unprecedented constraints
448 on the seafloor and frontal-wedge deformation near the trench (Fig. 10) [Fujiwara *et al.*, 2017;
449 Fujiwara *et al.*, 2011; Kodaira *et al.*, 2020; Kodaira *et al.*, 2012]. An ocean bottom survey of the
450 distribution of coseismic turbidites near the trench was also performed after the earthquake in
451 2012, 2013 and 2016 [Ikehara *et al.*, 2016; McHugh *et al.*, 2016; Molenaar *et al.*, 2019]. The
452 Japan Trench Fast Drilling project in 2012 (JFAST) retrieved fault material from 820 m below
453 the seafloor (location in Fig. 10) and recorded temperature time series for ~6 months around the
454 recently ruptured fault, suggesting a very low frictional strength [e.g., Brodsky *et al.*, 2020;
455 Chester *et al.*, 2013; Fulton *et al.*, 2013; Ujiie *et al.*, 2013]. Emergency observations of land
456 areas by the phased-array-type L-band SAR (PALSAR) on Japan's ALOS satellite allowed for
457 repeat image acquisitions 4 – 38 days after the Tohoku-oki earthquake, which provided
458 centimeter-level crustal deformation at 10s of meter spatial resolution [Kobayashi *et al.*, 2011; Y
459 Takada and Fukushima, 2013]. The large-scale coseismic and postseismic deformation of the
460 lithosphere also produced permanent changes in the Earth's gravity field that were captured by
461 the pair of Gravity Recovery And Climate Experiment (GRACE) satellites [Matsuo and Heki,
462 2011; Lei Wang *et al.*, 2012b]. Along the coast, post-earthquake field surveys revealed details of
463 the spatial distribution of tsunami run up, inundation heights and area (H Nakajima and Koarai
464 [2011]; Sugawara *et al.* [2013]; Tsunami Joint Survey Group [2011] Fig. 3c). The distribution of
465 sandy tsunami deposits and long-lasting geochemical tracers of seawater in flooded areas
466 provided new insights into the nature of tsunami inundation processes and allowed for more
467 accurate estimation of the tsunami inundation area of paleo-tsunamis from sand and geochemical
468 signatures [Chagué-Goff *et al.*, 2012; K Goto *et al.*, 2011].

469 In 2013, the deployment of a 5800 km-long cable hosting a network of seismometers and
470 pressure gauges at 150 observation points (the S-net) was initiated, and S-net now provides
471 seismic and geodetic data directly from above the megathrust fault [Aoi *et al.*, 2020; National
472 Research Institute for Earth Science and Disaster Resilience, 2019]. In 2012, the GPS-Acoustic
473 network measuring sea-bottom deformation was also enhanced to 26 stations, capturing the
474 enduring postseismic deformation transients of the Tohoku-oki earthquake along the trench (Fig.
475 9b) [Honsho *et al.*, 2019; Tomita *et al.*, 2017; S-i Watanabe *et al.*, 2014].
476

477 3.2 Coseismic slip and tsunami

478 Early knowledge of the magnitude and location of the Mw9.0 Tohoku-oki earthquake
479 was provided and disseminated in real time. An earthquake early warning was issued during this
480 earthquake on the basis of coastal seismic records and successfully delivered to people in the
481 Tohoku area [Hoshihara and Iwakiri, 2011]. The warning was issued before the S wave arrival and
482 more than 15 s earlier than the strongest ground motion (intensity 5-lower or greater on the JMA
483 scale) everywhere in the Tohoku area. The estimated magnitude, which was estimated from
484 maximum displacement amplitudes, was only 7.2 for the first warning to the public. 116.8 s after
485 the first trigger, the estimated magnitude was raised to 8.1 [Hoshihara and Iwakiri, 2011]. This is
486 lower than the estimates from long-period or geodetic data analysis (Mw 9.0) provided later but
487 comparable to the upper limit of the JMA displacement magnitude, which saturates for
488 earthquakes $M_w \geq 8$. The initial tsunami warning was issued around three minutes after the
489 earthquake based on the earthquake location and magnitude (M7.9) available at that time [Japan
490 Meteorological Agency, 2013]. This first warning was only for 6 m, 3 m and 3 m run-up for the
491 coast along the Miyagi, Fukushima and Iwate prefectures, respectively (Fig. 8), which was too

492 small compared with the observed heights of 10-20 m, 15-40 m and 8-15 m in the three
 493 prefectures (Fig. 4c) [*Tsunami Joint Survey Group*, 2011]. JMA upgraded its estimate of the
 494 maximum tsunami height twice based on observations on a GPS buoy 10 km offshore the coast
 495 and at coastal tide gauges. The final estimate issued 44 minutes after the earthquake was for a
 496 ≥ 10 m tsunami along a ≥ 200 km extent of the coast [*Japan Meteorological Agency*, 2013] (Fig.
 497 8). JMA determined a magnitude of Mw 8.8 around 50 minutes after the earthquake by
 498 analyzing global seismic data which was not used to update the local warning because of the late
 499 timing (Fig. 8).

500 The coseismic slip of the Mw 9.0 Tohoku-oki earthquake was estimated from seismic
 501 waveform data [*Ammon et al.*, 2011; *Hayes*, 2011; *Ide et al.*, 2011; *Satriano et al.*, 2014; *Shao et*
 502 *al.*, 2011; *Suzuki et al.*, 2011; *Uchide*, 2013; *Yagi and Fukahata*, 2011; *Kunikazu Yoshida et al.*,
 503 2011], geodetic surface deformation measurements [*Iinuma et al.*, 2012; *T Ito et al.*, 2011a;
 504 *Kyriakopoulos et al.*, 2013; *Ozawa et al.*, 2012; *Perfettini and Avouac*, 2014; *Pollitz et al.*, 2011;
 505 *Silverii et al.*, 2014; *Zhou et al.*, 2014], high-rate GPS time series [*Z Wang et al.*, 2016; *H. Yue*
 506 *and Lay*, 2011], tsunami wave observations [*Fujii et al.*, 2011; *Hossen et al.*, 2015; *Maeda et al.*,
 507 2011; *Saito et al.*, 2011; *Satake et al.*, 2013], InSAR, and various combinations of these data
 508 [*Bletery et al.*, 2014; *Gusman et al.*, 2012; *Hooper et al.*, 2013; *Koketsu et al.*, 2011; *Kubo and*
 509 *Kakehi*, 2013; *Lee et al.*, 2011; *Melgar and Bock*, 2015; *Minson et al.*, 2014; *Romano et al.*,
 510 2012; *Romano et al.*, 2014; *C Wang et al.*, 2012a; *R Wang et al.*, 2013; *Shengji Wei et al.*, 2012;
 511 *Yamazaki et al.*, 2018; *Yokota et al.*, 2011; *Han Yue and Lay*, 2013] (Fig. 11). Resolution tests of
 512 models constrained by individual datasets indicate that the strong motion data alone have limited
 513 resolution of slip updip from the hypocenter, while inversions of on-land static geodetic data can
 514 resolve slip out to the hypocenter but have no resolution of slip near the trench [*Shengji Wei et*
 515 *al.*, 2012]. On the other hand, Tsunami data and seafloor geodetic data are important to constrain
 516 shallow slip near the trench [*Koketsu et al.*, 2011; *Shengji Wei et al.*, 2012; *Yokota et al.*, 2011].
 517 The seafloor deformation data off Miyagi provide resolution in the shallow updip area off
 518 Miyagi (central part of the peak-slip area and near the hypocenter) but the northern and southern
 519 regions remain unresolved due to the lack of stations [*Iinuma et al.*, 2016] (Fig. 9a).

520 According to the large number of studies, the overall feature of the coseismic slip can be
 521 summarized as follows. The Tohoku-oki earthquake rupture initiated in the Miyagi-oki area to
 522 the south of the foreshock (Fig. 5a). During the initial 20 second, the rupture first propagated to
 523 the north and then changed direction to the west (downdip) after the rupture reached the
 524 foreshock slip area [*Uchide*, 2013]. The downdip part of the coseismic slip includes the slip area
 525 of recurrent M~7.5 Miyagi-oki earthquakes [*Iinuma et al.*, 2012; *Pollitz et al.*, 2011]. Then,
 526 substantial slip continued for more than 100 seconds in the updip shallow part of the plate
 527 boundary [*Z Wang et al.*, 2016]. Some studies suggest repeated rupture of some sections
 528 occurred in this shallow updip area [*Ide et al.*, 2011; *Lee et al.*, 2011; *Z Wang et al.*, 2016]. The
 529 large slip area reaching to the trench produced seafloor uplift that caused the tsunami and led to
 530 the high tsunami run up along the Sanriku Coast and wide inundation in the Sendai plane [*Mori*
 531 *et al.*, 2011; *H Nakajima and Koarai*, 2011]. A deep southern expansion of the rupture with
 532 modest slip occurred after 110s [*Han Yue and Lay*, 2013]. In this downdip area, high-frequency
 533 radiation was prominent [e.g., *Koketsu et al.*, 2011; *Kurahashi and Irikura*, 2011; *Yokota et al.*,
 534 2011; *Kunikazu Yoshida et al.*, 2011] (Fig. 12d). The existence of this southern extension of the
 535 rupture is consistent with the zone of reduced interplate seismicity extending from the northern
 536 large-slip area, as well as with the surrounding enhanced aftershock activity, indicative of stress
 537 drop in the coseismic slip area and stress increase in the surrounding areas (Fig. 2, Fig. 12a-c,

538 [Kato and Igarashi, 2012; W Nakamura et al., 2016]. This southern extension corresponds to the
 539 location of many previous M~7 earthquakes, including the 1938 sequence (Fig. 5).

540 The duration of the rupture was estimated to be 171 s from high-frequency energy
 541 radiation [Hara, 2011] and 150 s from the joint inversion of seismic and geodetic data [Minson
 542 et al., 2014]. The mean stress drop is 2.3 ± 1.3 MPa, based on the area within the 5 m slip
 543 contour from 40 published slip models and assuming a uniform rigidity of 40 GPa. However,
 544 locally the stress drop well exceeds 20 MPa for the majority of models [Brown et al., 2015].
 545 Some models using tsunami data or joint inversion suggest a northern extension of slip near the
 546 trench to $\sim 40.0^\circ\text{N}$ [e.g., Hossen et al., 2015; Satake et al., 2013; Yokota et al., 2011]. However,
 547 slip models constrained by other data and aftershocks [W Nakamura et al., 2016], differential
 548 seafloor bathymetry [Kodaira et al., 2020], and near-trench turbidities [Ikehara et al., 2016]
 549 (Fig. 10) suggest that the main coseismic slip is limited to the south of 39.2°N . The higher-
 550 frequency tsunami waves [Tappin et al., 2014] and seismic profiles of shallow structure [Y
 551 Nakamura et al., 2020] showed that gravitational slope failures of the trench inner wall can also
 552 explain the proposed tsunami source around $39\text{-}40^\circ\text{N}$.

553

554 3.3 Implications of the coseismic slip

555 An especially important feature of the coseismic slip, we think, is that the main slip
 556 occurred in the area where a large slip deficit had been estimated from the GPS data before the
 557 earthquake [e.g., C Hashimoto et al., 2012; Loveless and Meade, 2010; Suwa et al., 2006]. The
 558 repeating earthquake data had also indicated a large slip deficit in the coseismic slip area before
 559 the earthquake [Uchida and Matsuzawa, 2011] and the trend of the compressional axis in the
 560 upper plate before the Tohoku-Oki earthquake also supported strain accumulation in the near-
 561 trench large-slip area [Hasegawa et al., 2012]. Therefore, to first order the Tohoku-oki
 562 earthquake compensated the slip deficit that had accumulated in the wide area off Tohoku. There
 563 were arguments that other processes, such as slow slip events or tsunami earthquakes, could
 564 make up the slip deficit inferred from the discrepancy between geodetic and seismic coupling
 565 discussed in Section 2.1 [Kanamori et al., 2006]; however, such events did not occur. This
 566 suggests that it is important to understand the variability of slip mode of the fault surface.
 567 Obviously, the instrumental record of ~ 100 years was insufficiently long to evaluate seismic
 568 coupling that is dominated by the largest earthquake. Scholz and Campos [2012] re-estimated the
 569 seismic coupling ratio to be 0.59 by considering M~9 Tohoku-oki earthquakes and assuming the
 570 a recurrence interval of 1000 years, based on the tsunami deposit observation of the 869 Jyogan
 571 earthquake. Despite the great uncertainties involved in either estimate, this updated value is
 572 consistent with the coupling from geodetic data (0.54 - 0.65).

573 The large near-trench slip was the second important feature of the Tohoku-oki earthquake
 574 that heightened the devastating tsunami and casualties. Although the variability of the slip
 575 models is large especially in the near-trench areas (Fig. 13), Sun et al. [2017] confirmed that \geq
 576 62 m slip reached to the trench by modeling the high-resolution bathymetry-change data of
 577 Fujiwara et al. [2011] (track MY101 and MY102 of Fig. 10) observed above the large-slip area.
 578 Closest to the trench, the change in shallow structure from seismic reflection data obtained
 579 before and after the earthquake, differential bathymetry, and sediment core data suggest that the
 580 slip reached to the seafloor at the trench axis [Kodaira et al., 2012; Strasser et al., 2013]. The
 581 near-trench slip in coseismic slip models occurred along a $\sim 120\text{-km}$ -long section of the trench
 582 off Miyagi, which is consistent with the distribution of turbidite deposits in the trench [Ikehara et

583 *al.*, 2016; *Ikehara et al.*, 2018] and the along-trench extent of the bathymetry change [*Kodaira et*
584 *al.*, 2020] (Fig. 10). Due to the unconsolidated nature of fault-zone material in the shallow
585 megathrust, many studies assumed the area closest to the trench represents an aseismic slip zone
586 [e.g., *Bilek and Lay*, 2002; *Hyndman and Wang*, 1993; *Oleskevich et al.*, 1999]. Therefore, the
587 very large, near-trench seismic slip and resulting tsunami were a surprise to many, even though
588 the area was considered by some to be capable of generating tsunami earthquakes or sometimes
589 participating in larger ruptures [e.g., *Kanamori*, 1972; *Lay et al.*, 2012; *Tanioka and Satake*,
590 1996]. Dynamic weakening mechanisms [e.g., *Noda and Lapusta*, 2013; *Shengji Wei et al.*,
591 2012] and dynamic overshoot [e.g., *Fukuyama and Hok*, 2015; *Ide et al.*, 2011; *Kozdon and*
592 *Dunham*, 2013] may help explain the large slip all the way to the trench. Various models, for
593 example considering thermal pressurization [*Shibazaki et al.*, 2019], and rate- and state-
594 dependent friction with two state variables that lead to strong velocity weakening properties at
595 high slip velocities [*Shibazaki et al.*, 2011], have been proposed to explain such large shallow
596 slip. In addition, laboratory experiments on fault-zone material retrieved from the shallow
597 Tohoku plate-boundary by drilling suggest very low friction due to the presence of smectite
598 [*Ujiie et al.*, 2013]. The laboratory-derived properties of fault materials in combination with
599 dynamic rupture simulations of fault weakening and rupture propagation contribute to a more
600 realistic estimation of the near-trench slip mode [*Hirono et al.*, 2016]. The determination of near-
601 trench coupling and slip is now possible thanks to the recent addition of more GPS-Acoustic
602 stations [*Honsho et al.*, 2019]. As the shallow coseismic slip is directly linked to the height of the
603 resulting tsunami, it is generally important to accurately quantify the near-trench slip deficit in
604 all subduction zones.

605 In addition to the near-fault material, the large-scale structure was also examined to infer
606 the structure related to the Tohoku-oki earthquake. *Zhao et al.* [2011] used seismic tomography
607 and found that a high-velocity body exists above the plate boundary in the Miyagi-oki region
608 where the peak coseismic slip occurred. *K Wang and Bilek* [2014] suggest that relatively smooth
609 subducting seafloor is responsible for large megathrust earthquakes, including the 2011 Tohoku-
610 oki earthquake, from the global review of seismic and geodetic studies. *Bassett et al.* [2016]
611 found that the slip area of the Tohoku-oki earthquake is located to the north of a geologic
612 boundary revealed by residual topography and gravity anomalies (Fig. 2b), suggesting some
613 control of coseismic slip by the upper plate. *Kubo et al.* [2013] also found that the coseismic slip
614 and largest aftershock at the southern end of the coseismic rupture stopped to the north of the
615 area where the upper plate is the Philippine Sea plate (not the North America or Okhotsk plate
616 where the main slip occurred) (Fig. 2b). *Satriano et al.* [2014] interpreted the broadband
617 characteristics of the slip to along-dip differences of material properties and structure, including
618 the material of the overlying plate (crust/mantle), thermal structure and plate geometry. *Hua et*
619 *al.* [2020] used offshore seismometers (S-net) to find weak material above the shallow large slip
620 area from seismic tomography. *Lay et al.* [2012] related often-observed along-dip changes in
621 rupture characteristics of megathrust ruptures to first-order changes in material properties and
622 structure, including the Tohoku-oki earthquake (Fig. 12d). The material properties of the
623 overriding plate, morphology of the plate interface and fault zone and along-dip segmentation
624 may all contribute to the characteristics and size of the coseismic rupture. These observations
625 support an important influence of structural heterogeneities on the megathrust rupture mode.

626

627 3.4 Postseismic deformation and seismicity

628 Substantial postseismic deformation and seismicity were observed starting immediately
629 following the Tohoku-oki earthquake, as captured by land and ocean bottom stations. The land
630 GPS stations showed seaward movement (Fig. 9b) that can be explained by aseismic afterslip
631 downdip of the coseismic slip area and near the coastline (Fig. 14) [e.g., *Inuma et al.*, 2016;
632 *Yamagiwa et al.*, 2015] as well as viscoelastic relaxation in the mantle wedge above the
633 subducting slab [e.g., *Hu et al.*, 2016; *Sun et al.*, 2014]. The offshore geodetic data [*Honsho et al.*, 2019; *Tomita et al.*, 2017] again provided important constraints on the spatial distribution of
634 offshore afterslip and allowed for the characterization of the viscoelastic response of the mantle
635 above and below the Pacific plate. The offshore GPS-Acoustic stations above the large coseismic
636 slip area showed landward movement (Fig. 9b) and subsidence, which can only be explained by
637 relaxation of stresses induced by the thrust earthquake in the mantle below the downgoing plate
638 [*Hu et al.*, 2016; *Sun et al.*, 2014]. On the other hand, the GPS-Acoustic stations to the north and
639 south of the coseismic slip zone exhibit postseismic seaward motions caused by the rapid
640 afterslip on the adjacent, poorly coupled sections of the plate boundary [*Honsho et al.*, 2019;
641 *Tomita et al.*, 2017].

642 The afterslip of the Tohoku-oki earthquake was estimated by *Diao et al.* [2014]; *Hu et al.*
643 [2016]; *Inuma et al.* [2016]; *Johnson et al.* [2012]; *Ozawa et al.* [2012]; *Ozawa et al.* [2011];
644 *Shirzaei et al.* [2014]; *Silverii et al.* [2014]. In most studies, the contribution of viscoelastic
645 relaxation was first removed to estimate postseismic slip on the plate boundary [e.g., *Diao et al.*,
646 2014; *Inuma et al.*, 2016]. The postseismic slip area showed a complementary distribution with
647 the coseismic slip (Fig. 14a, c) [*Inuma et al.*, 2016; *Ozawa et al.*, 2012]. The distribution of
648 accelerated repeating earthquakes on the plate interface also confirmed near-trench afterslip to
649 the north of the coseismic rupture in addition to downdip and the shallow portion of the
650 megathrust to the south (Fig. 14b) [*Uchida and Matsuzawa*, 2013]. The repeating earthquake
651 data also indicated delayed acceleration in the afterslip at larger distances from the coseismic slip
652 area, suggesting spatio-temporal propagation of the afterslip. The repeating earthquake data was
653 also used with GNSS data to better constrain the interplate postseismic slip [*Shirzaei et al.*, 2014]
654 and to improve the discrimination of interplate afterslip and viscoelastic response of the earth
655 [*Hu et al.*, 2016].

656 Most of the interplate aftershocks occurred near the edge of the coseismic slip and can be
657 considered as a proxy of afterslip. Two large, M7.4 and M7.6 aftershocks occurred just beyond
658 the northern and southern edges of the coseismic slip area, on the day of the Tohoku-oki
659 earthquake [*Kubo and Nishikawa*, 2020; *W Nakamura et al.*, 2016] (Fig. 2). The slip areas of the
660 2011 Tohoku-oki earthquake and these immediate aftershocks don't appear to overlap with the
661 inferred areas of postseismic repeating earthquakes, earthquake swarms, tremors, and very low-
662 frequency earthquakes on the plate interface (Fig. 2). Conversely, these seismic phenomena were
663 strongly enhanced in the area surrounding the coseismic slip, which suggests the occurrence of
664 aseismic slip there. The spatial distribution of tremors, very low-frequency earthquakes and
665 repeating earthquakes in the subduction thrust before the Tohoku-oki earthquake are largely the
666 same as in the postseismic period but they may have been more active near the large slip area
667 [*Baba et al.*, 2020; *Katakami et al.*, 2018; *Takanori Matsuzawa et al.*, 2015; *Takahashi et al.*,
668 2020; *Uchida and Matsuzawa*, 2013]. The northern M 7.4 aftershock rupture area overlaps with
669 the slip zones of previous M~7 earthquakes (Fig. 2) [*Kubo and Nishikawa*, 2020; *Nishikawa et al.*,
670 2019]. In the downdip plate interface and along the updip edge of the rupture, no large
671

672 interplate aftershocks occurred and the near-trench plate-boundary was especially silent after the
673 Tohoku-oki earthquake [Asano *et al.*, 2011].

674 The aftershock focal mechanisms away from the plate interface were also consistent with
675 the stress changes due to the coseismic slip of the Tohoku-oki earthquake and the postseismic
676 slip [Diao *et al.*, 2014; W Nakamura *et al.*, 2016]. Seismicity on the updip side of the coseismic
677 rupture was characterized by normal faulting earthquakes in the subducting plate (outer-rise and
678 near-trench area) while the downdip side of the coseismic slip area was characterized by reverse-
679 faulting earthquakes in the subducting plate and normal-faulting earthquakes are prominent in
680 the upper plate [W Nakamura *et al.*, 2016]. On the downdip side, a significant rate increase of
681 intermediate-depth earthquakes in the upper plane of the double seismic zone was observed
682 [Delbridge *et al.*, 2017]. The upper plane of the double seismic zone is in downdip compression
683 [Hasegawa *et al.*, 1978; Kita *et al.*, 2010b], and the increase of the stress due to coseismic and
684 postseismic slip of the seismogenic plate interface apparently accelerated the deep intraplate
685 seismicity [Delbridge *et al.*, 2017]. A relatively large reverse faulting earthquake (M7.1 on April
686 7, 2011), consistent with the coseismic stress change, occurred in the subducting slab and near
687 the downdip end of the coseismic rupture. Based on a low-velocity feature observed by seismic
688 tomography and the dip of the fault plane of this event, J Nakajima *et al.* [2011] suggested
689 reactivation of a fault that was produced by the normal faulting in the outer-rise area. On the
690 updip side, Kubota *et al.* [2019] examined an earthquake doublet (Mw 7.2 and 7.1 on December
691 7, 2012) in the subducting plate consisting of shallow normal- and deep reverse-faulting
692 subevents near the trench, and pointed to the role of intraplate stress state changes due to the
693 Tohoku-oki earthquake. In the outer-rise region of the incoming plate, many normal-faulting
694 events, including a Mw7.7 event, were triggered. Obana *et al.* [2012] argued that the increase in
695 the depth extent of normal-faulting events in the outer-rise area can be explained by the
696 increased tensile bending stresses in the Pacific plate after the earthquake. Large interplate thrust
697 events and outer-rise normal-faulting earthquakes produce slip-encouraging stress changes on
698 each other, and paired interplate and outer-rise earthquakes are quite commonly observed in
699 global subduction zones [Lay *et al.*, 2011a; Lay *et al.*, 2010].

700 Seismicity rates also significantly changed in the inland seismogenic upper crust (Fig.
701 16a) [Okada *et al.*, 2011; Uchida *et al.*, 2018]. The seismicity sometimes started few days to few
702 weeks after the Tohoku-oki earthquake and many areas showed swarm activity and upward
703 migrations [e.g., Okada *et al.*, 2015; Okada *et al.*, 2011; Keisuke Yoshida and Hasegawa, 2018;
704 Keisuke Yoshida *et al.*, 2019](Fig. 16 c, d). Areas that were dominated by active thrust faulting
705 prior to the Tohoku-oki earthquake showed reduced postseismic seismicity rates. Dynamic
706 triggering of seismicity was also evident especially in the western part of Japan, consistent with
707 triggering by surface waves out to a distance of nearly 1,350 km [Kato *et al.*, 2013; Miyazawa,
708 2011]. Small events and tremors triggered by the passage of seismic waves from the Tohoku-oki
709 earthquake were also recognized globally [Chao *et al.*, 2013; Gonzalez-Huizar *et al.*, 2012].

710

711 3.5 Implications of the postseismic deformation and triggered seismicity

712 One of the most important features of the postseismic deformation revealed by the
713 Tohoku-oki earthquake is the immediate and far-reaching viscoelastic response of the earth. This
714 deformation represents the relaxation of coseismic stress changes by the flow of mantle and
715 crustal material below the brittle-ductile transition zone. Since the postseismic deformation is
716 caused by a combination of afterslip on the plate boundary, viscoelastic relaxation and

717 poroelastic rebound in the surrounding media, it is important to distinguish the contributions
718 from these processes. *Sun and Wang* [2015] suggest that immediately after large megathrust
719 earthquakes ($M_w > 8.0$), viscoelastic deformation should always lead to opposing motion of
720 inland and trench areas. Neglecting viscoelastic relaxation results in overestimation of
721 postseismic slip down-dip of the coseismic rupture and an underestimate of the afterslip at
722 shallower depths [*Sun et al.*, 2014], because the contribution of the viscoelastic relaxation is
723 trenchward in the land area and landward in the near-trench area (Fig. 15 a, b). Consideration of
724 contributions of viscoelastic relaxation in the mantle above and below the downgoing slab (Fig.
725 15 a, b) together with independent constraints on afterslip from repeating earthquakes (Fig. 14 b
726 & 15 c) improve the characterization of the different relaxation mechanisms following large
727 subduction earthquake [*Hu et al.*, 2016].

728 The post-mainshock seismicity also provided important insights into the ambient state of
729 stress and the frictional strength of the megathrust and surrounding faults. Prior to 2011, the
730 stress field of the Tohoku region reflected east-west compression and earthquakes with reverse
731 mechanisms dominated in the area. The coseismic Coulomb stress changes on the reverse faults
732 were negative (Fig. 17), including on many known active faults in the area [*Toda et al.*, 2011a].
733 A large number of normal-faulting aftershocks suggests that the stress change during the
734 mainshock was large enough, relative to the pre-earthquake ambient stress levels, to reverse the
735 dominant style of faulting close to the large slip area [*Chiba et al.*, 2013; *Hardebeck*, 2012;
736 *Hardebeck and Okada*, 2018; *Hasegawa et al.*, 2012; *Hasegawa et al.*, 2011]. A low background
737 differential stress, on the order of the earthquake stress drop, is also supported by the analysis of
738 ocean bottom borehole breakouts at the JFAST site (Fig. 10b) [*Brodsky et al.*, 2017; *Lin et al.*,
739 2013]. As the fault materials and temperature data collected at JFAST [e.g., *Brodsky et al.*, 2020;
740 *Chester et al.*, 2013; *Fulton et al.*, 2013; *Ujiie et al.*, 2013], the low regional heat flow [*Gao and*
741 *Wang*, 2014] and a forearc force-balance model [*K Wang et al.*, 2019] all suggest a weak fault,
742 the Tohoku-oki earthquake can be characterized as the rupture of a weak fault in a low-stress
743 environment [*Hardebeck*, 2015; *K Wang et al.*, 2019].

744 In the inland area, earthquakes with a variety of focal mechanisms were activated after
745 the earthquake (Fig. 16a). They can potentially be explained by small faults with highly variable
746 fault orientations [*Toda et al.*, 2011b], a heterogeneous local deviatoric stress field [*Keisuke*
747 *Yoshida et al.*, 2019] and/or the upward movement of fluids into the fault zone that can reduce
748 the effective normal stress on the faults (Fig. 16c) [*Keisuke Yoshida and Hasegawa*, 2018;
749 *Keisuke Yoshida et al.*, 2019]. The role of fluid migration as an important mechanism of
750 earthquake triggering is supported by the observation that many earthquake clusters only
751 initiated after a few days to few weeks after the Tohoku-oki earthquake (Fig. 16d) [*Keisuke*
752 *Yoshida et al.*, 2019]. Substantial spatial heterogeneity of stress orientations in the inland area
753 before the 2011 Tohoku-oki earthquake was identified from focal-mechanism data and the
754 anomalous areas corresponded to areas of increased seismic activity after the Tohoku-oki
755 mainshock [*Imanishi et al.*, 2012; *Keisuke Yoshida et al.*, 2019]. One of the areas with
756 anomalous stress orientations is located in region D of Fig. 16a. In this area, not only strong
757 seismicity occurred but also a repeating earthquake pair of $\sim M6$ that recurred within an
758 anomalously short interval (5 years), suggesting that the postseismic deformation of the Tohoku-
759 oki earthquake rapidly reloaded the shallow inland fault segment [*Fukushima et al.*, 2018].

760 Both postseismic deformation and aftershocks provide indirect evidence of the extent and
761 magnitude of coseismic slip. There have been efforts to improve constraints on the spatial
762 distribution of the coseismic slip by incorporating the postseismic seafloor geodetic (GPS-

763 Acoustic) time series and the inferred viscoelastic relaxation [*Tomita et al.*, 2020; *Yamagiwa et*
764 *al.*, 2015]. The concentration of aftershocks near the edges of the coseismic slip area helps
765 delineate details of the extent of coseismic rupture (Fig. 12 a-c). In turn, the interplate seismicity
766 was diminished in some areas due to the stress drop on the rupture and stress shadow effects (Fig.
767 12 a-c) [*Asano et al.*, 2011; *Kato and Igarashi*, 2012; *W Nakamura et al.*, 2016]. Thus,
768 postseismic observations can also be valuable to constrain the coseismic slip, independent of the
769 data obtained coseismically.

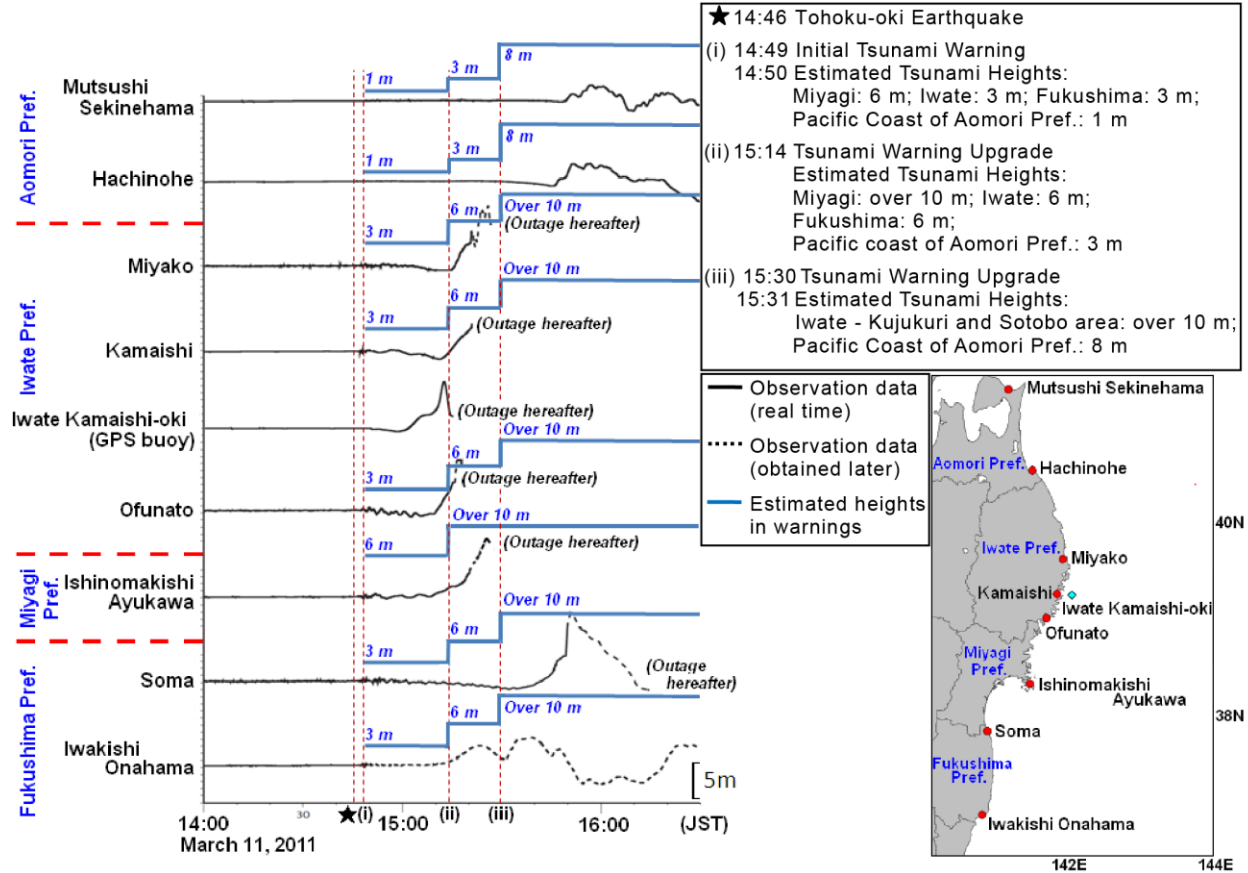
770

771

772

773

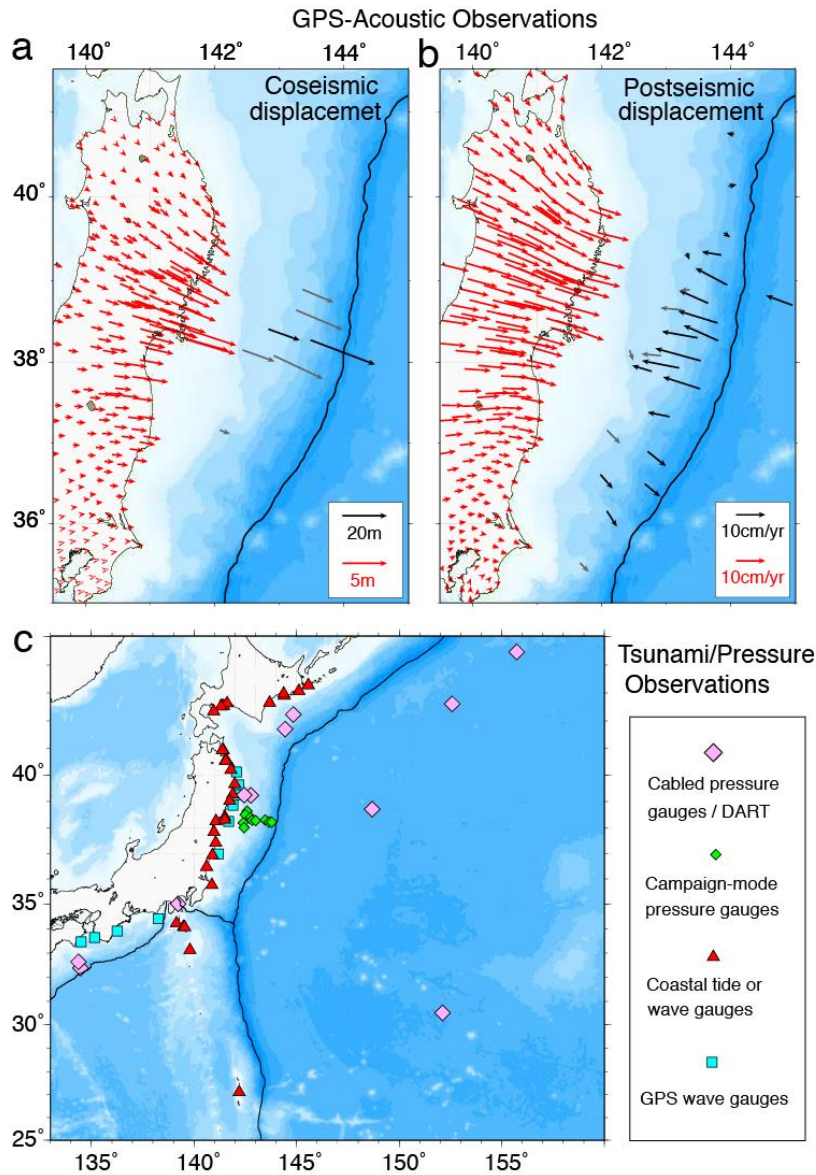
774
775



776
777

778 **Figure 8** Tsunami observations and issued warnings [after *Japan Meteorological Agency*,
779 2013]. The black lines show the observed data and blue lines show estimated tsunami heights in
780 the initial warning and two updates. The Iwate Kamaishi-oki GPS buoy 10 km offshore (green
781 diamond) captured the earliest direct evidence of the large tsunami amplitude. A magnitude of
782 Mw 8.8 was determined at around 15:40.

783



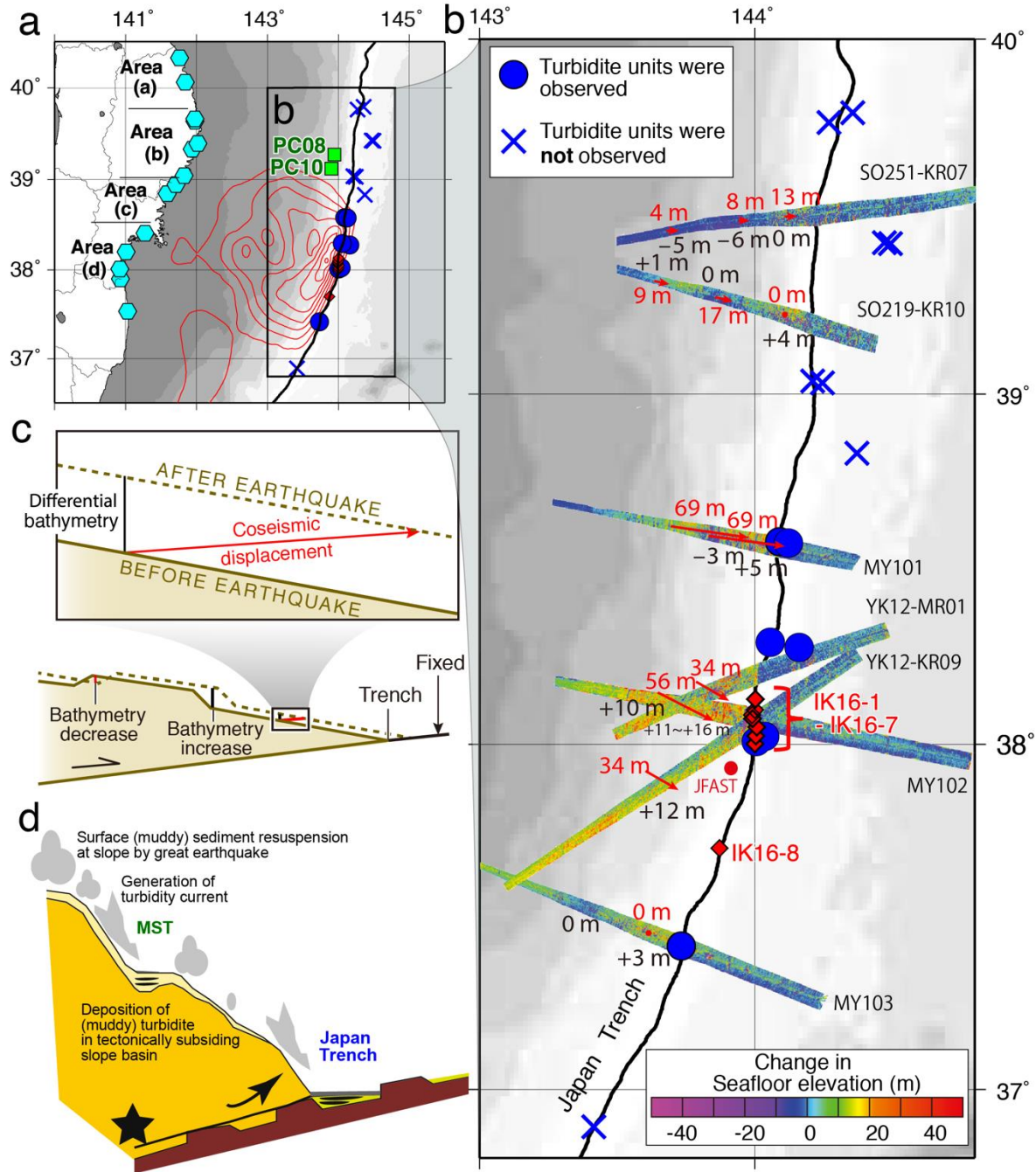
784

785

Figure 9 Offshore observations of the coseismic and postseismic phenomena of the Tohoku-oki earthquake. (a) Coseismic displacements from GPS-Acoustic observations (gray arrows from *Sato et al.* [2011a] and black arrows from *Kido et al.* [2011]) and land GPS data after *Inuma et al.* [2012]. (b) The average postseismic displacement rates determined from 2012 to 2016 (black, from *Honsho et al.* [2019], gray, from *Honsho et al.* [2019] based on *Yokota et al.* [2018]). The on-land velocities during the same period are from *Tomita et al.* [2020]. Note the reversal of postseismic displacement directions above the focal area. (c) Offshore tsunami and pressure observations by campaign-mode pressure sensors (green diamonds), cabled pressure sensors and DART systems (pink diamonds), GPS buoys (cyan squares), and coastal tide or wave gauges (red triangles). The locations of the campaign-mode pressure gauges are from *Y Ito et al.* [2013] and others are from *Satake et al.* [2013].

797

798

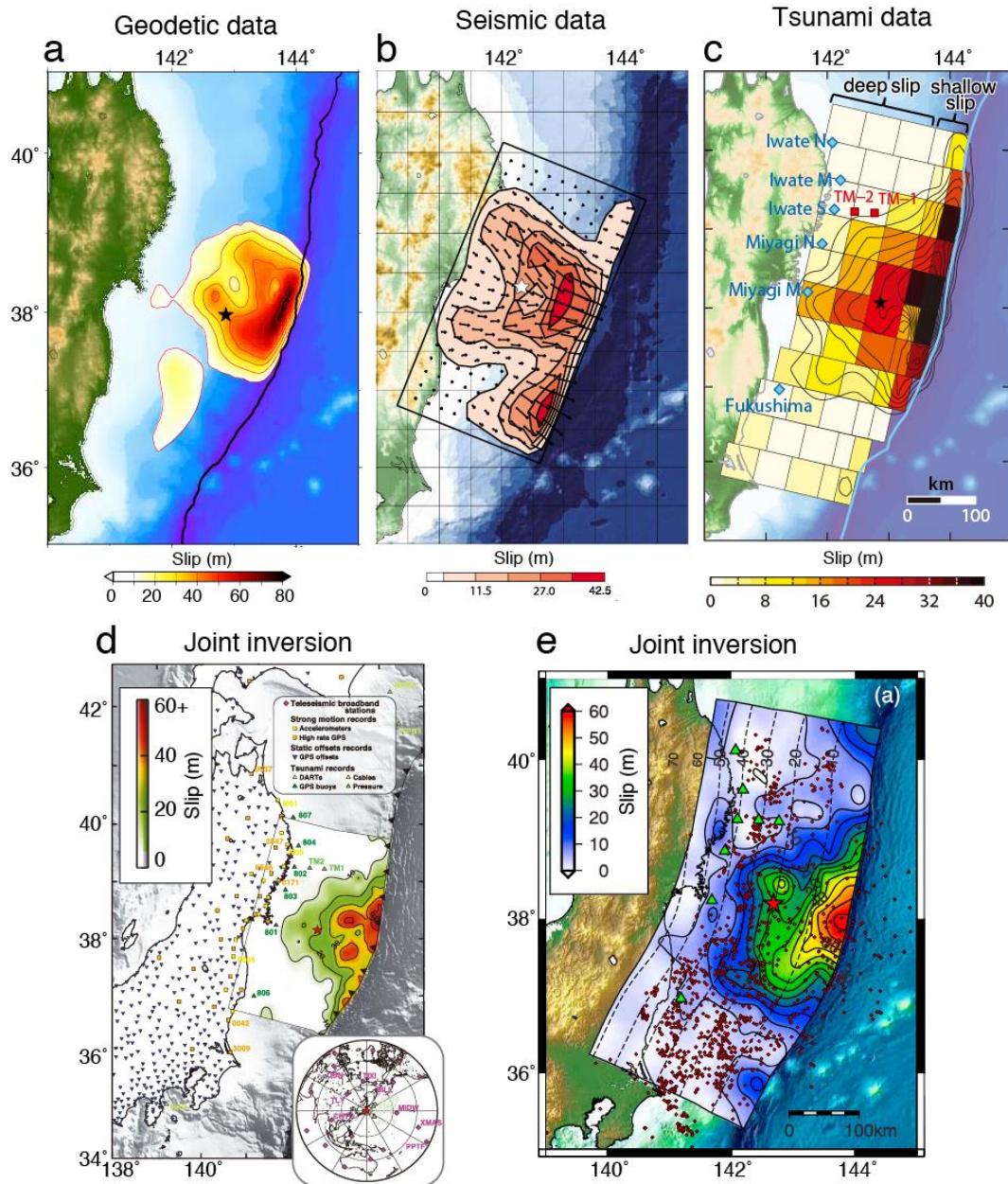


799
 800

801 **Figure 10** Coseismic change in seafloor elevation and distribution of turbidite deposits from the
 802 Tohoku-oki earthquake along the Japan trench axis. (a) Onshore sites of tsunami deposits (cyan
 803 hexagons) and offshore survey locations of turbidite units on the mid-slope terrace (green
 804 squares [K Usami *et al.*, 2018]) and along the Japan trench (blue crosses and circles [Ikehara
 805 *et al.*, 2018]). The circles show the surveyed locations with 2011 turbidites and crosses show
 806 locations without 2011 turbidites, showing that no turbidites were found to the north and south of
 807 the main coseismic slip area of the Tohoku-oki earthquake (red contour lines, [Inuma *et al.*,
 808 2012]). (b) Coseismic change in seafloor elevation (color contours) and inferred horizontal (red
 809 arrows and labels) and vertical (black labels) movements based on repeated bathymetry

810 observations (after *Kodaira et al.* [2020]). The data are from *Fujiwara et al.* [2011], *Kodaira et*
811 *al.* [2012], *Fujiwara et al.* [2017] and *Kodaira et al.* [2020]. Please note large displacements in
812 the middle four traces (MY101, YK12-MR01, YK12-KR09 and MY102) and negligible
813 displacements in the northern two (S0251-KR07) and southern (MY103) traces, considering
814 measurement uncertainties of ~20m in the horizontal and several meters in the vertical
815 component [*Kodaira et al.*, 2020]. Survey site locations shown by blue circles and crosses are the
816 same as those in (a), and the red diamonds show the sites of turbidite observations by *Ikehara et*
817 *al.* [2016]. (c) Schematic illustration of the relationship between differential bathymetry
818 (coseismic seafloor elevation change) and horizontal displacements (after *Sun et al.* [2017] and
819 *Kodaira et al.* [2020]). Note that both bathymetry increase and decrease may occur due to the
820 lateral offset of raised seafloor features. (d) Schematic showing the mechanism of deposition of
821 turbidites at the mid-slope terrace (MST) and in the Japan trench triggered by the strong ground
822 motion of megathrust earthquakes [after *Ikehara et al.*, 2020]. The strong motion due to the
823 seismic slip below the seaward slope of the Japan trench causes the resuspension of sediment,
824 turbidity current transport and deposition at the MST and Japan trench.
825

826



827

828

829

830

831

832

833

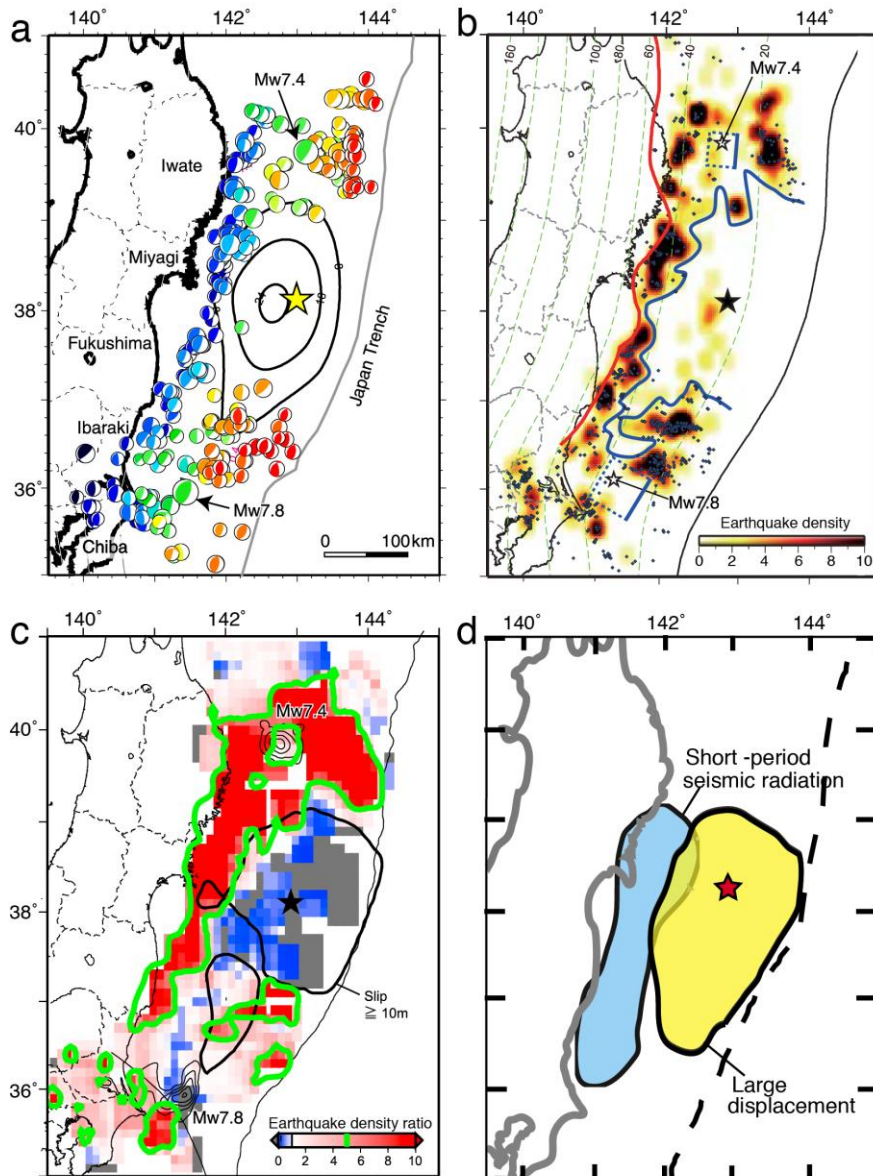
834

835

836

837

Figure 11 Examples of coseismic slip models. (a) Slip model from geodetic displacements [Iinuma *et al.*, 2012]. (b) Slip model from seismic waveforms Lay *et al.* [2011a]. (c) Slip model from and tsunami data [Satake *et al.*, 2013]. (d) Slip model from the joint inversion of teleseismic broadband data, strong motion records, static GPS displacements, and tsunami records [Bletery *et al.*, 2014]. The locations of sensors are shown in the main map and right bottom inset and the symbols are shown in right top inset. (e) Slip model from the joint inversion of high rate (>1 Hz) GPS time series, strong motion, cabled sea floor pressure sensors, and GPS buoys [Melgar and Bock, 2015]. The locations of cabled sea floor pressure, and GPS buoys are shown by green triangles.

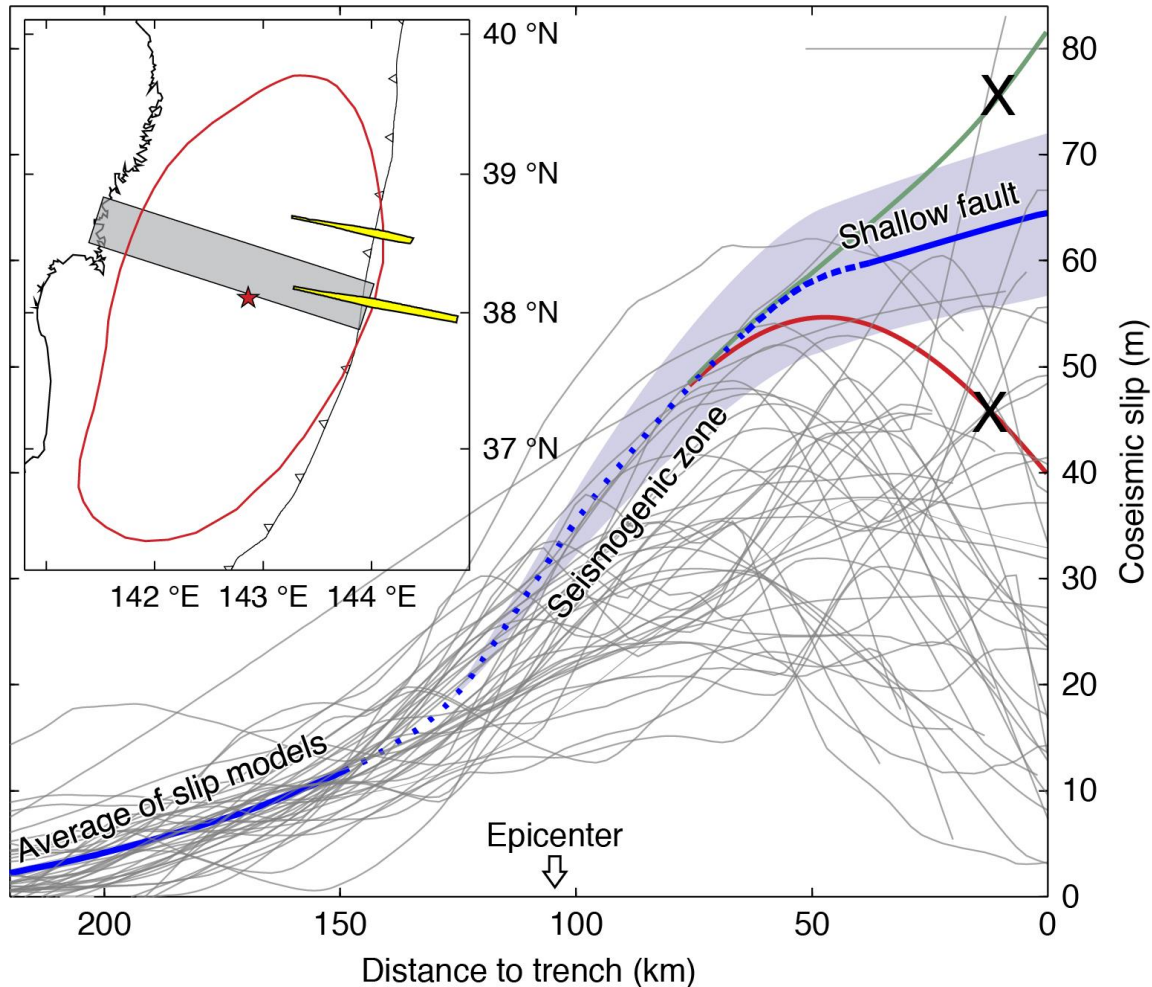


838
839

840 **Figure 12** Interplate seismicity after the Tohoku-oki earthquake in relation to coseismic slip area
 841 and the distribution of coseismic slip. (a) The distribution of interplate type aftershocks (beach
 842 balls showing shallow thrust focal mechanisms from CMT inversion) [after *Asano et al.*, 2011].
 843 The black contours show the coseismic slip model of *Geospatial Information Authority of Japan*
 844 [2011]. (b) Density of the interplate type aftershocks from one year of F-net focal mechanisms
 845 (color contours) and the distribution of postseismic repeating earthquakes (blue dots) [*Kato and*
 846 *Igarashi*, 2012]. The blue curve outlines the apparent extent of coseismic slip indicated by the
 847 seismicity data. The red line shows the downdip limit of interplate earthquakes [*Igarashi et al.*,
 848 2001]. (c) Ratio of rates of interplate earthquakes after the Tohoku-oki earthquake to rates before
 849 the mainshock based on a template-matching search for interplate events [after *W Nakamura et*
 850 *al.*, 2016]. The black lines show the coseismic slip model of [*Iinuma et al.*, 2012] and the green
 851 lines represent the factor-of-five contour of the seismicity ratio. Note the low interplate
 852 seismicity in the slip areas of the mainshock and the two largest aftershocks labeled Mw7.4 and

853 7.8. (d) Seismic radiation along the fault during the Tohoku-oki earthquake [after *Lay et al.*,
 854 2012]. Yellow patch shows the region of large coseismic fault displacements and the blue area
 855 indicates the region of coherent short-period (~ 1 s) teleseismic radiation. The stars in (a)-(d)
 856 show the mainshock epicenter.

857
 858

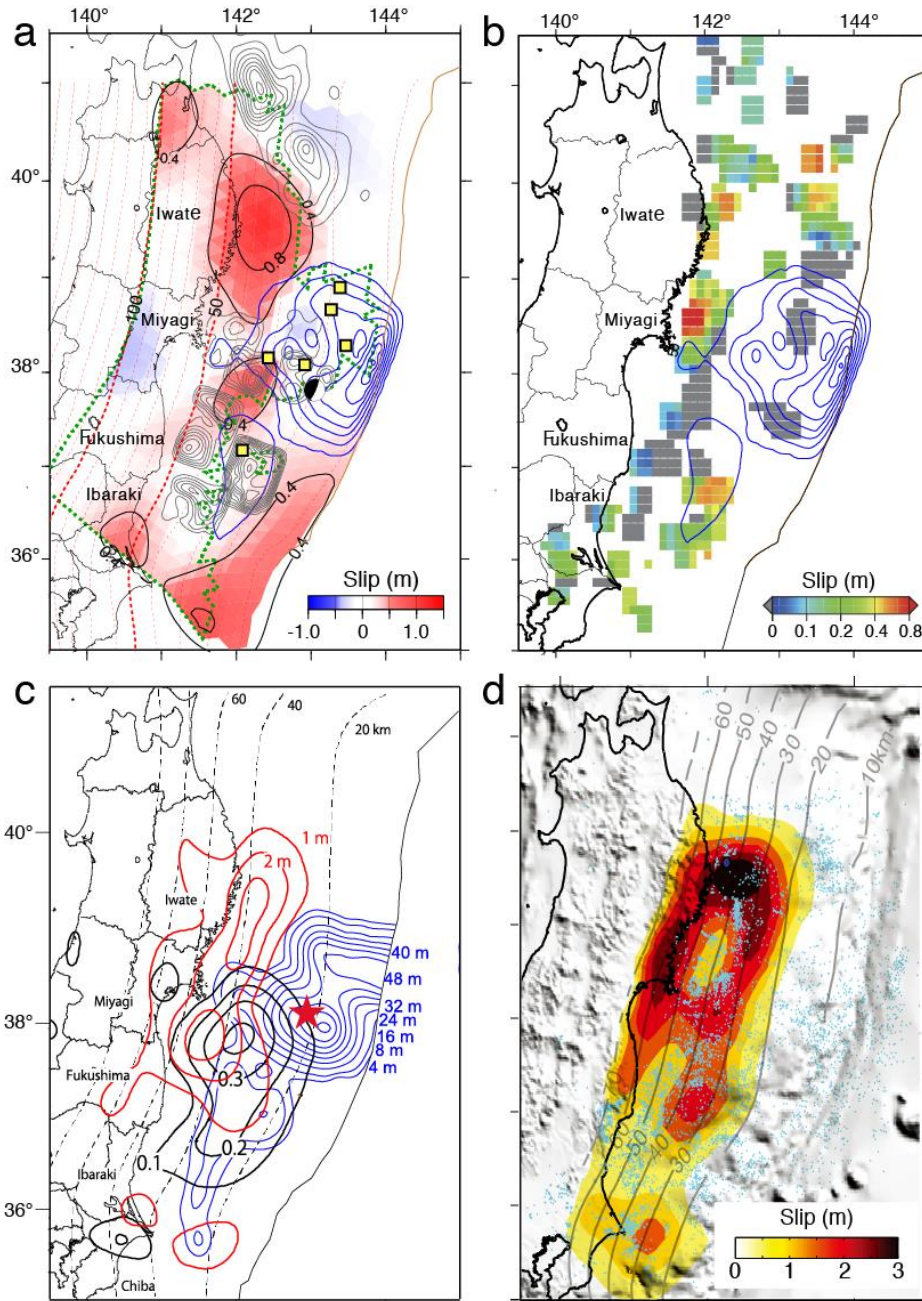


859
 860

861 **Figure 13** Compilation of 45 published coseismic slip models (gray lines) showing the slip
 862 distribution along the gray band in the inset and near-trench slip model (blue line with blue-
 863 shaded error ranges estimated from the models with root mean square deviations < 8.55 m) based
 864 on the modeling of near-trench bathymetry differences at the tracks shown in yellow in the inset
 865 [after *Sun et al.*, 2017]. The blue line at distances > 150 km from the trench represents the
 866 average of the published slip models and the dotted line represents a poorly constrained
 867 interpolation of slip at intermediate depths. In the inset map, the red outline shows the 2-m
 868 contour of coseismic slip [*K Wang and Bilek*, 2014] and the red star is the mainshock epicenter.
 869 The slip scenarios illustrated by the green and red lines are ruled out by the near-trench
 870 bathymetry difference data.

871

872



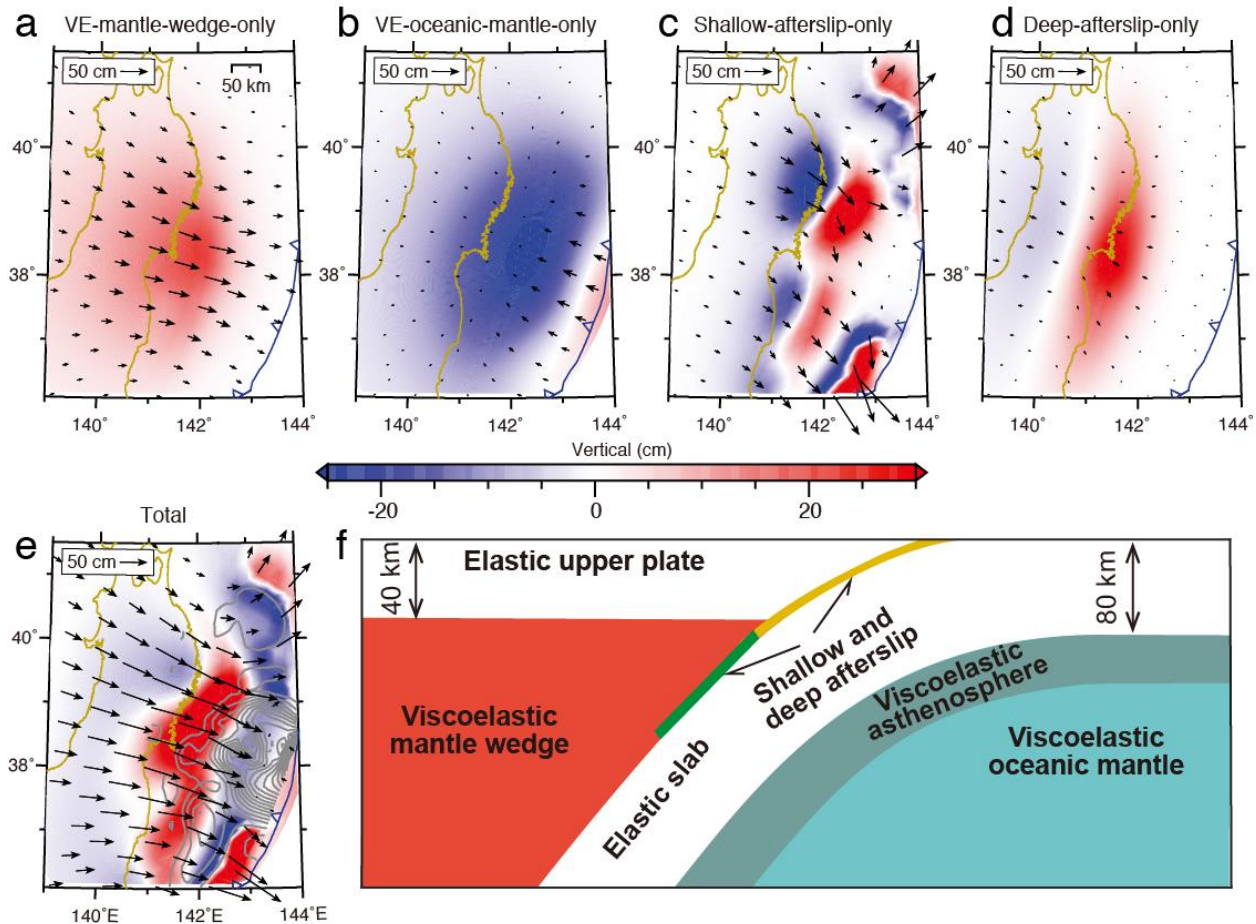
873

874

875 **Figure 14** Examples of postseismic afterslip models by (a) *Inuma et al.* [2016]; (b) *Inuma et al.*
 876 [2016] based on repeating-earthquake data from *Uchida and Matsuzawa* [2013] (c) *Ozawa et al.*
 877 [2012]; and (d) *Shirzaei et al.* [2014]. For (a) and (b), the study period of the color-contoured
 878 postseismic slip is the same (23 April 2011 to 10 December 2011). The coseismic slip
 879 distribution is also shown by the blue contour lines [*Inuma et al.*, 2016]. In (a), note that the
 880 GPS-Acoustic seafloor stations (yellow squares) are distributed only off Miyagi and Fukushima
 881 and consequently the uncertainty in the near-trench postseismic slip is large as shown by the
 882 green dotted line that surrounds the area with $< 0.3\text{m}$ slip uncertainty. In (c), the blue, red and
 883 black contours show coseismic slip, 4-month afterslip, and pre-earthquake (January 2003-

884 January 2011) aseismic slip. In (d) the postseismic slip was inverted from from on-land GPS and
 885 repeating earthquake data of the first 15 months following the mainshock. In (c) and (d) no
 886 seafloor geodetic data was used.

887
 888
 889
 890

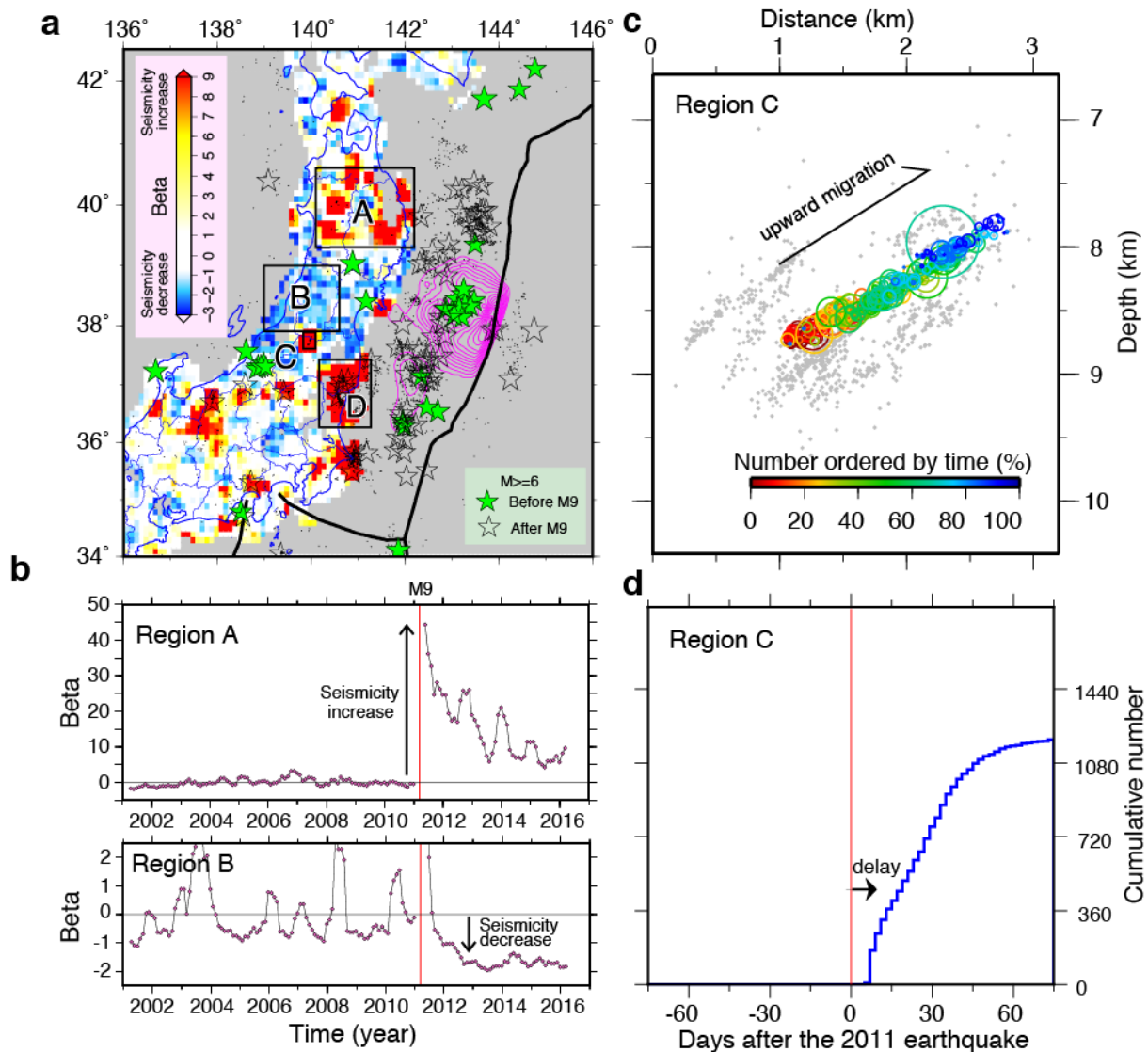


891
 892

893 **Figure 15** The modeled contribution of different postseismic deformation to the observed
 894 postseismic deformation at the surface [after *Hu et al.*, 2016]. Color contours and black arrows
 895 show total vertical and horizontal displacements during the first two years after the mainshock.
 896 (a) and (b) show contributions from viscoelastic mantle relaxation (VE) above and below the
 897 subducting Pacific plate. (c) and (d) show contributions from afterslip in the seismogenic zone
 898 (determined from repeating earthquakes) and downdip aseismic shear, respectively. (e) shows
 899 the sum of the contributions from viscous relaxation and afterslip in (a) through (d). (f) shows a
 900 cross-section through the 3D finite element model showing the locations of the elastic upper
 901 plate and elastic subduction slab (white), viscoelastic mantle wedge (red), viscoelastic oceanic
 902 mantle (dark and light cyan), and shear zone along the plate interface (green and yellow).

903
 904

905



906

907

908

909

910

911

912

913

914

915

916

917

918

919

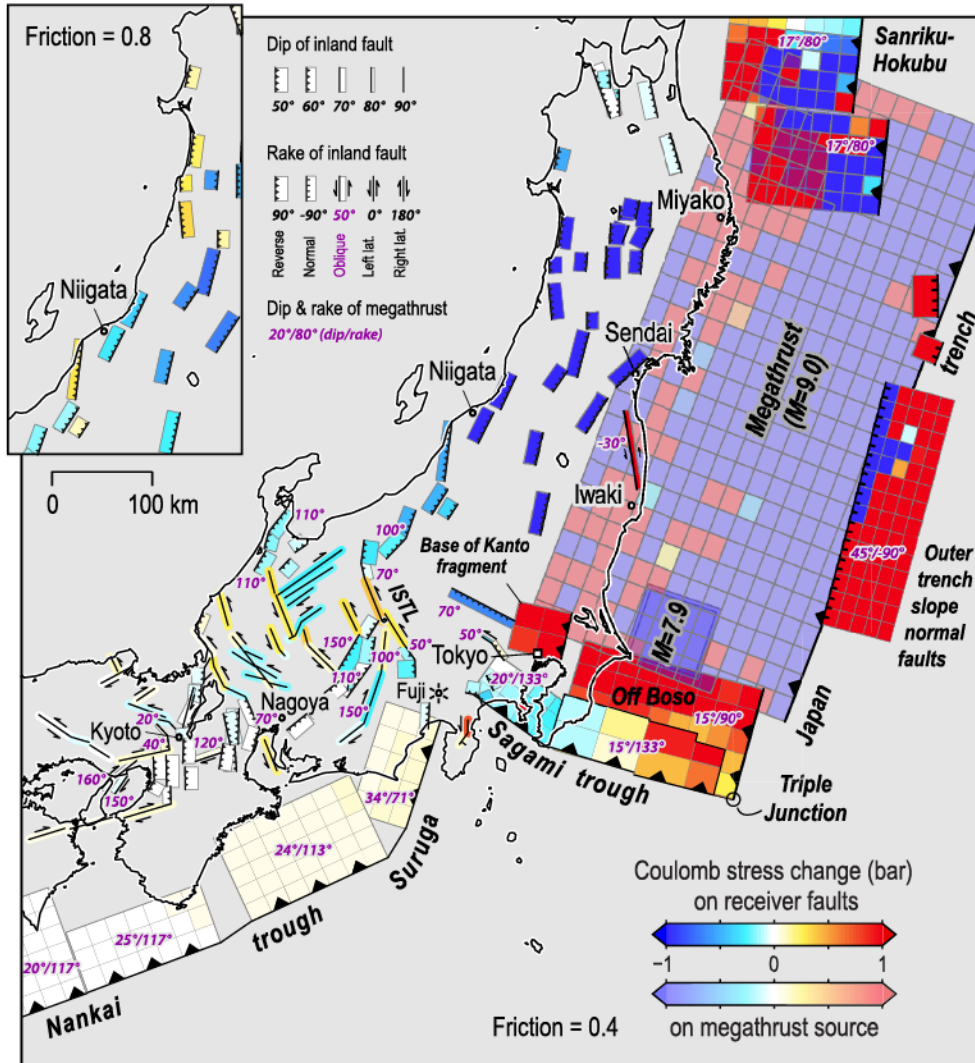
920

921

Figure 16 Inland seismicity rate changes after the Tohoku-oki earthquake. (a) Spatial distribution of beta statistic for March 2013 to March 2016, which is the excess rate of crustal earthquakes with respect to the pre-earthquake period from 2001 to March 11, 2011 normalized by the variance [Reasenber *et al.*, 1992]. The value is evaluated for every 0.3 by 0.3 degree spatial window. The values larger (smaller) than 1 (-1) represent significant increases (decreases) in the seismicity. Green and transparent stars denote $M6$ or larger earthquakes before the Tohoku-oki earthquake (2001 to March 11, 2011) and after the Tohoku-oki earthquake (March 11, 2011 to 2016). (b) Temporal change in beta value for regions A and B outlined in (a), using moving time windows of 0.4 year. (a) and (b) are modified from Uchida *et al.* [2018]. (c) Vertical cross section of earthquakes in a planar structure in the Aizu-swarm in region C shown in (a). The colors show the number ordered in time for a total duration of 800 days from the start of the activity. Sizes of circles correspond to fault diameter assuming a stress drop of 10 MPa. (d) Cumulative number of earthquakes in the earthquake cluster in region C for the first 75 days after the Tohoku-oki earthquake. (c) and (d) are modified from Keisuke Yoshida *et al.* [2019]. The red vertical lines in (b) and (d) are the occurrence time of the

922 Tohoku-oki earthquake. Region D outlined in (a) hosted a pair of M~6 repeating earthquakes
923 discussed in the main text.
924

925
926
927
928



929
930
931
932
933
934
935
936
937
938
939
940
941

Figure 17 Coulomb stress changes due to the coseismic slip of the 2011 Tohoku-oki earthquake and Mw 7.9 aftershock to the south of the rupture [after *Toda et al.*, 2011a]. The coseismic slip model is from *S. Wei et al.* [2011]. The receiver fault geometries are based on the compilation of active faults from the Research Group for Active Faults in Japan, 1991 and Headquarters for Earthquake Research Promotion, 2011. Top and bottom depths of most of the active faults are set to 0 and 15 km. A friction coefficient of 0.4 was used except for the result shown in top left inset.

942 **4 Earthquake cycle and pre-earthquake processes at various time scales**

943 4.1 Refined geologic evidence of recurrent great earthquakes

944 After the 2011 Tohoku-oki earthquake, new observations emerged about the prehistoric
 945 great earthquake occurrences along the Japan trench. Well-documented tsunami deposits along
 946 the coast that were emplaced during the last ~1500 years are summarized by *Sawai* [2017]. The
 947 data showed that the 2011 Tohoku-oki earthquake had similar inundation distances (4.5 km
 948 maximum) as those indicated by the distribution of the tsunami deposits from the 869 Jyogan
 949 earthquake, although the shoreline at the time of the Jyogan earthquake was 1-1.5 km inland
 950 from the present shoreline (Fig. 18b). This would suggest a smaller inundation distance for the
 951 Jyogan earthquake. However, it was recognized that the actual inundation of the tsunami of the
 952 2011 Tohoku-oki earthquake reached substantially further than the extent of sand deposits (about
 953 1.4-1.6 times larger than the inland limit of sandy tsunami deposit) [*T Abe et al.*, 2012; *K Goto et*
 954 *al.*, 2011; *Shishikura et al.*, 2012]. Therefore, the use of tsunami deposits as a measure of
 955 inundation can underestimate the tsunami size. A quantitative re-examination of the size of the
 956 869 Jyogan earthquake, which imposed a minimum flow depth (1m) and flow velocity (0.6m/s)
 957 based on the observation of 2011 sand deposit distribution, was performed by *Namegaya and*
 958 *Satake* [2014]. They recalculated the size of the Jyogan earthquake to be >Mw 8.6, which is
 959 much larger than the pre-2011 magnitude estimates (Mw 8.3-8.4, see section 2.2). *Satake et al.*
 960 [2013] assumed ~25m slip in the deep part of the Tohoku-oki rupture (Mw 8.6) as a Jyogan
 961 earthquake's slip model and showed that this model well explains the tsunami inundation of the
 962 869 Jyogan earthquake (Fig. 18). The scenarios of whole-area slip versus deep-only slip do not
 963 make a large difference in the simulations of tsunami inundation in the plains (Fig. 18), because
 964 the enduring relative coastal sea-level rise due to the long wavelength tsunami from the deep slip
 965 is the main cause of the far-reaching inundation. The impulsive tsunami resulting from the
 966 shallow slip increases the height of the tsunami, but cannot produce a long inundation distance
 967 because of the insufficient duration of the associated sea-level rise. This suggests that the
 968 distribution of tsunami deposits on the Sendai and Ishinomaki plains cannot tell whether large
 969 slip occurred near the trench at the time of the Jyogan earthquake.

970 For the events in between the 869 Jyogan and 2011 Tohoku-oki earthquakes, based on
 971 tsunami heights from additional historical documents and oral legends pertaining to the 1611
 972 Keicho earthquake [*Ebina and Imai*, 2014], *Imai et al.* [2015] estimated the source of the
 973 Keicho earthquake offshore Tohoku with M8.4-8.7 and considered it as a recurrent earthquake
 974 that shared the slip area with the 2011 Tohoku-oki earthquake (Fig. 3). On the other hand,
 975 [*Sawai et al.*, 2012; *Sawai et al.*, 2015] considered the 1454 Kyotoku earthquake as the
 976 penultimate great earthquake from their tsunami deposit data and historical documents
 977 [*Namegaya and Yata*, 2014]. Since the 1454 Kyotoku and 1611 Keicho earthquakes are close in
 978 time (Fig. 19), it is difficult to discriminate these earthquakes from the tsunami deposits alone [*T*
 979 *Goto et al.*, 2015; *Sawai*, 2017]. However, either way it appears that the recurrence interval of
 980 M~9 earthquakes in the Tohoku region is shorter than 1000 years.

981 The coastal and along-trench geologic data reveal an even longer history of large
 982 tsunamigenic earthquakes. Records of coastal tsunami deposits of the last 2000-4000 years
 983 suggest average recurrence intervals of 500-750 years from the data collected along the Sanriku
 984 coast (Fig. 19, reference 3) [*K Takada et al.*, 2016], ~360-year-long intervals on average at
 985 Koyadori on the Sanriku coast [*Ishimura and Miyauchi*, 2015], and 500-800-year-long intervals
 986 on the Sendai plain [*Sawai et al.*, 2012] (Fig. 19, reference 2). Many of these deposits along the

987 Tohoku coast appear to be coincident in time, consistent with their generation by great
988 megathrust earthquakes (Fig. 19).

989 The observations of offshore turbidite unit along the Japan trench provided new
990 constraints on the recurrence of megathrust earthquakes. [Ikehara *et al.*, 2016; Ikehara *et al.*,
991 2018] found that along-trench cores off Miyagi recorded two turbidites corresponding to the
992 1454 Kyotoku and 869 Jyogan earthquakes in addition to deposits associated with the 2011
993 Tohoku-oki earthquake, suggesting similar events occurred repeatedly. *K Usami et al.* [2018]
994 also used core samples at two sites on the landward mid-slope terrace ~40 km from the Japan
995 trench (Fig. 10 a, d) to find turbidites inferred to be caused by strong shaking. They used
996 radioisotopes, paleomagnetic secular variations and volcanic tephra to date the turbidite deposits
997 and found that only the 2011 Tohoku-oki, 1454 Kyotoku and the 869 Jyogan earthquake are
998 clearly recorded in the upper part of both cores (Fig. 19). At both sites, such turbidites recurred at
999 intervals of 400-900 years in the last 4000 years (Fig. 19). These observations also document that
1000 the timing of turbidites is well correlated with the coastal tsunami deposits, providing additional
1001 support for the tsunami deposits being due to local great ruptures off NE Japan (Fig. 19).

1002 From these along-coast and near-trench geodetic and historic constraints, the recurrence
1003 interval of earthquakes similar to the Tohoku-oki earthquake seems to be 400-900 years. If we
1004 consider the 62m maximum slip in 2011 constrained by near-trench bathymetry observations
1005 (Fig. 13, *Sun et al.* [2017]), about 730 year of slip-deficit accumulation at 8.5 cm/year plate
1006 convergence is needed to rebuild the slip potential for a similar-sized event at the Japan trench.
1007 Therefore, the recurrence-interval estimates are consistent with the coseismic slip amount, if the
1008 interplate coupling is close to 100% in the maximum-slip area.

1009

1010 4.2 Observations and models of long-term seismicity changes and decadal precursors

1011 There is a long history of discussion regarding seismicity changes leading up to large
1012 earthquakes [e.g., *Brodsky and Lay*, 2014; *Hardebeck et al.*, 2008; *Kato and Ben-Zion*, 2020;
1013 *Mogi*, 1969]. The 2011 Tohoku-oki earthquake provided a unique opportunity to learn more
1014 about seismicity changes over a wide range of time scales before and after the earthquake, inside
1015 and outside of the coseismic slip area. The hypocenter distribution of interplate earthquakes in
1016 the last ~100 years shows that several previous $M\sim 7$ earthquakes were located within the 2011
1017 coseismic slip area, as shown in Fig. 5. A number of small repeating earthquake sequences that
1018 are typically smaller than $M4$ were also distributed inside the coseismic slip area based on a
1019 record of ~20 years, suggesting the existence of poorly coupled patches within the larger rupture
1020 zone (Fig. 20a) [*Uchida and Matsuzawa*, 2011]. For the period after the Tohoku-oki earthquake,
1021 however, there is a clear lack of interplate seismicity in the main coseismic slip area [*Asano et*
1022 *al.*, 2011; *Kato and Igarashi*, 2012; *W Nakamura et al.*, 2016] (Fig. 12), and as of 2018 and 2020
1023 respectively, there have been no recurrences of the small repeating earthquakes or occurrences of
1024 interplate earthquakes there. This is an important feature of the earthquake, indicating that the
1025 seismicity patterns within a future rupture area evolve during the earthquake cycle.

1026 The careful reanalysis of land GPS data showed that the slip rate on the plate boundary
1027 increased off central and southern Tohoku, in the decade before the Tohoku-oki earthquake
1028 [*Inuma*, 2018; *Mavrommatis et al.*, 2014; *Ozawa et al.*, 2012; *Yokota and Koketsu*, 2015], as
1029 was partly recognized by the monitoring before the earthquake (See section 2.5 and Fig. 7). An
1030 independent analysis of repeating earthquakes [*Uchida and Matsuzawa*, 2013] and joint analysis
1031 of repeating earthquake sequences and GPS data [*Mavrommatis et al.*, 2015] (Fig. 20b) also

1032 showed unfastening of interplate coupling at decadal time scales in an area that showed relatively
1033 large pre-mainshock coupling but did not produce the largest coseismic slip during the 2011
1034 earthquake (Fig. 20a). However, investigation of the long-term (46 years) seismicity suggests
1035 there was a seismic quiescence offshore Miyagi between 1978 (M 7.4) and 2005 (M7.2)
1036 earthquakes [Katsumata, 2011], which suggests there have been more long-term variations in the
1037 interplate coupling [Meade and Loveless, 2009]. Thus, the progressive interplate uncoupling in
1038 the decade preceding the earthquake may represent a preparatory process before the Tohoku-oki
1039 earthquake, but it is unclear if this acceleration was unique to just before the eventual rupture.

1040 There are also decadal changes that were newly identified after the earthquake and are
1041 not directly related to interplate slip. Tanaka [2012] reported enhanced tidal triggering of
1042 earthquakes for several to ten years near the epicenter of the Tohoku-oki earthquake. Nanjo *et al.*
1043 [2012] and Tormann *et al.* [2015] reported a b-value decrease in the coseismic slip area at a
1044 decadal timescale, indicating a relative increase of the number of larger earthquakes relative to
1045 smaller events of the Tohoku-oki earthquake. While it has been suggested that b-value decreases
1046 may reflect a rise in differential stress, the underlying physical mechanisms for these
1047 observations are not well understood [Bürgmann *et al.*, 2016].

1048 The long-term changes in seismicity associated with the earthquake cycle of the Tohoku-
1049 oki earthquake can be modeled in earthquake simulations based on frictional failure laws and
1050 fault geometry. Nakata *et al.* [2016] simulated the earthquake cycle of M~9 earthquakes offshore
1051 Tohoku by considering realistic plate geometry and heterogeneous friction parameters. The
1052 model successfully reproduces the overall patterns of seismicity such as frequent recurrences of
1053 M ~ 7 earthquakes, as well as the coseismic slip, afterslip, the largest foreshock, and the largest
1054 aftershock of the 2011 earthquake. This model also suggests that the asperity of recurrent
1055 Miyagi-oki earthquakes (M~7) in the deeper section of the plate boundary will likely rupture at
1056 equal or shorter intervals after the Tohoku-oki earthquake. Barbot [2020] modeled super-cycles
1057 of partial and full ruptures of the Miyagi-oki segment by considering depth-dependent frictional
1058 properties that are consistent with the forearc structure. The model can explain the occurrence of
1059 smaller size (M~7) 1981 and 2003 earthquakes near the hypocenter of the Tohoku-oki
1060 earthquake by introducing a large velocity-weakening fault area with a small nucleation size and
1061 also captures other observed features, including slow slip and the development of a foreshock
1062 preparatory phase.

1063 4.3 Precursory processes just before the earthquake, real, uncertain and imagined

1064 After many significant earthquakes, attention is being paid to finding potential precursory
1065 activity of various kinds, whose recognition might have allowed for anticipating a destructive
1066 event. The hope is to better understand physical processes leading up to the nucleation of a
1067 mainshock, but also to assess the potential of such precursors for the purpose of improved short-
1068 term earthquake forecasting or even prediction. As such studies are generally done
1069 retrospectively, it is important to very critically assess if such precursor candidates are real; in
1070 the sense that they are based on reliable observations, are statistically significant, and represent
1071 plausible physical processes. It is human nature to conjure up anomalous patterns, which after
1072 more critical analysis may turn out to be non-unique or imagined [e.g., Hardebeck *et al.*, 2008;
1073 Orihara *et al.*, 2019; Woith *et al.*, 2018]. Thanks to improved geophysical monitoring
1074 capabilities, apparently meaningful precursors have been recognized preceding several recent
1075 large events, including the Tohoku-oki earthquake, leading to renewed interest in such
1076 phenomena [Kato and Ben-Zion, 2020; Nakatani, 2020; Pritchard *et al.*, 2020].

1077 The pressure gauges offshore Miyagi detected temporal changes of sea bottom pressure that
1078 are best explained by slow slip on the plate interface near the hypocenters of the M 7.3 foreshock
1079 and the mainshock (red rectangle in Fig. 21), extending from the end of January 2011 to March 9
1080 [Y Ito *et al.*, 2013]. The seafloor pressure gauge data also show that a similar event occurred in
1081 2008. In contrast, the pressure gauge data did not show any short-term precursory accelerations
1082 at the time scale of hours or minutes [Hino *et al.*, 2014]. From seismicity, a migrating pattern of
1083 events propagating from north to south was identified between February and March 9 (magenta
1084 circles in Fig. 21) [Kato *et al.*, 2012], culminating in the March 9 M7.3 foreshock of the 2011
1085 Tohoku-oki earthquake (slip area shown by blue in Fig. 21, [Ohta *et al.*, 2012a]). After the large
1086 foreshock, a second two-day-long seismicity migration toward the south and the hypocenter of
1087 the Tohoku-oki earthquake occurred (yellow circles, [R Ando and Imanishi, 2011; Kato *et al.*,
1088 2012], Fig. 21). The migrating seismicity included repeating earthquakes [Kato *et al.*, 2012;
1089 Uchida and Matsuzawa, 2013], suggesting aseismic slip was involved. The M 7.3 afterslip zone
1090 estimated from GPS data (green in Fig. 21) also lies in the earthquake-migration area [Ohta *et*
1091 *al.*, 2012a]). These data suggest a transient slow slip process accompanied by foreshock activity
1092 preceded the Tohoku-oki earthquake.

1093 There have also been attempts to capture precursory phenomena at various spatial and
1094 temporal scales before the Tohoku-oki earthquake from other space geodetic data. Kosuke Heki
1095 [2011] reported a positive anomaly of ionospheric total electron content starting ~40 minutes
1096 before the Tohoku-oki earthquake using continuous GPS data. Panet *et al.* [2018] reported a
1097 gravity field change at the scale of the whole Japanese-islands starting a few months before
1098 March 2011 by using time series of GRACE satellite data. Bedford *et al.* [2020] reported surface
1099 displacement variations that lasted several months and spanned thousands of kilometers using
1100 time series from on-land GPS stations. However, debate continues on the significance of these
1101 results. Kamogawa and Kakinami [2013], Masci *et al.* [2015] and Ikuta *et al.* [2020] suggest the
1102 preseismic disturbance of the total electron content reported by Kosuke Heki [2011] and Kosuke
1103 Heki and Enomoto [2015] represent artifacts associated with the time series analysis and indicate
1104 frequent occurrences of similar anomalies in the total-electron-content data, suggesting
1105 coincidence by chance. Lei Wang and Bürgmann [2019] showed that the proposed precursory
1106 changes in gravity [Panet *et al.*, 2018] are not statistically unique, either in time or in space.
1107 More research is warranted to thoroughly and critically assess any precursor candidates and to
1108 better understand the physical processes that might underly them [Pritchard *et al.*, 2020].
1109

1110 4.4 Could the Tohoku-oki earthquake have been predicted today?

1111 A decade of study since the 2011 Tohoku-oki earthquake established its detailed rupture
1112 characteristics, revealed pre- and postseismic deformation processes of the earthquake, and
1113 clarified the recurrence history of large megathrust earthquakes in NE Japan. There has also been
1114 much discussion addressing why the Tohoku-oki earthquake was not anticipated before the
1115 earthquake [e.g., Hasegawa, 2011; Hori *et al.*, 2011; Kagan and Jackson, 2013; Toru Matsuzawa,
1116 2011]. This discussion has led to the establishment of new offshore seismic and geodetic
1117 monitoring systems (S-net and GPS-Acoustic stations). In this regard, we now understand the
1118 occurrence of the 2011 Tohoku-oki earthquake and the nature of preceding seismicity and
1119 deformation much better than before, and we have substantially improved capabilities to monitor
1120 the subduction zone. In this section, we try to evaluate the present ability in terms of forecasting
1121 or even predicting earthquakes. For this purpose, we envision a scenario in which the Tohoku-

1122 oki earthquake had not yet happened, but the improved technology and geophysical
1123 infrastructure, as well as various lessons learned in the last decade were in place.

1124 As for long-term earthquake forecasts of great megathrust earthquakes, which rely on
1125 recurrence intervals and the time since the last earthquake, this is now feasible thanks to the new
1126 geologic event occurrence data and some evidence of the earlier earthquakes having occurred in
1127 the same area (i.e., characteristic earthquakes). However, the recurrence intervals (400-900
1128 years) and the rupture area and size of the previous earthquakes are still not very well
1129 constrained (see section 4.1). A retrospective calculation of the long-term probability of a great
1130 Tohoku-oki subduction earthquake at the time just before the 2011 mainshock obtained values of
1131 10-20% within 30 years, assuming a 600-year recurrence interval and time of the most recent
1132 event about 500-600 years ago [*Headquarters for Earthquake Research Promotion*, 2020]. Just
1133 knowing that $M > 8.5$ earthquakes and associated devastating tsunamis are possible along the
1134 Japan Trench, and considering the high 30-year occurrence probability, would likely have led to
1135 increased earthquake and tsunami hazard mitigation efforts in NE Japan.

1136 The decadal and months-long pre-earthquake slip rate variations and foreshock activity
1137 represent candidate observations that have potential to improve the timing accuracy of
1138 intermediate-term forecasts. They were largely detected by monitoring from land before the 2011
1139 Tohoku-oki earthquake (section 2.5) and if such changes in megathrust behavior were to occur
1140 today, we could more easily detect them both from land and offshore observations. We could
1141 also more easily link these phenomena to increased probabilities of an impending earthquake,
1142 because we know the large slip deficit area off Tohoku is capable of producing large seismic slip
1143 and approaches exist to assess the changes in stress and earthquake probabilities in response to
1144 such deformation processes [*Freed*, 2004; *Kano et al.*, 2019; *Kato and Ben-Zion*, 2020; *Mazzotti
1145 and Adams*, 2004; *Obara and Kato*, 2016]. However, it is not certain at all that such slow slips or
1146 foreshock candidates are prone to occur just before the final rupture of a $M \sim 9$ earthquake.
1147 *Uchida et al.* [2016] found periodic slow slip episodes that were activated before the 2011
1148 Tohoku-oki and other $M > 7$ earthquake, but similar episodic slip transients often did not result in
1149 large earthquakes. Near the May 9, 2011 foreshock, there were also similar-sized ($M \sim 7$)
1150 earthquakes with foreshock activity in 2003, 1980, 1962 and 1915 (Fig. 5). In any case, it seems
1151 important to use the potential foreshocks and slow slips to develop time-dependent earthquake
1152 probability estimates [*Mazzotti and Adams*, 2004] and to enhance efforts aimed at operational
1153 earthquake forecasting in subduction zones [e.g., *Field et al.*, 2016; *Jordan et al.*, 2011].

1154 With regards to foreshocks, a global search for successive occurrences of earthquakes
1155 suggests that 0.4-0.6% of $M \sim 7$ earthquakes were followed by $M \sim 8$ or larger earthquakes, within
1156 one week [*Fukushima and Nishikawa*, 2020; *T Hashimoto and Yokota*, 2019]. This is a low value
1157 but the probability is several to 30 times larger than the average determined in long-term
1158 forecasts. For slow slip, there are not many data to evaluate the relationship with, and enhanced
1159 probability of large earthquakes, but there are several examples of precursory transients besides
1160 the Tohoku-oki earthquake [e.g., *Brodsky and Lay*, 2014; *Obara and Kato*, 2016; *Ruiz et al.*,
1161 2014]. Earthquake cycle simulations and laboratory experiments also suggest that such slow slip
1162 events in or near the area of final rupture may be common [e.g., *Barbot*, 2020; *Takanori
1163 Matsuzawa et al.*, 2013; *McLaskey*, 2019; *Nakata et al.*, 2016].

1164 In 2019, the Japanese government implemented a procedure that JMA issue forecast
1165 information regarding a $M 8$ or larger earthquake, when the Nankai Trough Earthquake
1166 Assessment Committee finds that a $M 7$ to 8 earthquake occurred in the wide coupled area along
1167 the Nankai trough in SW Japan or a highly anomalous slow slip episode occurred nearby [*Japan*

1168 *Meteorological Agency, 2019*]. JMA is also to declare a status of "under investigation" even
1169 before the final judgement when the committee has convened, given observations of possible
1170 partial ruptures of the locked area or notable changes in interplate coupling. It seems reasonable
1171 to assume such events are associated with changes in hazard level, and thus to assess the degree
1172 to which they may trigger large earthquakes, and to rigorously quantify by how much the
1173 probability of earthquakes is raised above background levels.

1174 Compared to the above-mentioned improvements in long-term earthquake forecasts and
1175 estimates of time-dependent earthquake probabilities, the short-term (< ~week) precursory
1176 processes that were identified retrospectively after the Tohoku-oki earthquake could be more
1177 effective to mitigate earthquake disasters if they also reflect a substantial probability gain, thus
1178 allowing for meaningful short-term earthquake prediction. However, the debate continues
1179 regarding the significance and uniqueness of such precursors as discussed in section 4.3. We
1180 consider it is immature to implement them for the purpose of earthquake prediction and more
1181 tests are needed to associate the phenomena with the occurrence of large earthquakes and to
1182 better understand the underlying physical mechanisms. Our current understanding of the
1183 earthquake process suggests that while some earthquakes are preceded by a variety of precursory
1184 processes over a wide range of spatial and temporal scales, many and possibly most are not.

1185 In any case, the new offshore real-time seismic and geodetic observations (S-net) can
1186 now detect seismic and tsunami signals ~20 sec and ~20 min earlier than the previously available
1187 observation networks (Fig. 22). These data have been used since January 2019 to stop the
1188 Shinkansen high-speed trains before they experience large shaking [*JR East, 2019*], and have
1189 been incorporated in the public earthquake early warning system of JMA, since June 2019. [*JR*
1190 *East, 2019*] The underestimation of initial earthquake size, which was a problem at the time of
1191 the Tohoku-oki earthquake (Fig. 8), was also seriously considered. In 2016, the REal-time
1192 GEONET Analysis system for Rapid Deformation monitoring (REGARD) [*Ohta et al., 2012b*],
1193 which uses the high-rate displacements of land GPS stations, was implemented at the Geospatial
1194 Information Authority of Japan. In March 2019, the use of real-time offshore tsunami data for
1195 estimating accurate costal tsunami heights (tsunami Forecasting based on Inversion for initial
1196 sea-Surface Height (tFISH)) [*Tsushima et al., 2014*] was implemented as part of the JMA's
1197 official tsunami warning system. Thus, while the prediction of disastrous earthquakes like the
1198 2011 Tohoku-oki event is still impossible, the much improved ability to assess the earthquake
1199 potential, and the establishment of offshore real-time observations for earthquake and tsunami
1200 warning, have greatly improved the preparation of society and enabled actions immediately after
1201 the occurrence of large earthquakes to mitigate the disaster and save human life.

1202

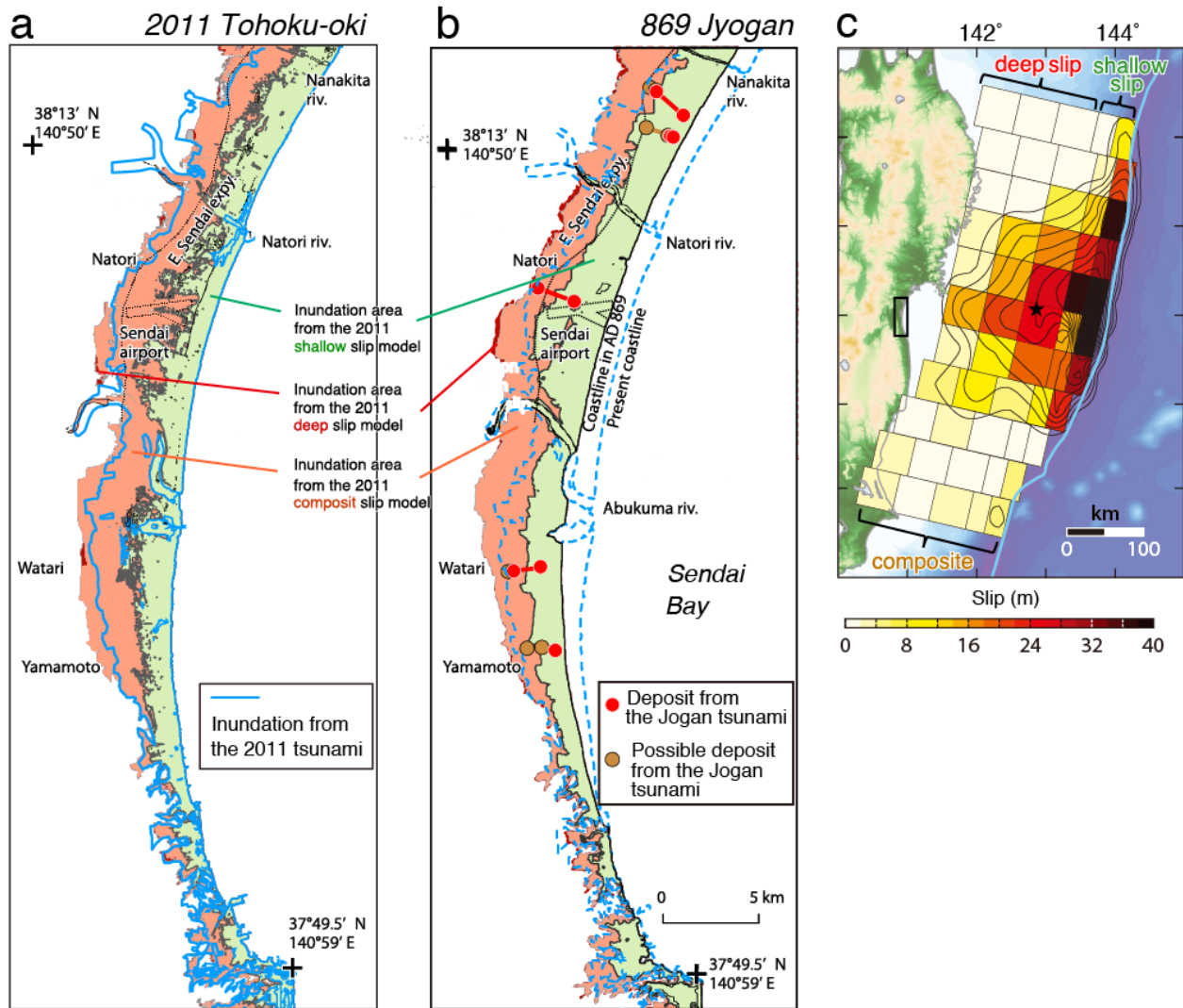
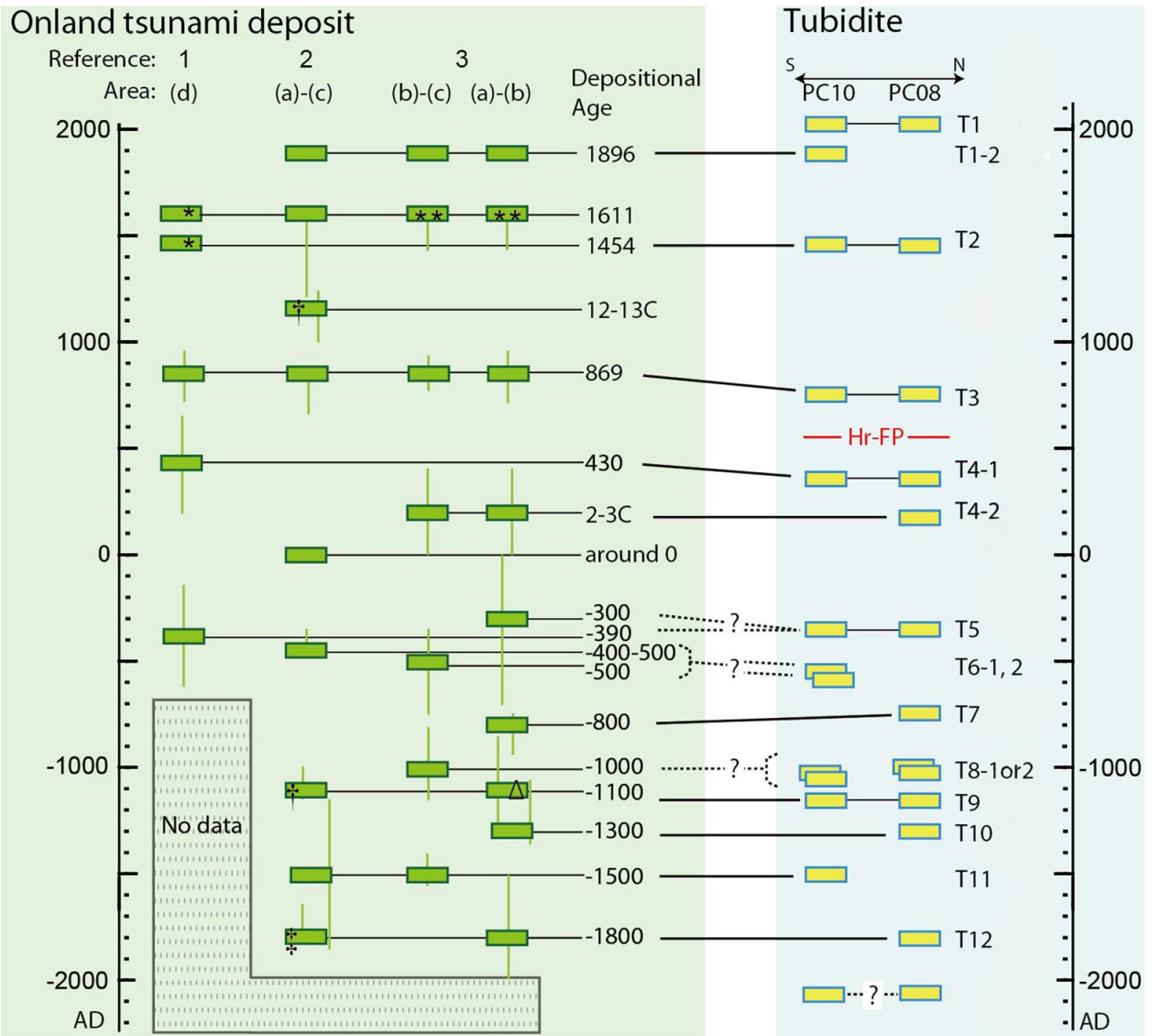
1203
12041205
1206

Figure 18 Observed and simulated tsunami inundations due to the 2011 Tohoku-oki (a) and 869 Jyogan (b) earthquakes in the Sendai plane [Satake *et al.*, 2013]. For the simulation the source fault models are the same for both cases but reconstructed near-shore bathymetry and topography are used for the 869 Jyogan earthquake. Three source-fault model scenarios are considered including final (composite) slip model (orange), slip only in shallow near-trench fault area (green), and slip only in the deep area. The slip of composite, deep and near-trench fault areas (the same as Fig. 11c) and the region (black rectangle) shown in (a) and (b) are shown in (c). The inundation area is defined as the land areas where the modeled flow depth is >0.5 m. Note the simulated inundation areas for the deep and composite models are almost identical. The observed inundation from the 2011 Tohoku-oki earthquake is shown by blue lines in (a) [H Nakajima and Koarai, 2011] and by blue dashed lines in (b) for reference. The locations of certain and possible 869 tsunami deposits [Sawai *et al.*, 2012; Sawai *et al.*, 2008; Sawai *et al.*, 2007] are shown by red and brown circles, respectively.

1220
1221

1222

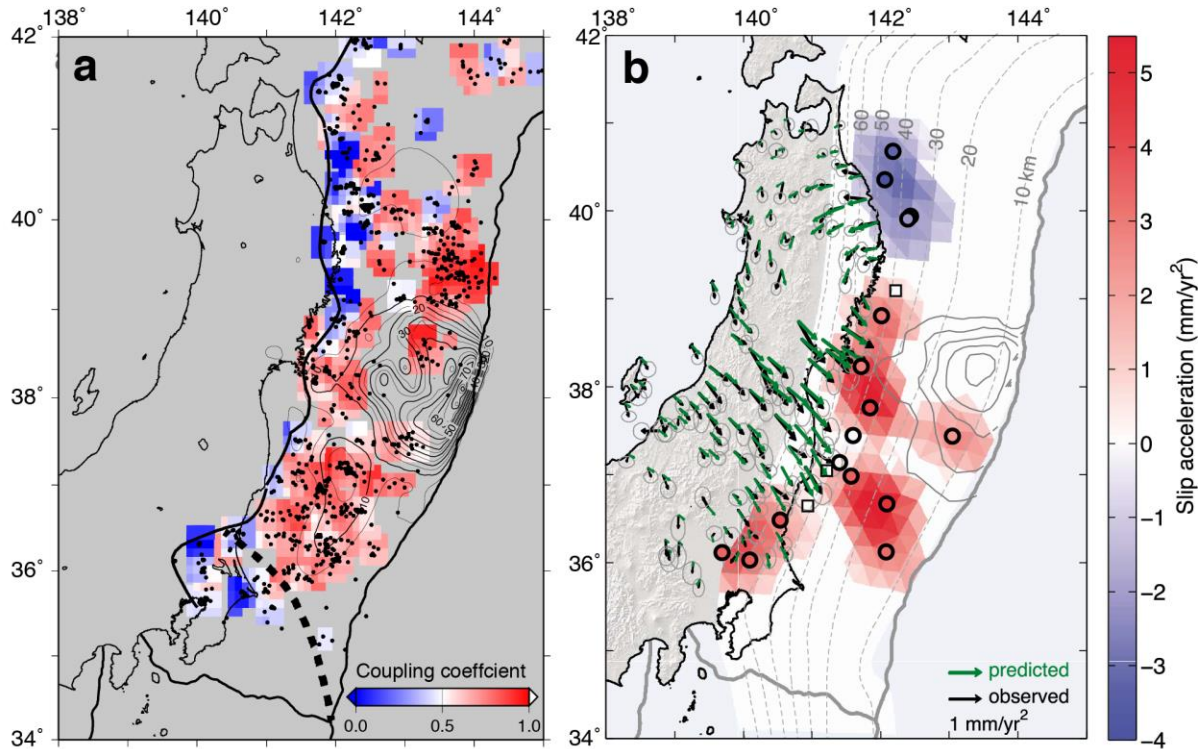


1223
1224

1225 **Figure 19** The comparison of dated on-land tsunami deposits and turbidites near the trench [after
1226 *K Usami et al.*, 2018]. References 1, 2, and 3 are *Sawai et al.* [2012], *Hirakawa* [2012] and *K*
1227 *Takada et al.* [2016]. Estimated depositional age of the tsunami deposits is shown by green
1228 rectangles with error bars (2σ). The locations of areas (a)–(d), PC08 and PC10 are shown in Fig.
1229 10a. * means northern part of area (d) and ** means that deposits may be associated with the
1230 earthquake in A.D. 1454 [*K Takada et al.*, 2016]. † and ‡ mean the northern part of area (b) and
1231 Δ means the northern part of area (a). Hr-FP means tephra of Mt. Haruna eruption in the 6th
1232 century.

1233
1234
1235
1236
1237
1238
1239

1240
1241
1242
1243
1244



1245
1246

Figure 20 Interplate coupling estimated from (a) repeating earthquakes before the Tohoku-oki earthquake (1993-2007), [after *Uchida and Matsuzawa, 2011*] and (b) decadal acceleration (in mm/yr^2) of interplate slip estimated from the joint inversion of GPS and repeating earthquake data [after *Mavrommatis et al., 2015*]. The dots in (a) show the locations of repeating earthquake sequences and circles in (b) show the estimated slip accelerations at the locations of the selected repeating earthquake sequences with frequent recurrences. In (a) the black line shows the downdip limit of interplate earthquakes [*Igarashi et al., 2001; Kita et al., 2010a; Uchida et al., 2009*] and the black dashed line indicates the northeastern limit of the Philippine Sea plate on the Pacific plate [*Uchida et al., 2009*]. In (b) black arrows on land show observed GPS accelerations with 2σ error ellipses and green arrows show model predicted values.

1257
1258
1259
1260
1261
1262

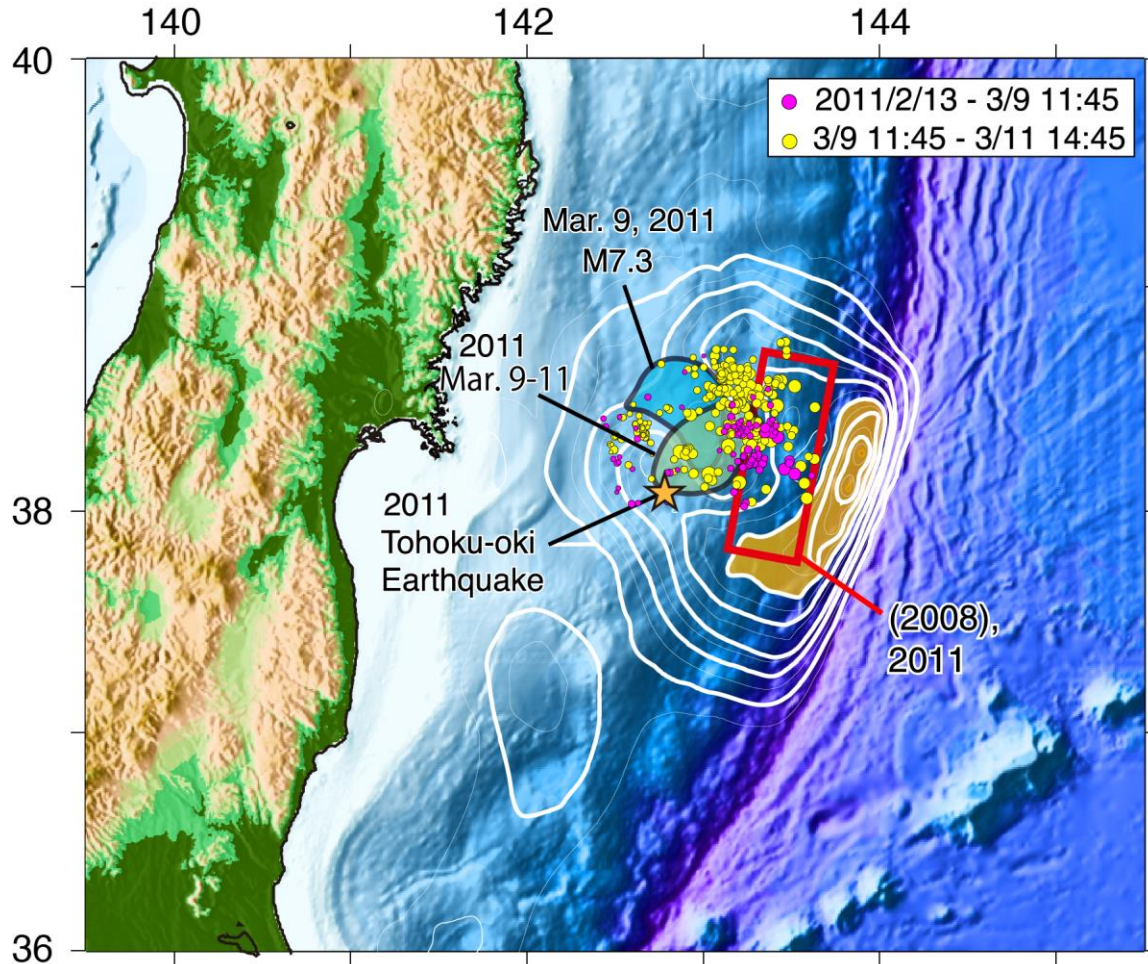
1263
12641265
1266
1267
1268
1269
1270
1271
1272
1273
1274
1275
1276

Figure 21 Various phenomena that occurred before the 2011 Tohoku-oki earthquake in the final slip area. The white contour lines show the coseismic slip model by *Iinuma et al.* [2012] with 10 m contour intervals for thick white lines. The area with >50m slip is filled with orange color. The inferred area of the slow slip events detected in 2008 and 2011 from pressure gauge data are shown by red bold rectangle [*Y Ito et al.*, 2013]. Slip areas of the M7.3 foreshock on March 9, 2011 and its afterslip are shown by blue and green polygons, respectively [*Ohta et al.*, 2012a]. The seismicity that showed migration toward the M9 mainshock hypocenter from Feb. 13, 2011 to March 9 (before the foreshock) and from March 9 (after the foreshock) to March 11 (before the M9 mainshock) are shown by magenta and yellow circles, respectively [*Kato et al.*, 2012].

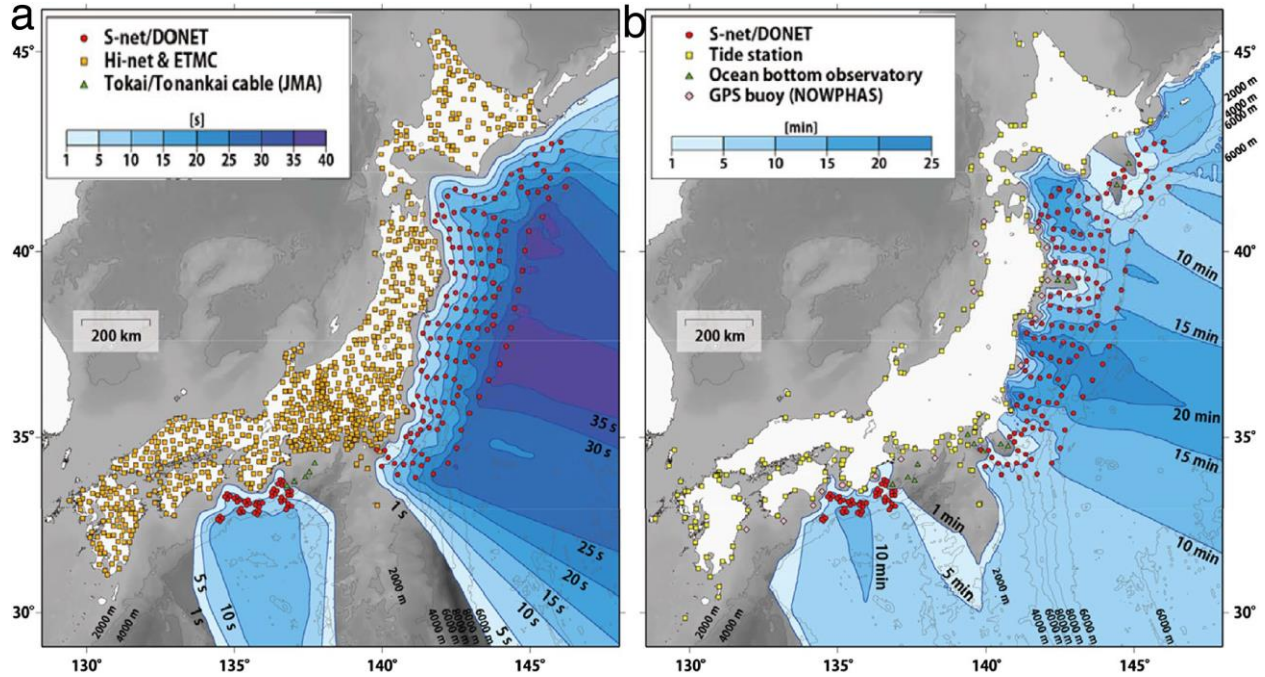
1277
12781279
1280
1281
1282
1283
1284
1285
1286
1287

Figure 22. The time advancement of (a) seismic and (b) tsunami wave detection thanks to the seafloor observation network for earthquakes and tsunami along the Japan trench (S-net, small red circles off NE Japan) and Dense Oceanfloor Network system for Earthquakes and Tsunamis (DONET, small red circles off SW Japan). The labeled blue color contours indicate the time advance over the warning times from the land seismic networks alone (yellow squares), if an earthquake occurred in a given location in the offshore area [after Aoi *et al.*, 2020].

1288

1289 5 Summary of the lessons learned and implications for future megathrust earthquakes

1290 The 2011 Tohoku-oki earthquake occurred where geodetic data showed large interplate
1291 coupling (slip deficit) along the Japan trench (Fig. 3), which confirms that interseismically
1292 locked areas are the likely source areas of future earthquakes. However, the zone of strong
1293 geodetic coupling inferred before the earthquake did not extend to the near-trench area that
1294 produced the largest slip during the earthquake. The incorrect shallow geodetic coupling was due
1295 to poor model resolution in the near-trench area from the land deformation data, and offshore
1296 sea-bottom displacements from GPS-Acoustic observations are key to better resolving the near-
1297 trench coupling. Seismic data, including slip rate estimates from small repeating earthquakes
1298 (Fig. 20a), and the pattern of focal mechanisms in the upper plate, are also useful to discriminate
1299 the main coupling areas that produced the megathrust earthquake. The characterization of
1300 interplate coupling is fundamental to assessing the potential of megathrust earthquakes in
1301 subduction zones.

1302 Geological observations of tsunami deposits along the coast and historical documents and
1303 legends provide further indication of great megathrust earthquakes that occurred before the
1304 instrumental era (Fig. 4a and 18b). The evidence of recurrent great earthquakes similar to the
1305 2011 earthquake comes not only from the coastal tsunami deposits and historical accounts, but
1306 also from earthquake-induced turbidites near the trench axis (Figs. 10 and 19). One important
1307 lesson from these results is the reminder that instrumentally observed seismic data easily miss
1308 the rare largest events in an area and that it is fundamentally important to find evidence of large
1309 previous earthquakes from a variety of data to recognize the possibility of such events. The
1310 geological data document a recurrence history of great off-Tohoku ruptures with 400-900 year
1311 intervals (Fig. 19), characterizing the earthquake cycle and further quantifying the hazard of
1312 great ruptures.

1313 Examination of near-fault materials and structural anomalies (e.g., Fig. 2b) can also
1314 improve our understanding of the fault behavior and inform computational models of subduction
1315 zone mechanics. Increasingly advanced earthquake cycle simulations can also contribute to
1316 assessing the earthquake hazard, constrained by the observed coupling, large-earthquake
1317 recurrence history, distribution of seismicity and slow slip in space and time, fault geometry, and
1318 frictional properties. Since most observations are inherently incomplete, it is important to
1319 integrate the knowledge from many scientific fields to better understand the likelihood of an
1320 impending great earthquake and optimally prepare for it.

1321 The aftershocks and postseismic deformation processes that occurred in response to the
1322 large coseismic slip helped advance our understanding of earthquake mechanisms and the
1323 subduction system. Coseismic and postseismic slip showed complementary distribution (Fig. 14),
1324 and interplate aftershocks (Fig. 12), repeating earthquakes and tremors, and very low frequency
1325 earthquakes (Fig. 2b) were activated in the afterslip zone, driven by the coseismic stress
1326 concentration. Within the coseismic slip zone, the seismic activity diminished (Fig. 12), probably
1327 indicating a nearly full stress drop and long-term interplate seismicity changes through the
1328 earthquake cycle. The widespread triggered earthquakes away from the plate interface and
1329 postseismic deformation document the far reach of the mainshock and the enduring viscoelastic
1330 relaxation in the mantle (Fig. 15). The post-mainshock observations provided new insights on
1331 earthquake generation processes including static and dynamic triggering (Fig. 16a and Fig. 17),
1332 have illuminated the role of fluid pressure and migration (Fig. 16c and d), highlighted the

1333 heterogeneous pre-Tohoku-oki stress and structure, contributed to the better understanding of the
1334 rheological structure beneath the arc, and revealed the low ambient stress levels and low fault
1335 strength in the subduction zone.

1336 The Tohoku-oki earthquake also illuminated the importance of real-time observation and
1337 processing of earthquake data. The offshore GPS tsunami buoy contributed to recognizing the
1338 large tsunami earlier than is possible with only the coastal tsunami observations (Fig. 8). Many
1339 more offshore cabled pressure gauges (S-net) are now deployed based on this lesson and
1340 contribute to the time advancement of earthquake early warning and tsunami forecasts (Fig. 22).
1341 Another lesson regarding the real-time processing of earthquake data is the difficulty of rapid
1342 estimation of earthquake size for very large earthquakes. In 2011, the delay caused initial
1343 underestimation of the area affected by strong earthquake shaking and tsunami heights.
1344 Improved real-time analysis methods of the complementary data types, including on-land
1345 geodetic data and offshore tsunami data assimilation, will contribute to a more rapid and more
1346 accurate source-size determination.

1347 Offshore geophysical and geological observations provided crucial information about the
1348 interplate coupling, evidence of previous great megathrust earthquakes, fault-zone to asperity-
1349 size characterization of structure and fault behavior, and real-time observation and warning of
1350 the earthquake and tsunami. The data include sea-bottom GPS-Acoustic displacements (Fig. 9a
1351 and b), pressure and tsunami observations (Figs. 9c and 22), coseismic differential bathymetry
1352 (Fig. 10b) and seismic imaging, near-trench, earthquake-induced turbidites (Fig. 10c), cored
1353 fault-zone material and near-fault borehole observations, and seismometers just above the
1354 shallow subduction zone (Fig. 22).

1355 The decadal evolution of seismicity and changes in megathrust coupling (e.g., Fig. 20b)
1356 are new observations, which appear related to the physical state of the plate boundary
1357 approaching the final stage of the earthquake cycle. The accumulation of such observations, also
1358 in other subduction zones, will promote improved understanding of the whole earthquake cycle
1359 and nature of earthquakes. However, it is uncertain if this apparent preparation process observed
1360 before the Tohoku-oki earthquake occurred only before the final rupture or if it is a recurring
1361 feature; thus, uncertainty remains with regards to its relevance for earthquake forecasting.

1362 Finally, the apparent short-term precursors of the Tohoku-oki earthquake, including
1363 foreshocks and slow slip transients (e.g., Fig. 21), represent important phenomena that have been
1364 intensively investigated. These observations have contributed to better understanding of the
1365 earthquake generation process and can potentially lead to improved time-dependent operational
1366 earthquake forecasting. However, similar fault slip anomalies have been observed without being
1367 followed by large ruptures, and there is little evidence of a unique nucleation or preparation
1368 process that is diagnostic of the size and time of an eventual mainshock. Other intriguing
1369 observations, including changes in b-values and tidal modulation, regional-scale deformation and
1370 gravity anomalies, and ionospheric perturbations, have been put forward as potential precursor
1371 candidates, but neither the observations themselves nor the physics of underlying processes are
1372 well established. In the next decade, we have the opportunity to further improve our
1373 understanding of the complex dynamics of subduction zones and to implement that knowledge
1374 for the assessment of probability gains in increasingly accurate time-dependent earthquake
1375 forecasts.

1376

1377 **6 Future Issues**

- 1378 1. Due to the centuries-long intervals between ~M9 interplate earthquakes offshore
 1379 Tohoku, more accurate paleoseismic information is key to confirming the existence,
 1380 recurrence pattern and hazard of such great earthquakes.
- 1381 2. The coseismic rupture, afterslip, aftershocks, slow earthquakes, and viscoelastic
 1382 deformation are all related to each other. Further examining their interactions will
 1383 contribute to more advanced modeling of these phenomena and will improve our overall
 1384 understanding of this dynamic system.
- 1385 3. Further improvements of a wide range of geophysical observations and the development
 1386 of more advanced computational models are necessary to gain a deeper understanding of
 1387 the megathrust earthquake cycle and physical processes associated with the spectrum of
 1388 fault slip processes in subduction zones.
- 1389 4. Comparative studies illuminating the variety of fault system environments, properties
 1390 and mechanical behaviors will be important to better understand the factors underlying
 1391 variable behaviors among the world's subduction zones.
- 1392 5. Offshore observations greatly improve the monitoring capabilities in subduction systems
 1393 and enable more accurate earthquake hazard assessment. Such capabilities should be
 1394 developed in other subduction zones to improve our knowledge of the range of fault
 1395 system behaviors.
- 1396 6. It is important to make optimal use of real-time observations and to further develop the
 1397 methodologies and accuracy of earthquake and tsunami early warning systems.
- 1398 7. Although the Tohoku-oki earthquake provided unprecedented observations of active
 1399 processes leading up to, during and following the megathrust rupture, it is important to
 1400 understand which features are likely to be applicable only to the Tohoku subduction zone
 1401 or even just this one particular rupture.
- 1402 8. While it remains a daunting challenge, we should not rule out the possibility of much
 1403 improved short-term forecasting of large earthquakes based on the careful analysis and
 1404 interpretation of high-quality geophysical observations.

1406

1407 **Glossary**

1408

1409 Coulomb stress change: Coulomb stress change is the stress change on a fault that determines the
 1410 degree to which fault slip is encouraged or suppressed. Increasing shear stress in the slip
 1411 direction and decreasing fault-normal stress cause positive Coulomb stress changes that promote
 1412 earthquakes. It depends on the imparted stress change, the geometry and slip direction of a fault,
 1413 the friction coefficient, and the pore pressure [*Freed, 2004*].

1414

1415 Double seismic zone: Double seismic zones feature two planar earthquake concentrations in the
 1416 subducted plate in subduction zones that are near-parallel to the plate surface. One is located near
 1417 the surface and the other is located ~30km below in the case of the NE Japan subduction zone
 1418 [*Hasegawa et al., 1978*].

1419

1420 Dynamic weakening: Dynamic weakening of faults is a transient decrease in the friction of faults
1421 during the slip [*Di Toro et al.*, 2011].

1422
1423 GPS-Acoustic observation: GPS-Acoustic systems estimate water (sea) bottom displacements by
1424 combining repeated GPS measurements of the position of a platform at the sea surface and
1425 acoustic ranging between the surface and acoustic transponders on the seafloor [*Bürgmann and*
1426 *Chadwell*, 2014].

1427
1428 GRACE: GRACE (Gravity Recovery and Climate Experiment) is a system that measure Earth's
1429 gravity field at ~350 km resolution by using accurate distance measurements between a pair of
1430 satellites [*Tapley et al.*, 2004].

1431
1432 Poroelastic rebound: Poroelastic rebound is a postseismic deformation process that is caused by
1433 the movement of fluids within poroelastic media induced by coseismic pressure changes [*Peltzer*
1434 *et al.*, 1996].

1435
1436 Repeating earthquakes: Repeating earthquakes are effectively identical earthquakes that occur at
1437 the same place but different time. The overlapping events suggest the existence of fault creep in
1438 the surrounding area. Multiple repeating earthquake sequences provide information about the
1439 spatio-temporal distribution of fault creep [*Uchida and Bürgmann*, 2019].

1440
1441 Seafloor pressure gauge: Seafloor pressure gauges measure the ocean bottom pressure that can
1442 be transformed into the water thickness above the site. It can thus measure vertical displacements
1443 of the seafloor and temporal changes of sea height (e.g., tsunami) [*Bürgmann and Chadwell*,
1444 2014].

1445
1446 Slip deficit: Slip deficit is the amount of fault displacement that is not released by earthquakes or
1447 other types of slip. Slip deficit on a fault builds up due to plate motion across faults and will be
1448 compensated by future slip [*Lifeng Wang et al.*, 2015].

1449
1450 Tremor: Tremors and low frequency earthquakes represent a type of slow earthquake on a fault.
1451 They are dominated by shaking at several Hz and do not have clear P and S phases that are
1452 observed for regular earthquakes [*Beroza and Ide*, 2011].

1453
1454 Very low frequency earthquakes: Very low frequency earthquakes are a type of slow earthquake
1455 that are dominated by low-frequency seismic waves (below 0.1 Hz) [*Beroza and Ide*, 2011].

1456

1457 **Acknowledgments, Samples, and Data**

1458 We thank Yukitoshi Fukahata and Tatsuhiko Saito for discussions regarding the
1459 significance of the Tohoku-oki earthquake, Toru Matsuzawa, Ryota Hino and Akira Hasegawa
1460 for comment on the manuscript. We also thank Keisuke Yoshida, Takeshi Iinuma and Fumiaki
1461 Tomita for original data for figures. Data were not used, nor created for this research. This work
1462 was supported in part by JSPS KAKENHI 16H06473, 17KK0081, and 19H05596 and MEXT of
1463 Japan, under its Earthquake and Volcano Hazards Observation and Research Program. RB

1464 acknowledges support by NSF award EAR-1801720. This work is dedicated to the people
 1465 affected by the Tohoku-oki earthquake on March 11, 2011.

1466

1467 **References**

1468

1469 Abe, H., Y. Sugeno, and A. Chigama (1990), Estimation of the Height of the Sanriku Jogan 11 Earthquake-Tsunami
 1470 (A. D. 869) in the Sendai Plain, *Zisin* 2, 43(4), 513-525, doi:10.4294/zisin1948.43.4_513.

1471 Abe, T., K. Goto, and D. Sugawara (2012), Relationship between the maximum extent of tsunami sand and the
 1472 inundation limit of the 2011 Tohoku-oki tsunami on the Sendai Plain, Japan, *Sedimentary Geology*, 282, 142-150,
 1473 doi:<https://doi.org/10.1016/j.sedgeo.2012.05.004>.

1474 Ammon, C. J., T. Lay, H. Kanamori, and M. Cleveland (2011), A rupture model of the 2011 off the Pacific coast of
 1475 Tohoku Earthquake, *Earth, Planets and Space*, 63(7), 33, doi:10.5047/eps.2011.05.015.

1476 Ando, M. (1975), Source mechanisms and tectonic significance of historical earthquakes along the nankai trough,
 1477 Japan, *Tectonophysics*, 27(2), 119-140, doi:[http://dx.doi.org/10.1016/0040-1951\(75\)90102-X](http://dx.doi.org/10.1016/0040-1951(75)90102-X).

1478 Ando, R., and K. Imanishi (2011), Possibility of Mw 9.0 mainshock triggered by diffusional propagation of after-
 1479 slip from Mw 7.3 foreshock, *Earth, Planets and Space*, 63(7), 47, doi:10.5047/eps.2011.05.016.

1480 Aoi, S., Y. Asano, T. Kunugi, T. Kimura, K. Uehira, N. Takahashi, H. Ueda, K. Shiomi, T. Matsumoto, and H.
 1481 Fujiwara (2020), MOWLAS: NIED observation network for earthquake, tsunami and volcano, *Earth, Planets and*
 1482 *Space*, 72(1), 126, doi:10.1186/s40623-020-01250-x.

1483 Asano, Y., T. Saito, Y. Ito, K. Shiomi, H. Hirose, T. Matsumoto, S. Aoi, S. Hori, and S. Sekiguchi (2011), Spatial
 1484 distribution and focal mechanisms of aftershocks of the 2011 off the Pacific coast of Tohoku Earthquake, *Earth*
 1485 *Planets and Space*, 63(7), 669-673, doi:10.5047/eps.2011.06.016.

1486 Baba, S., A. Takeo, K. Obara, T. Matsuzawa, and T. Maeda (2020), Comprehensive Detection of Very Low
 1487 Frequency Earthquakes Off the Hokkaido and Tohoku Pacific Coasts, Northeastern Japan, *Journal of Geophysical*
 1488 *Research: Solid Earth*, 125(1), e2019JB017988, doi:<https://doi.org/10.1029/2019JB017988>.

1489 Barbot, S. (2020), Frictional and structural controls of seismic super-cycles at the Japan trench, *Earth, Planets and*
 1490 *Space*, 72(1), 63, doi:10.1186/s40623-020-01185-3.

1491 Bassett, D., D. T. Sandwell, Y. Fialko, and A. B. Watts (2016), Upper-plate controls on co-seismic slip in the 2011
 1492 magnitude 9.0 Tohoku-oki earthquake, *Nature*, 531(7592), 92-96, doi:10.1038/nature16945.

1493 Bedford, J. R., M. Moreno, Z. Deng, O. Oncken, B. Schurr, T. John, J. C. Báez, and M. Bevis (2020), Months-long
 1494 thousand-kilometre-scale wobbling before great subduction earthquakes, *Nature*, 580(7805), 628-635,
 1495 doi:10.1038/s41586-020-2212-1.

1496 Beroza, G. C., and S. Ide (2011), Slow Earthquakes and Nonvolcanic Tremor, *Annual Review of Earth and*
 1497 *Planetary Sciences*, 39(1), 271-296, doi:10.1146/annurev-earth-040809-152531.

1498 Bilek, S. L., and T. Lay (2002), Tsunami earthquakes possibly widespread manifestations of frictional conditional
 1499 stability, *Geophysical Research Letters*, 29(14), 18-11-18-14, doi:doi:10.1029/2002GL015215.

1500 Bletery, Q., A. Sladen, B. Delouis, M. Vallée, J.-M. Nocquet, L. Rolland, and J. Jiang (2014), A detailed source
 1501 model for the Mw9.0 Tohoku-Oki earthquake reconciling geodesy, seismology, and tsunami records, *Journal of*
 1502 *Geophysical Research: Solid Earth*, 119(10), 7636-7653, doi:10.1002/2014JB011261.

1503 Brodsky, E. E., and T. Lay (2014), Recognizing Foreshocks from the 1 April 2014 Chile Earthquake, *Science*,
 1504 344(6185), 700, doi:10.1126/science.1255202.

1505 Brodsky, E. E., et al. (2020), The State of Stress on the Fault Before, During, and After a Major Earthquake, *Annual*
 1506 *Review of Earth and Planetary Sciences*, 48(1), 49-74, doi:10.1146/annurev-earth-053018-060507.

1507 Brodsky, E. E., D. Saffer, P. Fulton, F. Chester, M. Conin, K. Huffman, J. C. Moore, and H.-Y. Wu (2017), The
 1508 postearthquake stress state on the Tohoku megathrust as constrained by reanalysis of the JFAST breakout data,
 1509 *Geophysical Research Letters*, 44(16), 8294-8302, doi:<https://doi.org/10.1002/2017GL074027>.

1510 Brown, L., K. Wang, and T. Sun (2015), Static stress drop in the Mw 9 Tohoku-oki earthquake: Heterogeneous
 1511 distribution and low average value, *Geophysical Research Letters*, 42(24), 10,595-510,600,
 1512 doi:10.1002/2015GL066361.

1513 Bürgmann, R., and D. Chadwell (2014), Seafloor Geodesy, *Annual Review of Earth and Planetary Sciences*, 42(1),
 1514 509-534, doi:10.1146/annurev-earth-060313-054953.

1515 Bürgmann, R., N. Uchida, Y. Hu, and T. Matsuzawa (2016), Tohoku rupture reloaded?, *Nature Geosci*, 9(3), 183-
 1516 184, doi:10.1038/ngeo2649

- 1517 <http://www.nature.com/ngeo/journal/v9/n3/abs/ngeo2649.html#supplementary-information>.
- 1518 Chagué-Goff, C., A. Andrew, W. Szczuciński, J. Goff, and Y. Nishimura (2012), Geochemical signatures up to the
- 1519 maximum inundation of the 2011 Tohoku-oki tsunami — Implications for the 869AD Jogan and other
- 1520 palaeotsunamis, *Sedimentary Geology*, 282, 65-77, doi:<https://doi.org/10.1016/j.sedgeo.2012.05.021>.
- 1521 Chao, K., Z. Peng, H. Gonzalez - Huizar, C. Aiken, B. Enescu, H. Kao, A. A. Velasco, K. Obara, and T. Matsuzawa
- 1522 (2013), A Global Search for Triggered Tremor Following the 2011 Mw 9.0 Tohoku Earthquake, *B Seismol Soc Am*,
- 1523 103(2B), 1551-1571, doi:10.1785/0120120171.
- 1524 Chester, F. M., et al. (2013), Structure and Composition of the Plate-Boundary Slip Zone for the 2011 Tohoku-Oki
- 1525 Earthquake, *Science*, 342(6163), 1208, doi:10.1126/science.1243719.
- 1526 Chiba, K., Y. Iio, and Y. Fukahata (2013), Detailed stress fields in the focal region of the 2011 off the Pacific coast
- 1527 of Tohoku Earthquake—Implication for the distribution of moment release—, *Earth, Planets and Space*, 64(12), 10,
- 1528 doi:10.5047/eps.2012.07.008.
- 1529 Delbridge, B. G., S. Kita, N. Uchida, C. W. Johnson, T. Matsuzawa, and R. Bürgmann (2017), Temporal variation
- 1530 of intermediate-depth earthquakes around the time of the M9.0 Tohoku-oki earthquake, *Geophysical Research*
- 1531 *Letters*, 44(8), 3580-3590, doi:10.1002/2017GL072876.
- 1532 Di Toro, G., R. Han, T. Hirose, N. De Paola, S. Nielsen, K. Mizoguchi, F. Ferri, M. Cocco, and T. Shimamoto
- 1533 (2011), Fault lubrication during earthquakes, *Nature*, 471(7339), 494-498, doi:10.1038/nature09838.
- 1534 Diao, F., X. Xiong, R. Wang, Y. Zheng, T. R. Walter, H. Weng, and J. Li (2014), Overlapping post-seismic
- 1535 deformation processes: afterslip and viscoelastic relaxation following the 2011 Mw 9.0 Tohoku (Japan) earthquake,
- 1536 *Geophysical Journal International*, 196(1), 218-229, doi:10.1093/gji/ggt376.
- 1537 Ebina, Y., and K. Imai (2014), Tsunami traces survey of the 1611 Keicho Ohshyu earthquake tsunami based on
- 1538 historical documents and traditions, *Report of Tsunami Engineering*, 31, 139-148.
- 1539 Field, E. H., T. H. Jordan, L. M. Jones, A. J. Michael, M. L. Blanpied, and P. Other Workshop (2016), The Potential
- 1540 Uses of Operational Earthquake Forecasting, *Seismological Research Letters*, 87(2A), 313-322,
- 1541 doi:10.1785/0220150174.
- 1542 Fire and disaster management agency, Japan, (2020), On the 2011 off the Pacific coast of Tohoku earthquake (report
- 1543 no. 160), <https://www.fdma.go.jp/disaster/higashinihon/items/160.pdf>.
- 1544 Freed, A. M. (2004), EARTHQUAKE TRIGGERING BY STATIC, DYNAMIC, AND POSTSEISMIC STRESS
- 1545 TRANSFER, *Annual Review of Earth and Planetary Sciences*, 33(1), 335-367,
- 1546 doi:10.1146/annurev.earth.33.092203.122505.
- 1547 Fujii, Y., K. Satake, S. i. Sakai, M. Shinohara, and T. Kanazawa (2011), Tsunami source of the 2011 off the Pacific
- 1548 coast of Tohoku Earthquake, *Earth, Planets and Space*, 63(7), 55, doi:10.5047/eps.2011.06.010.
- 1549 Fujiwara, T., C. dos Santos Ferreira, A. K. Bachmann, M. Strasser, G. Wefer, T. Sun, T. Kanamatsu, and S. Kodaira
- 1550 (2017), Seafloor Displacement After the 2011 Tohoku-oki Earthquake in the Northern Japan Trench Examined by
- 1551 Repeated Bathymetric Surveys, *Geophysical Research Letters*, 44(23), 11,833-811,839,
- 1552 doi:10.1002/2017GL075839.
- 1553 Fujiwara, T., S. Kodaira, T. No, Y. Kaiho, N. Takahashi, and Y. Kaneda (2011), The 2011 Tohoku-Oki Earthquake:
- 1554 Displacement Reaching the Trench Axis, *Science*, 334(6060), 1240, doi:10.1126/science.1211554.
- 1555 Fukushima, Y., and T. Nishikawa (2020), New Earthquake Warning Framework in the Nankai Trough Subduction
- 1556 Zone in Japan and Scientific Rationale that the Society Need to Know for Effective Countermeasures, *AGU 2020*
- 1557 *Fall Meeting*.
- 1558 Fukushima, Y., S. Toda, S. Miura, D. Ishimura, J. i. Fukuda, T. Demachi, and K. Tachibana (2018), Extremely early
- 1559 recurrence of intraplate fault rupture following the Tohoku-Oki earthquake, *Nature Geoscience*,
- 1560 doi:10.1038/s41561-018-0201-x.
- 1561 Fukuyama, E., and S. Hok (2015), Dynamic Overshoot Near Trench Caused by Large Asperity Break at Depth, *Pure*
- 1562 *and Applied Geophysics*, 172(8), 2157-2165, doi:10.1007/s00024-013-0745-z.
- 1563 Fulton, P. M., E. E. Brodsky, Y. Kano, J. Mori, F. Chester, T. Ishikawa, R. N. Harris, W. Lin, N. Eguchi, and S.
- 1564 Toczko (2013), Low Coseismic Friction on the Tohoku-Oki Fault Determined from Temperature Measurements,
- 1565 *Science*, 342(6163), 1214, doi:10.1126/science.1243641.
- 1566 Gao, X., and K. Wang (2014), Strength of stick-slip and creeping subduction megathrusts from heat flow
- 1567 observations, *Science*, 345(6200), 1038, doi:10.1126/science.1255487.
- 1568 Geospatial Information Authority of Japan (2011), The 2011 off the Pacific coast of Tohoku Earthquake, Coseismic
- 1569 and postseismic
- 1570 slip distribution on the plate interface (preliminary result), <http://www.gsi.go.jp/cais/topic110315.2-index-e.html>.

- 1571 Gonzalez-Huizar, H., A. A. Velasco, Z. Peng, and R. R. Castro (2012), Remote triggered seismicity caused by the
 1572 2011, M9.0 Tohoku-Oki, Japan earthquake, *Geophysical Research Letters*, 39(10),
 1573 doi:<https://doi.org/10.1029/2012GL051015>.
- 1574 Goto, K., et al. (2011), New insights of tsunami hazard from the 2011 Tohoku-oki event, *Marine Geology*, 290(1),
 1575 46-50, doi:<https://doi.org/10.1016/j.margeo.2011.10.004>.
- 1576 Goto, T., K. Satake, T. Sugai, T. Ishibe, T. Harada, and S. Murotani (2015), Historical tsunami and storm deposits
 1577 during the last five centuries on the Sanriku coast, Japan, *Marine Geology*, 367, 105-117,
 1578 doi:<https://doi.org/10.1016/j.margeo.2015.05.009>.
- 1579 Gusman, A. R., Y. Tanioka, S. Sakai, and H. Tsushima (2012), Source model of the great 2011 Tohoku earthquake
 1580 estimated from tsunami waveforms and crustal deformation data, *Earth and Planetary Science Letters*, 341-344,
 1581 234-242, doi:<https://doi.org/10.1016/j.epsl.2012.06.006>.
- 1582 Hara, T. (2011), Magnitude determination using duration of high frequency energy radiation and displacement
 1583 amplitude: application to the 2011 off the Pacific coast of Tohoku Earthquake, *Earth, Planets and Space*, 63(7), 3,
 1584 doi:10.5047/eps.2011.05.014.
- 1585 Hardebeck, J. L. (2012), Coseismic and postseismic stress rotations due to great subduction zone earthquakes,
 1586 39(21), doi:<https://doi.org/10.1029/2012GL053438>.
- 1587 Hardebeck, J. L. (2015), Stress orientations in subduction zones and the strength of subduction megathrust faults,
 1588 *Science*, 349(6253), 1213, doi:10.1126/science.aac5625.
- 1589 Hardebeck, J. L., K. R. Felzer, and A. J. Michael (2008), Improved tests reveal that the accelerating moment release
 1590 hypothesis is statistically insignificant, *Journal of Geophysical Research: Solid Earth*, 113(B8),
 1591 doi:10.1029/2007JB005410.
- 1592 Hardebeck, J. L., and T. Okada (2018), Temporal Stress Changes Caused by Earthquakes: A Review, *Journal of*
 1593 *Geophysical Research: Solid Earth*, 123(2), 1350-1365, doi:<https://doi.org/10.1002/2017JB014617>.
- 1594 Hasegawa, A. (2011), Social function of seismologist and seismology community - on the relationship with
 1595 government, *The report of special committee for the Tohoku-oki earthquake*, *Seismological Society of Japan*, 18-22,
 1596 https://www.zisin.jp/publications/pdf/SSJ_final_report.pdf.
- 1597 Hasegawa, A., J. Nakajima, N. Uchida, T. Okada, D. Zhao, T. Matsuzawa, and N. Umino (2009), Plate subduction,
 1598 and generation of earthquakes and magmas in Japan as inferred from seismic observations: An overview, *Gondwana*
 1599 *Research*, 16, 370-400.
- 1600 Hasegawa, A., N. Umino, and A. Takagi (1978), Double-planed structure of the deep seismic zone in the
 1601 northeastern Japan arc, *Tectonophysics*, 47(1-2), 43-58, doi:[http://dx.doi.org/10.1016/0040-1951\(78\)90150-6](http://dx.doi.org/10.1016/0040-1951(78)90150-6).
- 1602 Hasegawa, A., N. Umino, and A. Takagi (1985), Seismicity in the Northeastern Japan Arc and Seismicity Patterns
 1603 before Large Earthquakes, *Kisslinger C., Rikitake T. (eds) Practical Approaches to Earthquake Prediction and*
 1604 *Warning*, doi:10.1007/978-94-017-2738-9_23.
- 1605 Hasegawa, A., and K. Yoshida (2015), Preceding seismic activity and slow slip events in the source area of the 2011
 1606 Mw 9.0 Tohoku-Oki earthquake: a review, *Geoscience Letters*, 2(1), 6, doi:10.1186/s40562-015-0025-0.
- 1607 Hasegawa, A., K. Yoshida, Y. Asano, T. Okada, T. Iinuma, and Y. Ito (2012), Change in stress field after the 2011
 1608 great Tohoku-Oki earthquake, *Earth and Planetary Science Letters*, 355-356, 231-243,
 1609 doi:<http://dx.doi.org/10.1016/j.epsl.2012.08.042>.
- 1610 Hasegawa, A., K. Yoshida, and T. Okada (2011), Nearly complete stress drop in the 2011 Mw 9.0 off the Pacific
 1611 coast of Tohoku Earthquake, *Earth, Planets and Space*, 63(7), 35, doi:10.5047/eps.2011.06.007.
- 1612 Hashimoto, C., A. Noda, and M. Matsu'ura (2012), The M w 9.0 northeast Japan earthquake: total rupture of a
 1613 basement asperity, *Geophysical Journal International*, 189(1), 1-5.
- 1614 Hashimoto, C., A. Noda, T. Sagiya, and M. Matsu'ura (2009), Interplate seismogenic zones along the Kuril-Japan
 1615 trench inferred from GPS data inversion, *Nature Geosci*, 2(2), 141-144,
 1616 doi:http://www.nature.com/ngeo/journal/v2/n2/supinfo/ngeo421_S1.html.
- 1617 Hashimoto, T., and T. Yokota (2019), Successively occurring large earthquakes in the world –comparison of real
 1618 cases with expectations by the space-time ETAS, *JpGU 2019 meeting*, SSS10-P02.
- 1619 Hatori, T. (1972), The Tsunamis generated off Cape Erimo on August 2, 1971 and off Hachijo Island on February
 1620 29, 1972: Tsunami source and distribution of the initial motion of Tsunami, *Zisin 2*, 25(4), 362-370,
 1621 doi:10.4294/zisin1948.25.4_362.
- 1622 Hatori, T. (1974), Tsunami sources on the Pacific side in northeast Japan, *Zisin(2)*, 27, 321-337.
- 1623 Hatori, T. (1975), Sources of Tsunamis generated off Boso Peninsula, *Bulletin of the Earthquake Research Institute*,
 1624 *University of Tokyo*, 50(1), 83-91.
- 1625 Hatori, T. (1976), Source Mechanisms of Tsunamis Associated with the Fukushima-oki Earthquake Swarm in 1938,
 1626 *Zisin 2*, 29(2), 179-190.

- 1627 Hatori, T. (1978), The Tsunami Generated off Miyagi Prefecture in 1978 and Tsunami Activity in the Region,
 1628 *Bulletin of the Earthquake Research Institute, University of Tokyo*, 53(4), 1177-1189.
- 1629 Hatori, T. (1989), Characteristic of Tsunamis Associated with Aftershock and Swarm near Japan, *Zisin* 2, 42, 183-
 1630 188.
- 1631 Hatori, T. (1996), The 1994 Sanriku-Oki Tsunami and Distribution of the Radiating Tsunami Energy in the Sanriku
 1632 Region, *Zisin* 2, 49(1), 19-26.
- 1633 Hatori, T. (2012), The size of the Tsunami of the 2011 Tohoku-oki earthquake, *Report of Tsunami Engineering*, 31,
 1634 325-328.
- 1635 Hayes, G. P. (2011), Rapid source characterization of the 2011 Mw 9.0 off the Pacific coast of Tohoku Earthquake,
 1636 *Earth, Planets and Space*, 63(7), 4, doi:10.5047/eps.2011.05.012.
- 1637 Headquarters for Earthquake Research Promotion (2020), The catalogue of long-term forecast of active faults and
 1638 subduction zone earthquakes, <https://www.jishin.go.jp/main/choukihyoka/ichiran.pdf>.
- 1639 Headquarters for Earthquake Research Promotion, Ministry of Education, Culture, Sports, Science and Technology,
 1640 Japan (2011), The Evaluation of Seismic Activities in Japan, February 2011,
 1641 https://www.static.jishin.go.jp/resource/monthly/2011/2011_02.pdf.
- 1642 Headquarters for Earthquake Research Promotion, Ministry of Education, Culture, Sports, Science and Technology,
 1643 Japan,, (2009), Summary report of the Research and Observation of the Miyagi-Oki Earthquake conducted in 2005-
 1644 2009, https://www.jishin.go.jp/database/project_report/miyagi_juten/.
- 1645 Headquarters of Earthquake Research Promotion, M. o. E., Culture, Sports, Science and Technology, Japan (2000),
 1646 The long-term earthquake forecast of the Miyagi-ken-oki earthquake,
 1647 <https://www.jishin.go.jp/main/chousa/00nov4/miyagi.htm>.
- 1648 Headquarters of Earthquake Research Promotion, M. o. E., Culture, Sports, Science and Technology, Japan (2002),
 1649 Longterm forecast of earthquakes from Sanriku-oki to Boso-oki,
 1650 https://www.jishin.go.jp/main/chousa/kaikou_pdf/sanriku_boso.pdf.
- 1651 Heki, K. (2011), Ionospheric electron enhancement preceding the 2011 Tohoku-Oki earthquake, *Geophysical*
 1652 *Research Letters*, 38(17), doi:10.1029/2011GL047908.
- 1653 Heki, K., and Y. Enomoto (2015), Mw dependence of the preseismic ionospheric electron enhancements, *Journal of*
 1654 *Geophysical Research: Space Physics*, 120(8), 7006-7020, doi:10.1002/2015JA021353.
- 1655 Heki, K., S. Miyazaki, and H. Tsuji (1997), Silent fault slip following an interplate thrust earthquake at the Japan
 1656 Trench, *Nature*, 386(6625), 595-598.
- 1657 Hino, R. (2015), An overview of the Mw 9, 11 March 2011, Tohoku earthquake, *Summary of the Bulletin of the*
 1658 *International Seismological Centre*, 48(1-6), 100-132, doi:10.5281/zenodo.998789.
- 1659 Hino, R., D. Inazu, Y. Ohta, Y. Ito, S. Suzuki, T. Inuma, Y. Osada, M. Kido, H. Fujimoto, and Y. Kaneda (2014),
 1660 Was the 2011 Tohoku-Oki earthquake preceded by aseismic preslip? Examination of seafloor vertical deformation
 1661 data near the epicenter, *Mar Geophys Res*, 35(3), 181-190, doi:10.1007/s11001-013-9208-2.
- 1662 Hino, R., T. Tanioka, T. Kanazawa, S. Sakai, M. Nishino, and K. Suyehiro (2001), Micro-tsunami from a local
 1663 interplate earthquake detected by cabled offshore tsunami observation in northeastern Japan, *Geophys. Res. Lett.*, 28,
 1664 3533-3536.
- 1665 Hirakawa, K. (2012), Outsize tsunami sediments since last years along the Japan and Kuril-Trench: a tentative idea
 1666 on source and supercycle, *Kagaku*, 82, 172-181.
- 1667 Hirono, T., K. Tsuda, W. Tanikawa, J.-P. Ampuero, B. Shibasaki, M. Kinoshita, and J. J. Mori (2016), Near-trench
 1668 slip potential of megaquakes evaluated from fault properties and conditions, *Scientific Reports*, 6(1), 28184,
 1669 doi:10.1038/srep28184.
- 1670 Honsho, C., M. Kido, F. Tomita, and N. Uchida (2019), Offshore Postseismic Deformation of the 2011 Tohoku
 1671 Earthquake Revisited: Application of an Improved GPS-Acoustic Positioning Method Considering Horizontal
 1672 Gradient of Sound Speed Structure, *124(6)*, 5990-6009, doi:10.1029/2018jb017135.
- 1673 Hooper, A., J. Pietrzak, W. Simons, H. Cui, R. Riva, M. Naeije, A. Terwisscha van Scheltinga, E. Schrama, G.
 1674 Stelling, and A. Socquet (2013), Importance of horizontal seafloor motion on tsunami height for the 2011 Mw=9.0
 1675 Tohoku-Oki earthquake, *Earth and Planetary Science Letters*, 361, 469-479,
 1676 doi:<https://doi.org/10.1016/j.epsl.2012.11.013>.
- 1677 Hori, T., T. Matsuzawa, and Y. Yagi (2011), Why the Tohoku-oki was not assumed - identifying problems for new
 1678 seismology, *The report of special committee for the Tohoku-oki earthquake, Seismological Society of Japan*, 125-
 1679 130, https://www.zisin.jp/publications/pdf/SSJ_final_report.pdf.
- 1680 Hori, T., and S. i. Miyazaki (2010), Hierarchical asperity model for multiscale characteristic earthquakes: A
 1681 numerical study for the off-Kamaishi earthquake sequence in the NE Japan subduction zone, *Geophys. Res. Lett.*,
 1682 37(10), L10304, doi:10.1029/2010gl042669.

- 1683 Hoshiba, M., and K. Iwakiri (2011), Initial 30 seconds of the 2011 off the Pacific coast of Tohoku Earthquake (Mw
1684 9.0)—amplitude and τ for magnitude estimation for Earthquake Early Warning—, *Earth, Planets and Space*, 63(7),
1685 8, doi:10.5047/eps.2011.06.015.
- 1686 Hossen, M. J., P. R. Cummins, J. Dettmer, and T. Baba (2015), Tsunami waveform inversion for sea surface
1687 displacement following the 2011 Tohoku earthquake: Importance of dispersion and source kinematics, *Journal of*
1688 *Geophysical Research: Solid Earth*, 120(9), 6452-6473, doi:10.1002/2015JB011942.
- 1689 Hu, Y., R. Bürgmann, N. Uchida, P. Banerjee, and J. T. Freymueller (2016), Stress-driven relaxation of
1690 heterogeneous upper mantle and time-dependent afterslip following the 2011 Tohoku earthquake, *Journal of*
1691 *Geophysical Research: Solid Earth*, 2015JB012508, doi:10.1002/2015JB012508.
- 1692 Hua, Y., D. Zhao, G. Toyokuni, and Y. Xu (2020), Tomography of the source zone of the great 2011 Tohoku
1693 earthquake, *Nature Communications*, 11(1), 1163, doi:10.1038/s41467-020-14745-8.
- 1694 Hyndman, R. D., and K. Wang (1993), Thermal Constraints on the Zone of Major Thrust Earthquake Failure - the
1695 Cascadia Subduction Zone, *J Geophys Res-Sol Ea*, 98(B2), 2039-2060.
- 1696 Ide, S., and H. Aochi (2005), Earthquakes as multiscale dynamic ruptures with heterogeneous fracture surface
1697 energy, *Journal of Geophysical Research: Solid Earth*, 110(B11), doi:doi:10.1029/2004JB003591.
- 1698 Ide, S., A. Baltay, and G. C. Beroza (2011), Shallow dynamic overshoot and energetic deep rupture in the 2011 Mw
1699 9.0 Tohoku-oki earthquake, *Science*, 332, 1427-1429.
- 1700 Igarashi, T., T. Matsuzawa, and A. Hasegawa (2003), Repeating earthquakes and interplate aseismic slip in the
1701 northeastern Japan subduction zone, *J. Geophys. Res.*, 108, 10.1029/2002JB001920.
- 1702 Igarashi, T., T. Matsuzawa, N. Umino, and A. Hasegawa (2001), Spatial distribution of focal mechanisms for
1703 interplate and intraplate earthquakes associated with the subducting Pacific plate beneath the northeastern Japan arc:
1704 A triple-plated deep seismic zone, *J. Geophys. Res.*, 106, 2177-2191.
- 1705 Iinuma, T. (2018), Monitoring of the spatio-temporal change in the interplate coupling at northeastern Japan
1706 subduction zone based on the spatial gradients of surface velocity field, *Geophysical Journal International*, 213(1),
1707 30-47, doi:10.1093/gji/ggx527.
- 1708 Iinuma, T., et al. (2012), Coseismic slip distribution of the 2011 off the Pacific Coast of Tohoku Earthquake (M9.0)
1709 refined by means of seafloor geodetic data, *J. Geophys. Res.*, 117, doi:10.1029/2012JB009186.
- 1710 Iinuma, T., R. Hino, N. Uchida, W. Nakamura, M. Kido, Y. Osada, and S. Miura (2016), Seafloor observations
1711 indicate spatial separation of coseismic and postseismic slips in the 2011 Tohoku earthquake, *Nature*
1712 *Communications*, 7, 13506, doi:10.1038/ncomms13506
1713 <http://www.nature.com/articles/ncomms13506#supplementary-information>.
- 1714 Ikeda, Y. (1996), Implications of active fault study for the present-day tectonics of the Japan arc, *Active Fault*
1715 *Research (Katsudanso Kenkyu)*, 15, 93-99.
- 1716 Ikehara, K., T. Kanamatsu, Y. Nagahashi, M. Strasser, H. Fink, K. Usami, T. Irino, and G. Wefer (2016),
1717 Documenting large earthquakes similar to the 2011 Tohoku-oki earthquake from sediments deposited in the Japan
1718 Trench over the past 1500 years, *Earth and Planetary Science Letters*, 445, 48-56,
1719 doi:<https://doi.org/10.1016/j.epsl.2016.04.009>.
- 1720 Ikehara, K., K. Usami, and T. Kanamatsu (2020), Repeated occurrence of surface-sediment remobilization along the
1721 landward slope of the Japan Trench by great earthquakes, *Earth, Planets and Space*, 72(1), 114,
1722 doi:10.1186/s40623-020-01241-y.
- 1723 Ikehara, K., K. Usami, T. Kanamatsu, K. Arai, A. Yamaguchi, and R. Fukuchi (2018), Spatial variability in
1724 sediment lithology and sedimentary processes along the Japan Trench: use of deep-sea turbidite records to
1725 reconstruct past large earthquakes, *Geological Society, London, Special Publications*, 456(1), 75,
1726 doi:10.1144/SP456.9.
- 1727 Ikuta, R., T. Hisada, G. Karakama, and O. Kuwano *Was the observed pre-seismic total electron content*
1728 *enhancement a true precursor of the 2011 Tohoku-Oki Earthquake?* %J *Earth and Space Science Open Archive*, 33
1729 pp., doi:doi:10.1002/essoar.10502392.2.
- 1730 Imai, K., T. Maeda, T. Iinuma, Y. Ebina, D. Sugawara, F. Imamura, and A. Hirakawa (2015), Paleo tsunami source
1731 estimation by using combination optimization algorithm - Case study of The 1611
1732 Keicho earthquake tsunami, *Tohoku Journal of Natural Disaster Science*, 51, 139-144.
- 1733 Imanishi, K., R. Ando, and Y. Kuwahara (2012), Unusual shallow normal-faulting earthquake sequence in
1734 compressional northeast Japan activated after the 2011 off the Pacific coast of Tohoku earthquake, *Geophysical*
1735 *Research Letters*, 39(9), L09306, doi:10.1029/2012GL051491.
- 1736 Ishimura, D., and T. Miyauchi (2015), Historical and paleo-tsunami deposits during the last 4000 years and their
1737 correlations with historical tsunami events in Koyadori on the Sanriku Coast, northeastern Japan, *Progress in Earth*
1738 *and Planetary Science*, 2(1), 16, doi:10.1186/s40645-015-0047-4.

- 1739 Ito, T., K. Ozawa, T. Watanabe, and T. Sagiya (2011a), Slip distribution of the 2011 off the Pacific coast of Tohoku
1740 Earthquake inferred from geodetic data, *Earth, Planets and Space*, 63(7), 21, doi:10.5047/eps.2011.06.023.
- 1741 Ito, Y., et al. (2013), Episodic slow slip events in the Japan subduction zone before the 2011 Tohoku-Oki
1742 earthquake, *Tectonophysics*, 600(0), 14-26, doi:<http://dx.doi.org/10.1016/j.tecto.2012.08.022>.
- 1743 Ito, Y., T. Tsuji, Y. Osada, M. Kido, D. Inazu, Y. Hayashi, H. Tsushima, R. Hino, and H. Fujimoto (2011b), Frontal
1744 wedge deformation near the source region of the 2011 Tohoku-Oki earthquake, *Geophysical Research Letters*,
1745 38(7), doi:10.1029/2011GL048355.
- 1746 Japan Meteorological Agency (2013), Lessons learned from the tsunami disaster caused by the 2011 Great East
1747 Japan Earthquake and improvements in JMA's tsunami warning system,
1748 <https://www.jma.go.jp/jma/en/Publications/publications.html>.
- 1749 Japan Meteorological Agency (2019), On the launch of the Nankai trough earthquake extra information
1750 https://www.jma.go.jp/jma/press/1905/31a/20190531_nreq_name.html.
- 1751 Johnson, K. M., J. i. Fukuda, and P. Segall (2012), Challenging the rate-state asperity model: Afterslip following the
1752 2011 M9 Tohoku-oki, Japan, earthquake, *Geophysical Research Letters*, 39(20), n/a-n/a,
1753 doi:10.1029/2012GL052901.
- 1754 Jordan, T. H., Y.-T. Chen, P. Gasparini, R. Madariaga, I. Main, W. Marzocchi, G. Papadopoulos, G. Sobolev, K.
1755 Yamaoka, and J. Zschau (2011), Operational earthquake forecasting. State of knowledge and guidelines for
1756 utilization, *Annals of Geophysics*, 54(4).
- 1757 JR East (2019), On the addition of sea-bottom seismometers to the Shinkansen Early Earthquake Detection System,
1758 <https://www.jreast.co.jp/press/2018/20190110.pdf>.
- 1759 Kagan, Y. Y. (1997), Seismic moment-frequency relation for shallow earthquakes: Regional comparison, *Journal of*
1760 *Geophysical Research: Solid Earth*, 102(B2), 2835-2852, doi:10.1029/96JB03386.
- 1761 Kagan, Y. Y., and D. D. Jackson (2013), Tohoku Earthquake: A Surprise?, *B Seismol Soc Am*, 103(2B), 1181-1194,
1762 doi:10.1785/0120120110.
- 1763 Kahoku-shinpo (2011), The relationship between the Sanriku-oki M7.3 earthquake and Miyagi-ken-oki earthquake -
1764 the possibility of a multisegment rupture decreased?, *March 10, 2011, Kahoku-shinpo (news paper)*.
- 1765 Kaizuka, S., and T. Imaizumi (1984), Horizontal strain rates of the Japanese islands estimated from quaternary fault
1766 data, *Geographical Reports of Tokyo Metropolitan University*, 19, 43-65.
- 1767 Kamogawa, M., and Y. Kakinami (2013), Is an ionospheric electron enhancement preceding the 2011 Tohoku-Oki
1768 earthquake a precursor?, *Journal of Geophysical Research: Space Physics*, 118(4), 1751-1754,
1769 doi:10.1002/jgra.50118.
- 1770 Kanamori, H. (1972), Mechanism of tsunami earthquakes, *Physics of the Earth and Planetary Interiors*, 6(5), 346-
1771 359, doi:[https://doi.org/10.1016/0031-9201\(72\)90058-1](https://doi.org/10.1016/0031-9201(72)90058-1).
- 1772 Kanamori, H., M. Miyazawa, and J. Mori (2006), Investigation of the earthquake sequence off Miyagi prefecture
1773 with historical seismograms, *Earth, Planets and Space*, 58(12), 1533-1541, doi:10.1186/BF03352657.
- 1774 Kano, M., A. Kato, and K. Obara (2019), Episodic tremor and slip silently invades strongly locked megathrust in the
1775 Nankai Trough, *Scientific Reports*, 9(1), 9270, doi:10.1038/s41598-019-45781-0.
- 1776 Katakami, S., Y. Ito, K. Ohta, R. Hino, S. Suzuki, and M. Shinohara (2018), Spatiotemporal Variation of Tectonic
1777 Tremor Activity Before the Tohoku-Oki Earthquake, *Journal of Geophysical Research: Solid Earth*, 123(11), 9676-
1778 9688, doi:10.1029/2018JB016651.
- 1779 Kato, A., and Y. Ben-Zion (2020), The generation of large earthquakes, *Nature Reviews Earth & Environment*,
1780 doi:10.1038/s43017-020-00108-w.
- 1781 Kato, A., J. i. Fukuda, and K. Obara (2013), Response of seismicity to static and dynamic stress changes induced by
1782 the 2011 M9.0 Tohoku-Oki earthquake, *Geophysical Research Letters*, 40(14), 3572-3578,
1783 doi:<https://doi.org/10.1002/grl.50699>.
- 1784 Kato, A., and T. Igarashi (2012), Regional extent of the large coseismic slip zone of the 2011 Mw 9.0 Tohoku-Oki
1785 earthquake delineated by on-fault aftershocks, *Geophysical Research Letters*, 39(15), n/a-n/a,
1786 doi:10.1029/2012gl052220.
- 1787 Kato, A., K. Obara, T. Igarashi, H. Tsuruoka, S. Nakagawa, and N. Hirata (2012), Propagation of Slow Slip Leading
1788 Up to the 2011 Mw 9.0 Tohoku-Oki Earthquake, *Science*, 335(6069), 705-708, doi:10.1126/science.1215141.
- 1789 Katsumata, K. (2011), A long-term seismic quiescence started 23 years before the 2011 off the Pacific coast of
1790 Tohoku Earthquake (M = 9.0), *Earth, Planets and Space*, 63(7), 36, doi:10.5047/eps.2011.06.033.
- 1791 Kawasaki, I., Y. Asai, and Y. Tamura (2001), Space-time distribution of interplate moment release including slow
1792 earthquakes and the seismo-geodetic coupling in the Sanriku-oki region along the Japan trench, *Tectonophysics*,
1793 330(3), 267-283, doi:[https://doi.org/10.1016/S0040-1951\(00\)00245-6](https://doi.org/10.1016/S0040-1951(00)00245-6).

- 1794 Kido, M., Y. Osada, H. Fujimoto, R. Hino, and Y. Ito (2011), Trench-normal variation in observed seafloor
1795 displacements associated with the 2011 Tohoku-Oki earthquake, *Geophysical Research Letters*, 38(24),
1796 doi:10.1029/2011GL050057.
- 1797 Kiser, E., and M. Ishii (2013), Hidden aftershocks of the 2011 Mw 9.0 Tohoku, Japan earthquake imaged with the
1798 backprojection method, *Journal of Geophysical Research: Solid Earth*, 118(10), 5564-5576,
1799 doi:10.1002/2013JB010158.
- 1800 Kita, S., T. Okada, A. Hasegawa, J. Nakajima, and T. Matsuzawa (2010a), Anomalous deepening of a seismic belt
1801 in the upper-plane of the double seismic zone in the Pacific slab beneath the Hokkaido corner : Possible evidence for
1802 thermal shielding caused by subducted forearc crust materials, *Earth Planet. Sci. Lett.*, 290, 415-426.
- 1803 Kita, S., T. Okada, A. Hasegawa, J. Nakajima, and T. Matsuzawa (2010b), Existence of interplane earthquakes and
1804 neutral stress boundary between the upper and lower planes of the double seismic zone beneath Tohoku and
1805 Hokkaido, northeastern Japan, *Tectonophysics*, 496(1-4), 68-82, doi:<http://dx.doi.org/10.1016/j.tecto.2010.10.010>.
- 1806 Kobayashi, T., M. Tobita, T. Nishimura, A. Suzuki, Y. Noguchi, and M. Yamanaka (2011), Crustal deformation
1807 map for the 2011 off the Pacific coast of Tohoku Earthquake, detected by InSAR analysis combined with GEONET
1808 data, *Earth, Planets and Space*, 63(7), 20, doi:10.5047/eps.2011.06.043.
- 1809 Kodaira, S., T. Fujiwara, G. Fujie, Y. Nakamura, and T. Kanamatsu (2020), Large Coseismic Slip to the Trench
1810 During the 2011 Tohoku-Oki Earthquake, *Annual Review of Earth and Planetary Sciences*, 48(1), 321-343,
1811 doi:10.1146/annurev-earth-071719-055216.
- 1812 Kodaira, S., T. No, Y. Nakamura, T. Fujiwara, Y. Kaiho, S. Miura, N. Takahashi, Y. Kaneda, and A. Taira (2012),
1813 Coseismic fault rupture at the trench axis during the 2011 Tohoku-oki earthquake, *Nature Geoscience*, 5(9), 646-
1814 650, doi:10.1038/ngeo1547.
- 1815 Koketsu, K., et al. (2011), A unified source model for the 2011 Tohoku earthquake, *Earth and Planetary Science*
1816 *Letters*, 310(3-4), 480-487, doi:10.1016/j.epsl.2011.09.009.
- 1817 Konca, A. O., et al. (2008), Partial rupture of a locked patch of the Sumatra megathrust during the 2007 earthquake
1818 sequence, *Nature*, 456(7222), 631-635, doi:10.1038/nature07572.
- 1819 Kozdon, J. E., and E. M. Dunham (2013), Rupture to the Trench: Dynamic Rupture Simulations of the 11 March
1820 2011 Tohoku Earthquake, *B Seismol Soc Am*, 103(2B), 1275-1289, doi:10.1785/0120120136.
- 1821 Kubo, H., K. Asano, and T. Iwata (2013), Source-rupture process of the 2011 Ibaraki-oki, Japan, earthquake (Mw
1822 7.9) estimated from the joint inversion of strong-motion and GPS Data: Relationship with seamount and Philippine
1823 Sea Plate, *Geophysical Research Letters*, 40(12), 3003-3007, doi:10.1002/grl.50558.
- 1824 Kubo, H., and Y. Kakehi (2013), Source Process of the 2011 Tohoku Earthquake Estimated from the Joint Inversion
1825 of Teleseismic Body Waves and Geodetic Data Including Seafloor Observation Data: Source Model with Enhanced
1826 Reliability by Using Objectively Determined Inversion Settings, *B Seismol Soc Am*, 103(2B), 1195-1220,
1827 doi:10.1785/0120120113.
- 1828 Kubo, H., and T. Nishikawa (2020), Relationship of preseismic, coseismic, and postseismic fault ruptures of two
1829 large interplate aftershocks of the 2011 Tohoku earthquake with slow-earthquake activity, *Scientific Reports*, 10(1),
1830 12044, doi:10.1038/s41598-020-68692-x.
- 1831 Kubota, T., R. Hino, D. Inazu, and S. Suzuki (2019), Fault model of the 2012 doublet earthquake, near the up-dip
1832 end of the 2011 Tohoku-Oki earthquake, based on a near-field tsunami: implications for intraplate stress state,
1833 *Progress in Earth and Planetary Science*, 6(1), 67, doi:10.1186/s40645-019-0313-y.
- 1834 Kurahashi, S., and K. Irikura (2011), Source model for generating strong ground motions during the 2011 off the
1835 Pacific coast of Tohoku Earthquake, *Earth, Planets and Space*, 63(7), 11, doi:10.5047/eps.2011.06.044.
- 1836 Kyriakopoulos, C., T. Masterlark, S. Stramondo, M. Chini, and C. Bignami (2013), Coseismic slip distribution for
1837 the Mw 9 2011 Tohoku-Oki earthquake derived from 3-D FE modeling, *Journal of Geophysical Research: Solid*
1838 *Earth*, 118(7), 3837-3847, doi:10.1002/jgrb.50265.
- 1839 Lay, T. (2018), A review of the rupture characteristics of the 2011 Tohoku-oki Mw 9.1 earthquake, *Tectonophysics*,
1840 733, 4-36, doi:<https://doi.org/10.1016/j.tecto.2017.09.022>.
- 1841 Lay, T., C. J. Ammon, H. Kanamori, M. J. Kim, and L. Xue (2011a), Outer trench-slope faulting and the 2011 Mw
1842 9.0 off the Pacific coast of Tohoku Earthquake, *Earth, planets and space*, 63(7), 713-718.
- 1843 Lay, T., C. J. Ammon, H. Kanamori, L. Rivera, K. D. Koper, and A. R. Hutko (2010), The 2009 Samoa-Tonga great
1844 earthquake triggered doublet, *Nature*, 466(7309), 964-968,
1845 doi:<http://www.nature.com/nature/journal/v466/n7309/abs/nature09214.html#supplementary-information>.
- 1846 Lay, T., C. J. Ammon, H. Kanamori, L. Xue, and M. J. Kim (2011b), Possible large near-trench slip during the 2011
1847 M(w) 9.0 off the Pacific coast of Tohoku Earthquake, *Earth Planets and Space*, 63(7), 687-692,
1848 doi:10.5047/eps.2011.05.033.

- 1849 Lay, T., H. Kanamori, C. J. Ammon, K. D. Koper, A. R. Hutko, L. Ye, H. Yue, and T. M. Rushing (2012), Depth-
 1850 varying rupture properties of subduction zone megathrust faults, *Journal of Geophysical Research: Solid Earth*,
 1851 *117*(B4), doi:10.1029/2011JB009133.
- 1852 Lee, S.-J., B.-S. Huang, M. Ando, H.-C. Chiu, and J.-H. Wang (2011), Evidence of large scale repeating slip during
 1853 the 2011 Tohoku-Oki earthquake, *Geophys. Res. Lett.*, *38*(19), L19306, doi:10.1029/2011gl049580.
- 1854 Lengliné, O., B. Enescu, Z. Peng, and K. Shiomi (2012), Decay and expansion of the early aftershock activity
 1855 following the 2011, Mw9.0 Tohoku earthquake, *Geophysical Research Letters*, *39*(18),
 1856 doi:<https://doi.org/10.1029/2012GL052797>.
- 1857 Lin, W., M. Conin, J. C. Moore, F. M. Chester, Y. Nakamura, J. J. Mori, L. Anderson, E. E. Brodsky, and N. Eguchi
 1858 (2013), Stress State in the Largest Displacement Area of the 2011 Tohoku-Oki Earthquake, *Science*, *339*(6120), 687,
 1859 doi:10.1126/science.1229379.
- 1860 Loveless, J. P., and B. J. Meade (2010), Geodetic imaging of plate motions, slip rates, and partitioning of
 1861 deformation in Japan, *Journal of Geophysical Research: Solid Earth*, *115*(B2), B02410, doi:10.1029/2008jb006248.
- 1862 Maeda, T., T. Furumura, S. i. Sakai, and M. Shinohara (2011), Significant tsunami observed at ocean-bottom
 1863 pressure gauges during the 2011 off the Pacific coast of Tohoku Earthquake, *Earth, Planets and Space*, *63*(7), 53,
 1864 doi:10.5047/eps.2011.06.005.
- 1865 Masci, F., J. N. Thomas, F. Villani, J. A. Secan, and N. Rivera (2015), On the onset of ionospheric precursors 40
 1866 min before strong earthquakes, *Journal of Geophysical Research: Space Physics*, *120*(2), 1383-1393,
 1867 doi:10.1002/2014JA020822.
- 1868 Matsuo, K., and K. Heki (2011), Coseismic gravity changes of the 2011 Tohoku-Oki earthquake from satellite
 1869 gravimetry, *Geophysical Research Letters*, *38*(7), doi:<https://doi.org/10.1029/2011GL049018>.
- 1870 Matsuzawa, T. (2011), Why could the M9 earthquake occur in the northeastern Japan subduction zone?: Why did
 1871 we believe it would not occur there?, *Kagaku*, *81*(10), 1020-1026.
- 1872 Matsuzawa, T., Y. Asano, and K. Obara (2015), Very low frequency earthquakes off the Pacific coast of Tohoku,
 1873 Japan, *Geophysical Research Letters*, *42*(11), 4318-4325, doi:<https://doi.org/10.1002/2015GL063959>.
- 1874 Matsuzawa, T., B. Shibazaki, K. Obara, and H. Hirose (2013), Comprehensive model of short- and long-term slow
 1875 slip events in the Shikoku region of Japan, incorporating a realistic plate configuration, *Geophysical Research*
 1876 *Letters*, *40*(19), 5125-5130, doi:10.1002/grl.51006.
- 1877 Mavrommatis, A. P., P. Segall, and K. M. Johnson (2014), A decadal-scale deformation transient prior to the 2011
 1878 Mw 9.0 Tohoku-oki earthquake, *Geophysical Research Letters*, *41*(13), 4486-4494, doi:10.1002/2014gl060139.
- 1879 Mavrommatis, A. P., P. Segall, N. Uchida, and K. M. Johnson (2015), Long-term acceleration of aseismic slip
 1880 preceding the Mw 9 Tohoku-oki earthquake: Constraints from repeating earthquakes, *Geophysical Research Letters*,
 1881 *2015GL066069*, doi:10.1002/2015GL066069.
- 1882 Mazzotti, S. p., and J. Adams (2004), Variability of Near-Term Probability for the Next Great Earthquake on the
 1883 Cascadia Subduction Zone, *B Seismol Soc Am*, *94*(5), 1954-1959, doi:10.1785/012004032.
- 1884 McCaffrey, R. (2008), Global frequency of magnitude 9 earthquakes, *Geology*, *36*(3), 263-266,
 1885 doi:10.1130/G24402A.1.
- 1886 McHugh, C. M., T. Kanamatsu, L. Seeber, R. Bopp, M.-H. Cormier, and K. Usami (2016), Remobilization of
 1887 surficial slope sediment triggered by the A.D. 2011 Mw 9 Tohoku-Oki earthquake and tsunami along the Japan
 1888 Trench, *Geology*, *44*(5), 391-394, doi:10.1130/G37650.1.
- 1889 McLaskey, G. C. (2019), Earthquake Initiation From Laboratory Observations and Implications for Foreshocks,
 1890 *Journal of Geophysical Research: Solid Earth*, *124*(12), 12882-12904, doi:<https://doi.org/10.1029/2019JB018363>.
- 1891 Meade, B. J., and J. P. Loveless (2009), Predicting the geodetic signature of MW \geq 8 slow slip events, *Geophysical*
 1892 *Research Letters*, *36*(1), doi:<https://doi.org/10.1029/2008GL036364>.
- 1893 Melgar, D., and Y. Bock (2015), Kinematic earthquake source inversion and tsunami runup prediction with regional
 1894 geophysical data, *Journal of Geophysical Research: Solid Earth*, *120*(5), 3324-3349, doi:10.1002/2014JB011832.
- 1895 Meneses-Gutierrez, A., and T. Sagiya (2016), Persistent inelastic deformation in central Japan revealed by GPS
 1896 observation before and after the Tohoku-oki earthquake, *Earth and Planetary Science Letters*, *450*, 366-371,
 1897 doi:<https://doi.org/10.1016/j.epsl.2016.06.055>.
- 1898 Minoura, K., F. Imamura, D. Sugawara, Y. Kono, and T. J. J. o. N. D. S. Iwashita (2001), The 869 Jogan tsunami
 1899 deposit and recurrence interval of large-scale tsunami on the Pacific coast of northeast Japan, *23*, 83-88.
- 1900 Minoura, K., and S. Nakaya (1991), Traces of Tsunami preserved in inter-tidal lacustrine and marsh deposits - Some
 1901 examples from northeast Japan, *J. Geol.*, *99*(2), 265-287.
- 1902 Minson, S. E., M. Simons, J. L. Beck, F. Ortega, J. Jiang, S. E. Owen, A. W. Moore, A. Inbal, and A. Sladen (2014),
 1903 Bayesian inversion for finite fault earthquake source models – II: the 2011 great Tohoku-oki, Japan earthquake,
 1904 *Geophysical Journal International*, *198*(2), 922-940, doi:10.1093/gji/ggu170.

- 1905 Miyazawa, M. (2011), Propagation of an earthquake triggering front from the 2011 Tohoku-Oki earthquake,
 1906 *Geophysical Research Letters*, 38(23), doi:10.1029/2011GL049795.
- 1907 Mogi, K. (1969), Some Features of Recent Seismic Activity in and near Japan (2) : Activity before and after Great
 1908 Earthquakes, *Bulletin of the Earthquake Research Institute, University of Tokyo*, 47(3), 395 - 417.
- 1909 Molenaar, A., J. Moernaut, G. Wiemer, N. Dubois, and M. Strasser (2019), Earthquake Impact on Active Margins:
 1910 Tracing Surficial Remobilization and Seismic Strengthening in a Slope Sedimentary Sequence, *Geophysical
 1911 Research Letters*, 46(11), 6015-6023, doi:10.1029/2019GL082350.
- 1912 Mori, N., T. Takahashi, T. Yasuda, and H. Yanagisawa (2011), Survey of 2011 Tohoku earthquake tsunami
 1913 inundation and run-up, *Geophysical Research Letters*, 38(7), doi:10.1029/2011GL049210.
- 1914 Murotani, T., M. Kikuchi, and Y. Yamanaka (2003), Rupture processes of large Fukushima-Oki Earthquakes in
 1915 1938, presented at the 2003 Japan Geoscience Union, Chiba, Japan, S052-004.
- 1916 Murray, J., and J. Langbein (2006), Slip on the San Andreas Fault at Parkfield, California, over Two Earthquake
 1917 Cycles, and the Implications for Seismic Hazard, *B Seismol Soc Am*, 96(4B), S283-S303, doi:10.1785/0120050820.
- 1918 Muto, J., B. Shibazaki, T. Iinuma, Y. Ito, Y. Ohta, S. Miura, and Y. Nakai (2016), Heterogeneous rheology
 1919 controlled postseismic deformation of the 2011 Tohoku-Oki earthquake, *Geophysical Research Letters*, 43(10),
 1920 4971-4978, doi:<https://doi.org/10.1002/2016GL068113>.
- 1921 Nakajima, H., and M. Koarai (2011), Assessment of tsunami flood situation from the Great East Japan Earthquake,
 1922 *Bulletin of the Geospatial Information Authority of Japan*, 59.
- 1923 Nakajima, J., A. Hasegawa, and S. Kita (2011), Seismic evidence for reactivation of a buried hydrated fault in the
 1924 Pacific slab by the 2011 M9.0 Tohoku earthquake, *Geophysical Research Letters*, 38(7),
 1925 doi:<https://doi.org/10.1029/2011GL048432>.
- 1926 Nakamura, W., N. Uchida, and T. Matsuzawa (2016), Spatial distribution of the faulting types of small earthquakes
 1927 around the 2011 Tohoku - oki earthquake: A comprehensive search using template events, *Journal of Geophysical
 1928 Research: Solid Earth*, 121(4), 2591-2607, doi:doi:10.1002/2015JB012584.
- 1929 Nakamura, Y., T. Fujiwara, S. Kodaira, S. Miura, and K. Obana (2020), Correlation of frontal prism structures and
 1930 slope failures near the trench axis with shallow megathrust slip at the Japan Trench, *Scientific Reports*, 10(1), 11607,
 1931 doi:10.1038/s41598-020-68449-6.
- 1932 Nakata, R., T. Hori, M. Hyodo, and K. Ariyoshi (2016), Possible scenarios for occurrence of M ~ 7 interplate
 1933 earthquakes prior to and following the 2011 Tohoku-Oki earthquake based on numerical simulation, *Scientific
 1934 Reports*, 6(1), 25704, doi:10.1038/srep25704.
- 1935 Nakatani, M. (2020), Evaluation of Phenomena Preceding Earthquakes and Earthquake Predictability, *Journal of
 1936 Disaster Research*, 15(2), 112-143, doi:10.20965/jdr.2020.p0112.
- 1937 Namegaya, Y., and K. Satake (2014), Reexamination of the A.D. 869 Jogan earthquake size from tsunami deposit
 1938 distribution, simulated flow depth, and velocity, *Geophysical Research Letters*, 41(7), 2297-2303,
 1939 doi:10.1002/2013GL058678.
- 1940 Namegaya, Y., K. Satake, and S. Yamaki (2010), Numerical simulation of the AD 869 Jogan tsunami in Ishinomaki
 1941 and Sendai
 1942 plains and Ukedo river-mouth lowland, *Annu. Rep. Active Fault Paleoequake Res.*, 10, 1-21.
- 1943 Namegaya, Y., and T. Yata (2014), Tsunamis which affected the Pacific coast of eastern Japan in medieval times
 1944 inferred from historical documents, *Zisin (Journal of the Seismological Society of Japan. 2nd ser.)*, 66, 73-81,
 1945 doi:10.4249/zisin.66.73.
- 1946 Nanayama, F., K. Satake, R. Furukawa, K. Shimokawa, B. F. Atwater, K. Shigeno, and S. Yamaki (2003),
 1947 Unusually large earthquakes inferred from tsunami deposits along the Kuril trench, *Nature*, 424(6949), 660-663,
 1948 doi:10.1038/nature01864.
- 1949 Nanjo, K. Z., N. Hirata, K. Obara, and K. Kasahara (2012), Decade-scale decrease in b value prior to the M9-class
 1950 2011 Tohoku and 2004 Sumatra quakes, *Geophysical Research Letters*, 39(20), doi:doi:10.1029/2012GL052997.
- 1951 Nanjo, K. Z., H. Tsuruoka, N. Hirata, and T. H. Jordan (2011), Overview of the first earthquake forecast testing
 1952 experiment in Japan, *Earth, Planets and Space*, 63(3), 1, doi:10.5047/eps.2010.10.003.
- 1953 National Research Institute for Earth Science and Disaster Resilience (2019), NIED S-net, *National Research
 1954 Institute for Earth Science and Disaster Resilience*, 10.17598/NIED.10007
- 1955 Nishikawa, T., T. Matsuzawa, K. Ohta, N. Uchida, T. Nishimura, and S. Ide (2019), The slow earthquake spectrum
 1956 in the Japan Trench illuminated by the S-net seafloor observatories, *Science*, 365, 808-813,
 1957 doi:doi:10.1126/science.aax5618.
- 1958 Nishimura, T., S. Miura, K. Tachibana, K. Hashimoto, T. Sato, S. Hori, E. Murakami, T. Kono, and M. M. K. Nida,
 1959 T. Hirasawa, S. Miyazaki (2000), Distribution of seismic coupling on the subducting plate boundary in northeastern
 1960 Japan inferred from GPS observations, *Tectonophysics*, 323, 217-238.

- 1961 Nishimura, T., M. Sato, and T. Sagiya (2014), Global Positioning System (GPS) and GPS-Acoustic Observations:
 1962 Insight into Slip Along the Subduction Zones Around Japan, *Annual Review of Earth and Planetary Sciences*, 42(1),
 1963 653-674, doi:10.1146/annurev-earth-060313-054614.
- 1964 Noda, H., and N. Lapusta (2013), Stable creeping fault segments can become destructive as a result of dynamic
 1965 weakening, *Nature*, 493(7433), 518-521,
 1966 doi:<http://www.nature.com/nature/journal/v493/n7433/abs/nature11703.html#supplementary-information>.
- 1967 Obana, K., G. Fujie, T. Takahashi, Y. Yamamoto, Y. Nakamura, S. Kodaira, N. Takahashi, Y. Kaneda, and M.
 1968 Shinohara (2012), Normal-faulting earthquakes beneath the outer slope of the Japan Trench after the 2011 Tohoku
 1969 earthquake: Implications for the stress regime in the incoming Pacific plate, *Geophysical Research Letters*, 39(7),
 1970 L00G24, doi:10.1029/2011gl050399.
- 1971 Obara, K., and A. Kato (2016), Connecting slow earthquakes to huge earthquakes, *Science*, 353(6296), 253-257,
 1972 doi:10.1126/science.aaf1512.
- 1973 Ohta, Y., et al. (2012a), Geodetic constraints on afterslip characteristics following the March 9, 2011, Sanriku-oki
 1974 earthquake, Japan, *Geophysical Research Letters*, 39(16), doi:10.1029/2012GL052430.
- 1975 Ohta, Y., et al. (2012b), Quasi real-time fault model estimation for near-field tsunami forecasting based on RTK-
 1976 GPS analysis: Application to the 2011 Tohoku-Oki earthquake (Mw 9.0), 117(B2), doi:10.1029/2011jb008750.
- 1977 Ohzono, M., Y. Yabe, T. Inuma, Y. Ohta, S. Miura, K. Tachibana, T. Sato, and T. Demachi (2013), Strain
 1978 anomalies induced by the 2011 Tohoku Earthquake (Mw 9.0) as observed by a dense GPS network in northeastern
 1979 Japan, *Earth, Planets and Space*, 64(12), 17, doi:10.5047/eps.2012.05.015.
- 1980 Okada, T., et al. (2015), Hypocenter migration and crustal seismic velocity distribution observed for the inland
 1981 earthquake swarms induced by the 2011 Tohoku-Oki earthquake in NE Japan: implications for crustal fluid
 1982 distribution and crustal permeability, *Geofluids*, 15(1-2), 293-309, doi:10.1111/gfl.12112.
- 1983 Okada, T., K. Yoshida, S. Ueki, J. Nakajima, N. Uchida, T. Matsuzawa, N. Umino, A. Hasegawa, and E. Group for
 1984 the aftershock observations of the off the Pacific coast of Tohoku (2011), Shallow inland earthquakes in NE Japan
 1985 possibly triggered by the 2011 off the Pacific coast of Tohoku Earthquake, *Earth, Planets and Space*, 63(7), 44,
 1986 doi:10.5047/eps.2011.06.027.
- 1987 Oleskevich, D. A., R. D. Hyndman, and K. Wang (1999), The updip and downdip limits to great subduction
 1988 earthquakes: Thermal and structural models of Cascadia, south Alaska, SW Japan, and Chile, *Journal of*
 1989 *Geophysical Research: Solid Earth*, 104(B7), 14965-14991, doi:10.1029/1999JB900060.
- 1990 Orihara, Y., M. Kamogawa, Y. Noda, and T. Nagao (2019), Is Japanese Folklore Concerning Deep - Sea Fish
 1991 Appearance a Real Precursor of Earthquakes?, *B Seismol Soc Am*, 109(4), 1556-1562, doi:10.1785/0120190014.
- 1992 Ozawa, S., T. Nishimura, H. Munekane, H. Suito, T. Kobayashi, M. Tobita, and T. Imakiire (2012), Preceding,
 1993 coseismic, and postseismic slips of the 2011 Tohoku earthquake, Japan, *J Geophys Res*, doi:10.1029/2011JB009120.
- 1994 Ozawa, S., T. Nishimura, H. Suito, T. Kobayashi, M. Tobita, and T. Imakiire (2011), Coseismic and postseismic slip
 1995 of the 2011 magnitude 9 Tohoku-oki earthquake, *Nature*, 10.1038/nature10227.
- 1996 Pacheco, J. F., L. R. Sykes, and C. H. Scholz (1993), Nature of seismic coupling along simple plate boundaries of
 1997 the subduction type, *Journal of Geophysical Research: Solid Earth*, 98(B8), 14133-14159, doi:10.1029/93jb00349.
- 1998 Panet, I., S. Bonvalot, C. Narteau, D. Remy, and J.-M. Lemoine (2018), Migrating pattern of deformation prior to
 1999 the Tohoku-Oki earthquake revealed by GRACE data, *Nature Geoscience*, 11(5), 367-373, doi:10.1038/s41561-018-
 2000 0099-3.
- 2001 Pararas-Carayannis, G. (2014), The Great Tohoku-Oki Earthquake and Tsunami of March 11, 2011 in Japan: A
 2002 Critical Review and Evaluation of the Tsunami Source Mechanism, *Pure and Applied Geophysics*, 171(12), 3257-
 2003 3278, doi:10.1007/s00024-013-0677-7.
- 2004 Peltzer, G., P. Rosen, F. Rogez, and K. Hudnut (1996), Postseismic Rebound in Fault Step-Overs Caused by Pore
 2005 Fluid Flow, *Science*, 273(5279), 1202-1204, doi:10.1126/science.273.5279.1202.
- 2006 Perfettini, H., and J. P. Avouac (2014), The seismic cycle in the area of the 2011 Mw9.0 Tohoku-Oki earthquake,
 2007 *Journal of Geophysical Research: Solid Earth*, 119(5), 4469-4515, doi:10.1002/2013JB010697.
- 2008 Peterson, E. T., and T. Seno (1984), Factors affecting seismic moment release rates in subduction zones, *Journal of*
 2009 *Geophysical Research: Solid Earth*, 89(B12), 10233-10248.
- 2010 Pollitz, F. F., R. Bürgmann, and P. Banerjee (2011), Geodetic slip model of the 2011 M9.0 Tohoku earthquake,
 2011 *Geophys. Res. Lett.*, 38, L00G08, doi:10.1029/2011gl048632.
- 2012 Pritchard, M. E., et al. (2020), New Opportunities to Study Earthquake Precursors, *Seismological Research Letters*,
 2013 91(5), 2444-2447, doi:10.1785/0220200089.
- 2014 Reasenberg, P. A., and R. W. Simpson (1992), Response of Regional Seismicity to the Static Stress Change
 2015 Produced by the Loma Prieta Earthquake, *Science*, 255(5052), 1687, doi:10.1126/science.255.5052.1687.

- 2016 Research Center for Prediction of Earthquakes and Volcanic Eruptions, Graduate School of Science, Tohoku
 2017 University (2011), On the M7.3 earthquake off-Sanriku on March 9, 2011,
 2018 <https://www.aob.gp.tohoku.ac.jp/info/topics/topics-110309/>.
 2019 Romano, F., A. Piatanesi, S. Lorito, N. D'Agostino, K. Hirata, S. Atzori, Y. Yamazaki, and M. Cocco (2012), Clues
 2020 from joint inversion of tsunami and geodetic data of the 2011 Tohoku-oki earthquake, *Scientific Reports*, 2(1), 385,
 2021 doi:10.1038/srep00385.
 2022 Romano, F., E. Trasatti, S. Lorito, C. Piromallo, A. Piatanesi, Y. Ito, D. Zhao, K. Hirata, P. Lanucara, and M. Cocco
 2023 (2014), Structural control on the Tohoku earthquake rupture process investigated by 3D FEM, tsunami and geodetic
 2024 data, *Scientific Reports*, 4(1), 5631, doi:10.1038/srep05631.
 2025 Ruff, L., and H. Kanamori (1980), Seismicity and the subduction process, *Physics of the Earth and Planetary*
 2026 *Interiors*, 23(3), 240-252, doi:[https://doi.org/10.1016/0031-9201\(80\)90117-X](https://doi.org/10.1016/0031-9201(80)90117-X).
 2027 Ruiz, S., M. Metois, A. Fuenzalida, J. Ruiz, F. Leyton, R. Grandin, C. Vigny, R. Madariaga, and J. Campos (2014),
 2028 Intense foreshocks and a slow slip event preceded the 2014 Iquique Mw 8.1 earthquake, *Science*,
 2029 doi:10.1126/science.1256074.
 2030 Saito, T., Y. Ito, D. Inazu, and R. Hino (2011), Tsunami source of the 2011 Tohoku-Oki earthquake, Japan:
 2031 Inversion analysis based on dispersive tsunami simulations, *Geophysical Research Letters*, 38(7),
 2032 doi:10.1029/2011GL049089.
 2033 Satake, K., and Y. Fujii (2014), Review: Source Models of the 2011 Tohoku Earthquake and Long-Term Forecast of
 2034 Large Earthquakes, *Journal of Disaster Research*, 9(3), 272-280, doi:10.20965/jdr.2014.p0272.
 2035 Satake, K., Y. Fujii, T. Harada, and Y. Namegaya (2013), Time and Space Distribution of Coseismic Slip of the
 2036 2011 Tohoku Earthquake as Inferred from Tsunami Waveform Data, *B Seismol Soc Am*, 103(2B), 1473-1492,
 2037 doi:10.1785/0120120122.
 2038 Satake, K., Y. Namegaya, and S. Yamaki (2008), Numerical simulation of the AD 869 Jogan tsunami in Ishinomaki
 2039 and Sendai plains, *Annual Report on Active Fault and Paleoequake Researches*, 8, 71-89.
 2040 Sato, M., T. Ishikawa, N. Ujihara, S. Yoshida, M. Fujita, M. Mochizuki, and A. Asada (2011a), Displacement
 2041 Above the Hypocenter of the 2011 Tohoku-Oki Earthquake, *Science*, 1207401, doi:10.1126/science.1207401.
 2042 Sato, M., H. Saito, T. Ishikawa, Y. Matsumoto, M. Fujita, M. Mochizuki, and A. Asada (2011b), Restoration of
 2043 interplate locking after the 2005 Off-Miyagi Prefecture earthquake, detected by GPS/acoustic seafloor geodetic
 2044 observation, 38(1), doi:10.1029/2010gl045689.
 2045 Satriano, C., V. Dionicio, H. Miyake, N. Uchida, J.-P. Vilotte, and P. Bernard (2014), Structural and thermal control
 2046 of seismic activity and megathrust rupture dynamics in subduction zones: Lessons from the Mw 9.0, 2011 Tohoku
 2047 earthquake, *Earth and Planetary Science Letters*, 403, 287-298, doi:<https://doi.org/10.1016/j.epsl.2014.06.037>.
 2048 Sawai, Y. (2017), Paleotsunami research along the Pacific coast of Tohoku region, *The Journal of the Geological*
 2049 *Society of Japan*, 123(10), 819-830, doi:10.5575/geosoc.2017.0055.
 2050 Sawai, Y., Y. Namegaya, Y. Okamura, K. Satake, and M. Shishikura (2012), Challenges of anticipating the 2011
 2051 Tohoku earthquake and tsunami using coastal geology, *Geophysical Research Letters*, 39(21), L21309,
 2052 doi:10.1029/2012gl053692.
 2053 Sawai, Y., Y. Namegaya, T. Tamura, R. Nakashima, and K. Tanigawa (2015), Shorter intervals between great
 2054 earthquakes near Sendai: Scour ponds and a sand layer attributable to A.D. 1454 overwash, *Geophysical Research*
 2055 *Letters*, 42(12), 4795-4800, doi:10.1002/2015GL064167.
 2056 Sawai, Y., M. Shishikura, and J. Komatsubara (2008), A study on paleotsunami using hand corer in Sendai plain
 2057 (Sendai City, Natori City, Iwanuma City, Watari Town, Yamamoto Town), Miyagi, Japan, *Annual report on active*
 2058 *fault and paleoearthquake researches*, 8, 17-70.
 2059 Sawai, Y., et al. (2007), A study on paleotsunami using handy geoslicer in Sendai Plain (Sendai, Natori, Iwanuma,
 2060 Watari, and Yamamoto), Miyagi, Japan, *Annual report on active fault and paleoearthquake researches*, 7, 47-80.
 2061 Sawazaki, K., H. Kimura, K. Shiomi, N. Uchida, R. Takagi, and R. Snieder (2015), Depth-dependence of seismic
 2062 velocity change associated with the 2011 Tohoku earthquake, Japan, revealed from repeating earthquake analysis
 2063 and finite-difference wave propagation simulation, *Geophysical Journal International*, 201(2), 741-763,
 2064 doi:10.1093/gji/ggv014.
 2065 Scholz, C. H., and J. Campos (2012), The seismic coupling of subduction zones revisited, 117(B5),
 2066 doi:10.1029/2011jb009003.
 2067 Schwartz, D. P., and K. J. Coppersmith (1984), Fault behavior and characteristic earthquakes: Examples from the
 2068 Wasatch and San Andreas fault zones, *J. Geophys. Res.*, 89, doi:10.1029/JB089iB07p05681.
 2069 Shao, G., X. Li, C. Ji, and T. Maeda (2011), Focal mechanism and slip history of the 2011 Mw 9.1 off the Pacific
 2070 coast of Tohoku Earthquake, constrained with teleseismic body and surface waves, *Earth Planets Space*, 63(7), 559-
 2071 564.

- 2072 Shennan, I., R. Bruhn, and G. Plafker (2009), Multi-segment earthquakes and tsunami potential of the Aleutian
2073 megathrust, *Quaternary Science Reviews*, 28(1), 7-13, doi:<https://doi.org/10.1016/j.quascirev.2008.09.016>.
- 2074 Shibazaki, B., T. Matsuzawa, A. Tsutsumi, K. Ujiie, A. Hasegawa, and Y. Ito (2011), 3D modeling of the cycle of a
2075 great Tohoku-oki earthquake, considering frictional behavior at low to high slip velocities, *Geophysical Research*
2076 *Letters*, 38(21), L21305, doi:10.1029/2011gl049308.
- 2077 Shibazaki, B., H. Noda, and M. J. Ikari (2019), Quasi-Dynamic 3D Modeling of the Generation and Afterslip of a
2078 Tohoku-oki Earthquake Considering Thermal Pressurization and Frictional Properties of the Shallow Plate
2079 Boundary, *Pure and Applied Geophysics*, 176(9), 3951-3973, doi:10.1007/s00024-018-02089-w.
- 2080 Shirzaei, M., R. Bürgmann, N. Uchida, Y. Hu, F. Pollitz, and T. Matsuzawa (2014), Seismic versus aseismic slip:
2081 Probing mechanical properties of the northeast Japan subduction zone, *Earth and Planetary Science Letters*, 406(0),
2082 7-13, doi:<http://dx.doi.org/10.1016/j.epsl.2014.08.035>.
- 2083 Shishikura, M., O. Fujiwara, Y. Sawai, Y. Namegaya, and K. Tanigawa (2012), Inland-limit of the tsunami deposit
2084 associated with the 2011 Off-Tohoku Earthquake in the Sendai and Ishinomaki Plains, Northeastern Japan, *Annu.*
2085 *Rep. Active Fault Paleoeearthquake Res.*, 12, 45-61.
- 2086 Shishikura, M., Y. Sawai, Y. Okamura, J. Komatsubara, T. T. Aung, T. Ishiyama, O. Fujiwara, and S. Fujino (2007),
2087 Age and distribution of tsunami deposit in the Ishinomaki Plain, Northeastern Japan, *Annual Report on Active Fault*
2088 *and Paleoeearthquake Researches*, 7, 31-46.
- 2089 Silverii, F., D. Cheloni, N. D'Agostino, G. Selvaggi, and E. Boschi (2014), Post-seismic slip of the 2011 Tohoku-
2090 Oki earthquake from GPS observations: implications for depth-dependent properties of subduction megathrusts,
2091 *Geophysical Journal International*, 198(1), 580-596, doi:10.1093/gji/ggu149.
- 2092 Somerville, P. G. (2014), A post-Tohoku earthquake review of earthquake probabilities in the Southern Kanto
2093 District, Japan, *Geoscience Letters*, 1(1), 10, doi:10.1186/2196-4092-1-10.
- 2094 Strasser, M., et al. (2013), A slump in the trench: Tracking the impact of the 2011 Tohoku-Oki earthquake, *Geology*,
2095 41(8), 935-938, doi:10.1130/G34477.1.
- 2096 Sugawara, D., F. Imamura, K. Goto, H. Matsumoto, and K. Minoura (2013), The 2011 Tohoku-oki Earthquake
2097 Tsunami: Similarities and Differences to the 869 Jogan Tsunami on the Sendai Plain, *Pure and Applied Geophysics*,
2098 170(5), 831-843, doi:10.1007/s00024-012-0460-1.
- 2099 Sugawara, D., F. Imamura, H. Matsumoto, K. Goto, and K. Minoura (2010), Quantitative reconstruction of
2100 historical tsunami: On the investigation of tsunami trace of the Jyogan earthquake and estimation of
2101 palaeotopography, *Res. Rep. Tsunami Eng.*, 27, 103-132.
- 2102 Sugawara, D., F. Imamura, H. Matsumoto, K. Goto, and K. Minoura (2011), Reconstruction of the AD869 Jogan
2103 earthquake induced tsunami by using the geological data, *Journal of Japan Society for Natural Disaster Science*,
2104 29(4), 501-516.
- 2105 Sugawara, D., K. Minoura, and F. Imamura (2001), Sedimentation associated with the AD 869 Jogan tsunami and
2106 its numerical reconstruction, *Res. Rep. Tsunami Eng.*, 18, 1-10.
- 2107 Sun, T., and K. Wang (2015), Viscoelastic relaxation following subduction earthquakes and its effects on afterslip
2108 determination, *Journal of Geophysical Research: Solid Earth*, 120(2), 2014JB011707, doi:10.1002/2014JB011707.
- 2109 Sun, T., K. Wang, T. Fujiwara, S. Kodaira, and J. He (2017), Large fault slip peaking at trench in the 2011 Tohoku-
2110 oki earthquake, *Nature Communications*, 8(1), 14044, doi:10.1038/ncomms14044.
- 2111 Sun, T., et al. (2014), Prevalence of viscoelastic relaxation after the 2011 Tohoku-oki earthquake, *Nature*,
2112 514(7520), 84-87, doi:10.1038/nature13778.
- 2113 Suwa, Y., S. Miura, A. Hasegawa, T. Sato, and K. Tachibana (2006), Interplate coupling beneath NE Japan inferred
2114 from three dimensional displacement field, *J. Geophys. Res.*, 111(B04402), doi:10.1029/102004JB003203.
- 2115 Suzuki, W., S. Aoi, H. Sekiguchi, and T. Kunugi (2011), Rupture process of the 2011 Tohoku-Oki mega-thrust
2116 earthquake (M9.0) inverted from strong-motion data, *Geophys. Res. Lett.*, 38, L00G16, doi:10.1029/2011gl049136.
- 2117 Tajima, F., J. Mori, and B. L. N. Kennett (2013), A review of the 2011 Tohoku-Oki earthquake (Mw 9.0): Large-
2118 scale rupture across heterogeneous plate coupling, *Tectonophysics*, 586, 15-34,
2119 doi:<https://doi.org/10.1016/j.tecto.2012.09.014>.
- 2120 Takada, K., et al. (2016), Distribution and ages of tsunami deposits along the Pacific Coast of the Iwate Prefecture,
2121 *Annu. Rep. Active Fault Paleoeearthquake Res.*, 16, 1-52.
- 2122 Takada, Y., and Y. Fukushima (2013), Volcanic subsidence triggered by the 2011 Tohoku earthquake in Japan,
2123 *Nature Geoscience*, 6(8), 637-641, doi:10.1038/ngeo1857.
- 2124 Takagi, R., and T. Okada (2012), Temporal change in shear velocity and polarization anisotropy related to the
2125 2011 M9.0 Tohoku-Oki earthquake examined using KiK-net vertical array data, *Geophysical Research Letters*,
2126 39(9), doi:10.1029/2012GL051342.

- 2127 Takahashi, H., R. Hino, N. Uchida, K. Ohta, and M. Shinohara (2020), Low-frequency tremor activity along
2128 northern Japan Trench before the 2011 Tohoku-Oki earthquake, *AGU 2020 Fall Meeting*, T003-0013.
- 2129 Tanaka, S. (2012), Tidal triggering of earthquakes prior to the 2011 Tohoku-Oki earthquake (Mw 9.1), *Geophysical*
2130 *Research Letters*, 39(7), L00G26, doi:10.1029/2012gl051179.
- 2131 Tanioka, Y., and K. Satake (1996), Fault parameters of the 1896 Sanriku Tsunami Earthquake estimated from
2132 Tsunami Numerical Modeling, *Geophysical Research Letters*, 23(13), 1549-1552, doi:10.1029/96gl01479.
- 2133 Tapley, B. D., S. Bettadpur, J. C. Ries, P. F. Thompson, and M. M. Watkins (2004), GRACE Measurements of Mass
2134 Variability in the Earth System, *Science*, 305(5683), 503, doi:10.1126/science.1099192.
- 2135 Tappin, D. R., S. T. Grilli, J. C. Harris, R. J. Geller, T. Masterlark, J. T. Kirby, F. Shi, G. Ma, K. K. S. Thingbaijam,
2136 and P. M. Mai (2014), Did a submarine landslide contribute to the 2011 Tohoku tsunami?, *Marine Geology*, 357,
2137 344-361, doi:<https://doi.org/10.1016/j.margeo.2014.09.043>.
- 2138 Toda, S., J. Lin, and R. S. Stein (2011a), Using the 2011 Mw 9.0 off the Pacific coast of Tohoku Earthquake to test
2139 the Coulomb stress triggering hypothesis and to calculate faults brought closer to failure, *Earth, Planets and Space*,
2140 63(7), 39, doi:10.5047/eps.2011.05.010.
- 2141 Toda, S., R. S. Stein, and J. Lin (2011b), Widespread seismicity excitation throughout central Japan following the
2142 2011 M=9.0 Tohoku earthquake and its interpretation by Coulomb stress transfer, *Geophysical Research Letters*,
2143 38(7), doi:10.1029/2011GL047834.
- 2144 Tomita, F., T. Iinuma, Y. Ohta, R. Hino, M. Kido, and N. Uchida (2020), Improvement on spatial resolution of a
2145 coseismic slip distribution using postseismic geodetic data through a viscoelastic inversion, *Earth, Planets and*
2146 *Space*, 72(1), 84, doi:10.1186/s40623-020-01207-0.
- 2147 Tomita, F., M. Kido, Y. Ohta, T. Iinuma, and R. Hino (2017), Along-trench variation in seafloor displacements after
2148 the 2011 Tohoku earthquake, *Science Advances*, 3(7), e1700113, doi:10.1126/sciadv.1700113.
- 2149 Tormann, T., B. Enescu, J. Woessner, and S. Wiemer (2015), Randomness of megathrust earthquakes implied by
2150 rapid stress recovery after the Japan earthquake, *Nature Geosci*, 8(2), 152-158, doi:10.1038/ngeo2343
2151 <http://www.nature.com/ngeo/journal/v8/n2/abs/ngeo2343.html#supplementary-information>.
- 2152 Tsuji, Y., K. Imai, Y. Mabuchi, T. Oie, K. Okada, Y. Iwabuchi, and F. Imamura (2012), Field Survey of the
2153 Tsunami of the 1677 Empo Boso-Oki and the 1611 Keicho Sanriku-Oki Earthquake, *Tsunami engineering technical*
2154 *report*, 29, 189-207.
- 2155 Tsuji, Y., Y. Mabuchi, T. Oie, and F. Imamura (2011), The tsunami record survey for the Keicho 16 Sanriku
2156 earthquake at the Iwate prefecture, *Tsunami engineering technical report*, 28, 173-180.
- 2157 Tsuji, Y., and K. Ueda (1995), The investigation of Keicho 16 (1611), Enpo 5 (1677), Hourei 12 (1768), Kansei 5
2158 (1793) and Ansei 3 (1856) earthquake tsunamis, *Historical Earthquakes*, 11.
- 2159 Tsunami Joint Survey Group, The Tohoku Earthquake (2011), NATIONWIDE FIELD SURVEY OF THE 2011
2160 OFF THE PACIFIC COAST OF TOHOKU EARTHQUAKE TSUNAMI, *Journal of Japan Society of Civil*
2161 *Engineers, Ser. B2 (Coastal Engineering)*, 67(1), 63-66, doi:10.2208/kaigan.67.63.
- 2162 Tsushima, H., R. Hino, Y. Ohta, T. Iinuma, and S. Miura (2014), tFISH/RAPiD: Rapid improvement of near-field
2163 tsunami forecasting based on offshore tsunami data by incorporating onshore GNSS data, *Geophysical Research*
2164 *Letters*, 41(10), 3390-3397, doi:10.1002/2014GL059863.
- 2165 Uchida, N., and R. Bürgmann (2019), Repeating earthquakes, *Annual Review of Earth and Planetary Sciences*, 47,
2166 10.1146/annurev-earth-053018-060119.
- 2167 Uchida, N., Y. Hu, and R. Bürgmann (2018), Co- and Postseismic Changes in Inland Seismicity and its Relationship
2168 with Transient Stress by the 2011 Tohoku-Oki Earthquake, *AOGS 2018*, SE28-A049.
- 2169 Uchida, N., T. Iinuma, R. M. Nadeau, R. Bürgmann, and R. Hino (2016), Periodic slow slip triggers megathrust
2170 zone earthquakes in northeastern Japan, *Science*, 351(6272), 488-492, doi:10.1126/science.aad3108.
- 2171 Uchida, N., and T. Matsuzawa (2011), Coupling coefficient, hierarchical structure, and earthquake cycle for the
2172 source area of the 2011 off the Pacific coast of Tohoku earthquake inferred from small repeating earthquake data,
2173 *Earth Planets and Space*, 63(7), 675-679, doi:10.5047/eps.2011.07.006.
- 2174 Uchida, N., and T. Matsuzawa (2013), Pre- and postseismic slow slip surrounding the 2011 Tohoku-oki earthquake
2175 rupture, *Earth and Planetary Science Letters*, 374(0), 81-91, doi:<http://dx.doi.org/10.1016/j.epsl.2013.05.021>.
- 2176 Uchida, N., T. Matsuzawa, W. L. Ellsworth, K. Imanishi, T. Okada, and A. Hasegawa (2007), Source parameters of
2177 a M4.8 and its accompanying repeating earthquakes off Kamaishi, NE Japan - implications for the hierarchical
2178 structure of asperities and earthquake cycle, *Geophys. Res. Lett.*, 34, doi:10.1029/2007GL031263.
- 2179 Uchida, N., J. Nakajima, A. Hasegawa, and T. Matsuzawa (2009), What controls interplate coupling?: Evidence for
2180 abrupt change in coupling across a border between two overlying plates in the NE Japan subduction zone, *Earth*
2181 *Planet. Sci. Lett.*, 283, 111-121.

- 2182 Uchide, T. (2013), High-speed rupture in the first 20 s of the 2011 Tohoku earthquake, Japan, *Geophysical Research*
 2183 *Letters*, 40(12), 2993-2997, doi:10.1002/grl.50634.
- 2184 Ujiie, K., H. Tanaka, T. Saito, A. Tsutsumi, J. J. Mori, J. Kameda, E. E. Brodsky, F. M. Chester, N. Eguchi, and S.
 2185 Toczko (2013), Low Coseismic Shear Stress on the Tohoku-Oki Megathrust Determined from Laboratory
 2186 Experiments, *Science*, 342(6163), 1211, doi:10.1126/science.1243485.
- 2187 Usami, K., K. Ikehara, T. Kanamatsu, and C. M. McHugh (2018), Supercycle in great earthquake recurrence along
 2188 the Japan Trench over the last 4000 years, *Geoscience Letters*, 5(1), 11, doi:10.1186/s40562-018-0110-2.
- 2189 Usami, T. (1996), Materials for Comprehensive List of De-structive Earthquakes in Japan 416-1995, *University of*
 2190 *Tokyo Press, (in Japanese)*, pp. 493.
- 2191 Wang, C., X. Ding, X. Shan, L. Zhang, and M. Jiang (2012a), Slip distribution of the 2011 Tohoku earthquake
 2192 derived from joint inversion of GPS, InSAR and seafloor GPS/acoustic measurements, *Journal of Asian Earth*
 2193 *Sciences*, 57, 128-136, doi:<https://doi.org/10.1016/j.jseaes.2012.06.019>.
- 2194 Wang, K., and S. L. Bilek (2014), Invited review paper: Fault creep caused by subduction of rough seafloor relief,
 2195 *Tectonophysics*, 610(0), 1-24, doi:<http://dx.doi.org/10.1016/j.tecto.2013.11.024>.
- 2196 Wang, K., L. Brown, Y. Hu, K. Yoshida, J. He, and T. Sun (2019), Stable Forearc Stressed by a Weak Megathrust:
 2197 Mechanical and Geodynamic Implications of Stress Changes Caused by the M = 9 Tohoku-Oki Earthquake, *Journal*
 2198 *of Geophysical Research: Solid Earth*, 124(6), 6179-6194, doi:10.1029/2018JB017043.
- 2199 Wang, L., and R. Bürgmann (2019), Statistical Significance of Precursory Gravity Changes Before the 2011 Mw 9.0
 2200 Tohoku-Oki Earthquake, *Geophysical Research Letters*, 46(13), 7323-7332, doi:10.1029/2019GL082682.
- 2201 Wang, L., S. Hainzl, and P. M. Mai (2015), Quantifying slip balance in the earthquake cycle: Coseismic slip model
 2202 constrained by interseismic coupling, *Journal of Geophysical Research: Solid Earth*, 120(12), 8383-8403,
 2203 doi:<https://doi.org/10.1002/2015JB011987>.
- 2204 Wang, L., C. K. Shum, F. J. Simons, B. Tapley, and C. Dai (2012b), Coseismic and postseismic deformation of the
 2205 2011 Tohoku-Oki earthquake constrained by GRACE gravimetry, *Geophysical Research Letters*, 39(7),
 2206 doi:<https://doi.org/10.1029/2012GL051104>.
- 2207 Wang, R., S. Parolai, M. Ge, M. Jin, T. R. Walter, and J. Zschau (2013), The 2011 Mw 9.0 Tohoku Earthquake:
 2208 Comparison of GPS and Strong - Motion Data, *B Seismol Soc Am*, 103(2B), 1336-1347, doi:10.1785/0120110264.
- 2209 Wang, Z., T. Kato, X. Zhou, and J. i. Fukuda (2016), Source process with heterogeneous rupture velocity for the
 2210 2011 Tohoku-Oki earthquake based on 1-Hz GPS data, *Earth, Planets and Space*, 68(1), 193, doi:10.1186/s40623-
 2211 016-0572-4.
- 2212 Watanabe, H. (2001), Is it possible to clarify the real state of past earthquakes and tsunamis on the basis of legends ?
 2213 -as an example of the 869 Jogan earthquake and tsunami -, *Historical Earthquakes*, 17, 130-146.
- 2214 Watanabe, S.-i., M. Sato, M. Fujita, T. Ishikawa, Y. Yokota, N. Ujihara, and A. Asada (2014), Evidence of
 2215 viscoelastic deformation following the 2011 Tohoku-Oki earthquake revealed from seafloor geodetic observation,
 2216 *Geophysical Research Letters*, 41(16), 5789-5796, doi:10.1002/2014GL061134.
- 2217 Wei, S., R. Graves, D. Helmberger, J.-P. Avouac, and J. Jiang (2012), Sources of shaking and flooding during the
 2218 Tohoku-Oki earthquake: A mixture of rupture styles, *Earth and Planetary Science Letters*, 333-334, 91-100,
 2219 doi:<https://doi.org/10.1016/j.epsl.2012.04.006>.
- 2220 Wei, S., A. Sladen, and t. A. group (2011), Updated Result 3/11/2011 (Mw 9.0), Tohoku-oki, Japan,
 2221 http://www.tectonics.caltech.edu/slip_history/2011_taiheiyo-oki/index.html, last accessed December 4, 2020.
- 2222 Woith, H., G. M. Petersen, S. Hainzl, and T. Dahm (2018), Review: Can Animals Predict Earthquakes?, *B Seismol*
 2223 *Soc Am*, 108(3A), 1031-1045, doi:10.1785/0120170313.
- 2224 Yagi, Y., and Y. Fukahata (2011), Rupture process of the 2011 Tohoku-oki earthquake and absolute elastic strain
 2225 release, *Geophysical Research Letters*, 38(19), L19307, doi:10.1029/2011GL048701.
- 2226 Yamagiwa, S., S. i. Miyazaki, K. Hirahara, and Y. Fukahata (2015), Afterslip and viscoelastic relaxation following
 2227 the 2011 Tohoku-oki earthquake (Mw9.0) inferred from inland GPS and seafloor GPS/Acoustic data, *Geophysical*
 2228 *Research Letters*, 42(1), 66-73, doi:10.1002/2014GL061735.
- 2229 Yamanaka, Y., and M. Kikuchi (2004), Asperity map along the subduction zone in northeastern Japan inferred from
 2230 regional seismic data, *J. Geophys. Res.*, 109(B7), B07307, doi:10.1029/2003jb002683.
- 2231 Yamazaki, Y., K. F. Cheung, and T. Lay (2018), A Self-Consistent Fault Slip Model for the 2011 Tohoku
 2232 Earthquake and Tsunami, *Journal of Geophysical Research: Solid Earth*, 123(2), 1435-1458,
 2233 doi:10.1002/2017JB014749.
- 2234 Yokota, Y., T. Ishikawa, and S.-i. Watanabe (2018), Seafloor crustal deformation data along the subduction zones
 2235 around Japan obtained by GNSS-A observations, *Scientific Data*, 5(1), 180182, doi:10.1038/sdata.2018.182.
- 2236 Yokota, Y., and K. Koketsu (2015), A very long-term transient event preceding the 2011 Tohoku earthquake, *Nat*
 2237 *Commun*, 6, doi:10.1038/ncomms6934.

- 2238 Yokota, Y., K. Koketsu, Y. Fujii, K. Satake, S. i. Sakai, M. Shinohara, and T. Kanazawa (2011), Joint inversion of
2239 strong motion, teleseismic, geodetic, and tsunami datasets for the rupture process of the 2011 Tohoku earthquake,
2240 *Geophysical Research Letters*, 38(7), doi:10.1029/2011GL050098.
- 2241 Yoshida, K., and A. Hasegawa (2018), Hypocenter Migration and Seismicity Pattern Change in the Yamagata-
2242 Fukushima Border, NE Japan, Caused by Fluid Movement and Pore Pressure Variation, *Journal of Geophysical*
2243 *Research: Solid Earth*, 123(6), 5000-5017, doi:10.1029/2018JB015468.
- 2244 Yoshida, K., A. Hasegawa, T. Yoshida, and T. Matsuzawa (2019), Heterogeneities in Stress and Strength in Tohoku
2245 and Its Relationship with Earthquake Sequences Triggered by the 2011 M9 Tohoku-Oki Earthquake, *Pure and*
2246 *Applied Geophysics*, 176(3), 1335-1355, doi:10.1007/s00024-018-2073-9.
- 2247 Yoshida, K., K. Miyakoshi, and K. Irikura (2011), Source process of the 2011 off the Pacific coast of Tohoku
2248 Earthquake inferred from waveform inversion with long-period strong-motion records, *Earth, Planets and Space*,
2249 63(7), 12, doi:10.5047/eps.2011.06.050.
- 2250 Yue, H., and T. Lay (2011), Inversion of high-rate (1 sps) GPS data for rupture process of the 11 March 2011
2251 Tohoku earthquake (Mw 9.1), *Geophys. Res. Lett.*, 38, L00G09, doi:10.1029/2011gl048700.
- 2252 Yue, H., and T. Lay (2013), Source Rupture Models for the Mw 9.0 2011 Tohoku Earthquake from Joint Inversions
2253 of High - Rate Geodetic and Seismic Data, *B Seismol Soc Am*, 103(2B), 1242-1255, doi:10.1785/0120120119.
- 2254 Zhao, D., Z. Huang, N. Umino, A. Hasegawa, and H. Kanamori (2011), Structural heterogeneity in the megathrust
2255 zone and mechanism of the 2011 Tohoku-oki earthquake (Mw 9.0), *Geophysical Research Letters*, 38(17), L17308,
2256 doi:10.1029/2011gl048408.
- 2257 Zhou, X., G. Cambiotti, W. Sun, and R. Sabadini (2014), The coseismic slip distribution of a shallow subduction
2258 fault constrained by prior information: the example of 2011 Tohoku (Mw 9.0) megathrust earthquake, *Geophysical*
2259 *Journal International*, 199(2), 981-995, doi:10.1093/gji/ggu310.
- 2260